1987

Numerical Solution Of Subsidence Mound Problems In Porous Media

Peter Laurens Schuck

CANADIAN THESES

THÈSES CANADIENNES

NOTICE

The quality of this microfiche is heavily dependent upon the quality of the original thesis submitted for microfilming. Every effort has been made to ensure the highest quality of reproduction possible.

If pages are missing, contact the university which granted the degree.

Some pages may have indistinct print especially if the original pages were typed with a poor typewriter ribbon or if the university sent us an inferior photocopy.

Previously copyrighted materials (journal articles, published tests, etc.) are not filmed.

Reproduction in full or in part of this film is governed by the Canadian Copyright Act, R.S.C. 1970, c. C-30.

AVIS

La qualité de cette microfiche dépend grandement de la qualité de la thèse soumise au microfilmage. Nous avons tout fait pour assurer une qualité supérieure de reproduction.

S'il manque des pages, veuillez communiquer avec l'université qui a conféré le grade.

La qualité d'impression de certaines pages peut laisser à désirer, surtout si les pages originales ont été dactylographiées à l'aide d'un ruban usé ou si l'université nous a fait parvenir une photocopie de qualité inférieure.

Les documents qui font déjà l'objet d'un droit d'auteur (articles de revue, examens publiés, etc.) ne sont pas microfilmés.

La reproduction, même partielle, de ce microfilm est soumise à la Loi canadienne sur le droit d'auteur, SRC 1970, c. C-30.

THIS DISSERTATION HAS BEEN MICROFILMED EXACTLY AS RECEIVED

LA THÈSE A ÉTÉ MICROFILMÉE TELLE QUE NOUS L'AVONS REÇUE

NUMERICAL SOLUTION OF SUBSIDENCE MOUND PROBLEMS IN POROUS MEDIA

by

Peter L. Schuck

Department of Applied Mathematics

Submitted in partial fulfilment
of the requirements for the degree of
Doctor of Philosophy

Faculty of Graduate Studies
The University of Western Ontario
London, Ontario
September 1986

ISBN 0-315-36072-0

Abstract

From the macroscopic equations of flow through a porous medium, a model is developed for the subsidence or decay of a mound of fluid over a horizontal impervious barrier. Three finite difference approaches are used to investigate the resulting moving boundary problem. In the first method, a coordinate transformation is used that fixes the toe or leading edge of the fluid location. The resulting problem is solved on a regular grid with interpolation near the moving boundary. In the second method, a coordinate transformation is employed that fixes the location of the entire boundary while in the third method, a transformed polar coordinate formulation is employed that maps the domain onto a quarter circle. For the latter two methods the resulting equations are solved using a regular grid. It is demonstrated that for all three methods, a predictor-corrector scheme gives satisfactory results for the boundary position without iteration. It was found that the first two methods were more accurate than the third for a given spatial discretization. A new similarity solution to the Bousinesq approximation to the problem for an initially parabolic mound is presented and is found to compare favourably to the numerical solution to the full problem for mounds with large initial aspect ratios.

The model is refined so that the effect on the mobility of the fluid of heating along the interface is incorporated. The fluid viscosity and density are assumed to be dependent on temperature. The problem is investigated using the latter two fully transformed finite difference grids above. The backwards Euler method is used for the temporal derivatives of both the temperature and boundary position equation and a successive substitution scheme with relaxation is used to iterate between the various coupled equations. Again it is found that the scheme based on rectangular coordinates is more accurate for a given spacial discretization than the scheme based on polar coordinates. Depending upon the choice of parameters in the problem the mound takes on a 'kinked' appearance with the quickly heated top area spreading out with a linear like profile and the central body of the fluid dropping slowly.

Acknowledgements

I would like to express my appreciation to Dr. H. Rasmussen for suggesting these porous flow problems and for his encouragement during this work.

A special thanks to Dave Meridith with whom I've has countless thought provoking conversations regarding aspects of numerical analysis and applied mathematics related to this work. Thanks also to the many other members of the Applied Mathematics Department, both students and faculty, with whom I've has numerous discussions concerning this work.

I am indepted to the Natural Science and Engineering Research Council of Canada for its financial support.

Finally, I most sincerely thank my family, my wife Joanne and our children Robyn and Mark, without whose moral support, patience and love, this work would certainly have suffered.

TABLE OF CONTENTS

CERTIFICATE OF EXAMINATION ii
ABSTRACT iii
ACKNOWLEDGEMENT v
TABLE OF CONTENTS vi
LIST OF TABLES vii
LIST OF FIGURES viii

CHAPTER 1 - GENERAL INTRODUCTION 1
1.1 Description of a Moving Boundary Problem ... 1
1.2 Description of a Porous Medium 3
1.3 Description of the Problem 4
1.4 Outline of Thesis 5

CHAPTER 2 - A SUBSIDENCE MOUND PROBLEM 8
2.1 Introduction 8
2.2 Equations for the Flow of Fluids Through a Porous Medium 10
2.3 Boundary Conditions on the Moving Surface 13
2.4 Statement of the Problem 18
2.5 Review of Previous Work 21
2.6 A Similarity Solution of the Bousinesq Equation 24
2.7 Numerical Method 28
2.7.1 The Potential Problem 28
2.7.2 The Movement of the Boundary 47
2.7.3 The Solution of the Linear Equations for the Potential and the Stream Function ... 53
2.8 Discussion of Numerical Results 64
2.9 Conclusions 86

CHAPTER 3 - A HEATED SUBSIDENCE MOUND PROBLEM 87
3.1 Introduction 87
3.2 Equations for the Flow of Heated Fluids Through a Porous Medium 89
3.3 Statement of the Problem 93
3.4 Review of Previous Work 98
3.5 Numerical Method 104
3.5.1 Coordinate Transformation 104
3.5.2 The Stream Function Equation 108
3.5.3 The Temperature Equation 114
3.5.4 Movement of the Boundary 126
3.5.5 Overview of the Numerical Proceedure 128
3.6 Discussion of Numerical Results 130
3.7 Conclusions 147

• • •

APPENDIX 1 148
APPENDIX 2 150
REFERENCES 156
VITA 163

LIST OF TABLES

Table	Description	Page
1a	Example 1 : Method 1 Results	66
1b	Example 1 : Method 1 Results (cont.)	67
2a	Example 1 : Method 2 Results	68
2b	Example 1 : Method 2 Results (cont.)	69
3	Example 1 : Method 3 Results	70
4a	Example 2 : Results	132
4b	Example 2 : Results (cont.)	133

LIST OF FIGURES

Figure	Description	Page
1	Subsidence Mound Problem	4
2	Alternate Subsidence Mound Problem	8
3	The Subsidence Mound Problem as Formulated	18
4	The Original and Transformed Domains for Method 1	29
5	Five Point Difference Molecule at an Interior Grid Point	31
6	Five Point Difference Molecule at a Grid Point Adjacent to the Boundary	32
7	The Original and Transformed Domains for Method 2	36
8	Nine Point Difference Molecule	39
9	The Original and Transformed Domains for Method 3	43
10	The Grids for Method 3 at Two Different Times	74
11	Comparison of Methods	75
12	Numerical vs Similarity Solution: $s(0) = 1$	76
13	Numerical vs Similarity Solution: $s(0) = 2$	78
14	Numerical vs Similarity Solution: $s(0) = 4$	79
15	Numerical vs Similarity Solution: $s(0) = 8$	80
16	Cubic Initial Mound: $s(0) = 1$	81
17	Cubic Initial Mound: $s(0) = 2$	82
18	Humped Initial Mound: $s(0) = 1$	83
19	Humped Initial Mound: $s(0) = 2$	84
20	The Heated Subsidence Mound Problem	93
21	Comparison of Methods	135
22	Isotherms at $t = 0$	137
23	Isotherms at $t = .06$	138
24a	Variation in Parameter K : $K = .5$	140
24b	Variation in Parameter K : $K = .7$	140
24c	Variation in Parameter K : $K = .9$	140
25a	Variation in Parameter m : $m = 2$	141
25b	Variation in Parameter m : $m = 3$	141
25c	Variation in Parameter m : $m = 4$	141
26a	Variation in Parameter Ra : $Ra = 1$	142
26b	Variation in Parameter Ra : $Ra = 10$	142
26c	Variation in Parameter Ra : $Ra = 50$	142
26d	Variation in Parameter Ra : $Ra = 200$	143
26e	Variation in Parameter Ra : $Ra = 800$	143
27a	Variation in Parameter $\delta\Delta T$: $\delta\Delta T = .05$	144
27b	Variation in Parameter $\delta\Delta T$: $\delta\Delta T = .1$	144
27c	Variation in Parameter $\delta\Delta T$: $\delta\Delta T = .2$	144
28a	Variation in Parameter $\frac{\alpha_1}{\alpha_2 P}$: $\frac{\alpha_1}{\alpha_2 P} = 1$	145
28b	Variation in Parameter $\frac{\alpha_1}{\alpha_2 P}$: $\frac{\alpha_1}{\alpha_2 P} = 3$	145
28c	Variation in Parameter $\frac{\alpha_1}{\alpha_2 P}$: $\frac{\alpha_1}{\alpha_2 P} = 5$	145

Chapter 1 - General Introduction

1.1 Description of a Moving Boundary Problem

Moving boundary problems occur naturally in many engineering and physics applications. The distinction between moving as opposed to free boundary problems is that the former are transient problems while the latter are steady-state. For example, melting/solidification fronts, surface water waves, unsteady flow over non-rigid bodies and the porous flow problems studied in the present thesis are all moving boundary problems. The major motivation for the porous flow problems as formulated in this thesis comes from aquifer drainage and heat storage in groundwater hydrology and from in situ heating of heavy oil in petroleum engineering.

A protoype moving boundary problem (MBP plural MBPS) consists of continuum equations of continuity, momentum and possibly energy for the interior of a domain as well as equations of state and appropriate initial and boundary conditions. After the initial time, the location of part or all of the boundary is unknown and must be determined as part of the solution. The major difficulty in solving MBPS is the non-linear coupling between the field equations and the equations locating the boundary. That

is, the domain of the field equations is unknown as time advances and must be calculated by solving additional partial differential equations for the boundary possition which in turn have coefficients depending on the field variables themselves.

1.2 Description of a Porous Medium

Much attention has been given to MBPS in the literature as witnessed by the survey of Fruzeland (1977). In this thesis the subsidence mound problem in porous flow is investigated. In order to further discuss this problem a description of flow in a porous medium is required.

A porous medium is a solid matrix which contains numerous void spaces or pores of various shapes, sizes and connectivity. If there is a connected path of pores from one region in the medium to another then flow can occur. For the present assume that the pores are evenly distributed and that in a region where there is fluid it completely fills all the pores. Furthermore, in such a saturated region the fluid/solid combination is assumed to be homogeneous . This allows the use of a macroscopic model where the microscopic details of the fluid flow in the pores is not considered. For the porous medium this macroscopic model deals with the properties of porosity and permeability. Porosity measures the fraction of void space of the medium while permeability measures the ease with which a fluid moves through the medium due to a pressure difference.

1.3 Description of the Problem

The subsidence mound problem under consideration can be described as the decay of an mound of fluid fully saturating a region of a porous medium above an impervious barrier as shown in Figure 1 below.

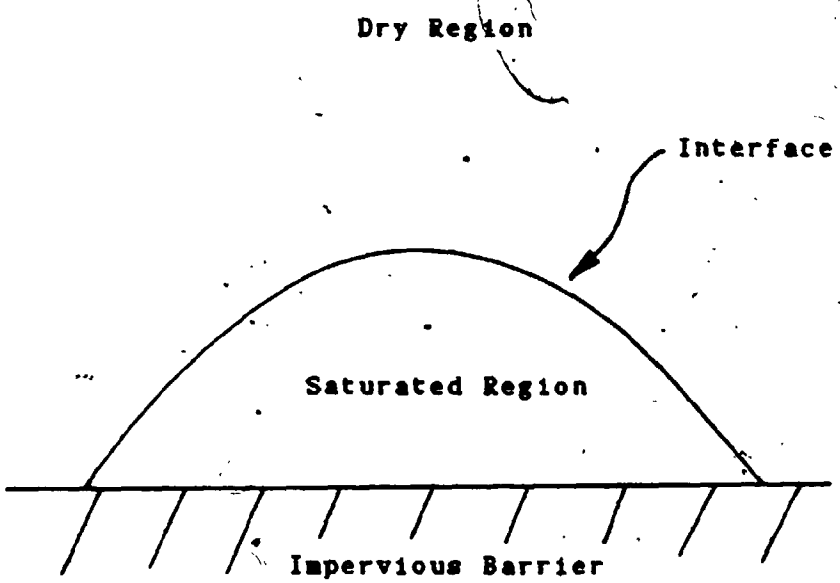

Figure 1 - Subsidence Mound Problem

1.4 Outline of Thesis

In this thesis finite difference methods are used to solve the system of partial differential equations resulting from the model problem. The solution of the subsidence mound problem has merit on its own since it has not been previously done, however the thrust of the thesis is to investigate the numerical methods for the solution of the mathematical model. In particular the technique of coordinate transformation which is used to handle the moving boundary is refined. This technique which is thought to be a natural method of handling moving or free boundaries has been previously investigated by Forsyth and Rasmussen (1979) & (1980), Rasmussen and Salhani (1981), Loh and Rasmussen (1985) and others. Under this transformation the unknown domain for the field equations becomes known but unfortunately the field equations themselves become more complex, typically with coefficients depending on the boundary position. They found the method to be useful from an ease of programming point of view but somewhat less efficient in CPU time than other methods.

In Chapter 2 three different finite difference methods for the subsidence mound problem are investigated. In the first two, the subsidence mound problem is formulated as a potential problem for the fluid velocity coupled to a

hyperbolic equation for the moving boundary. For the potential part of the problem comparisons are made between a scheme whereby the potential is calculated on a regular grid with interpolation near the moving boundary and a coordinate transformed scheme which fixes the boundary. Of interest here is whether the transformed scheme retains certain desirable properties of the other scheme. For both these schemes we propagate the boundary using a predictor-corrector procedure and investigate the necessity of iteration on the corrector as well as the stability of the scheme using various difference replacements for the slope of the boundary.

In the third method, the subsidence mound problem is formulated in polar coordinates as a stream function in the moving domain coupled to a non-linear equation for the boundary position. A coordinate transformation that maps the domain onto a quarter circle is employed. A finite difference scheme is set up for the stream function and a scheme similar to that for Methods 1 and 2 is used for moving the boundary.

In Chapter 3 heat transfer into the mound through the moving boundary is added in order to investigate the effect this has on the mobility of the fluid. The fluid viscosity is assumed to be dependent on temperature in a non-linear manner while density is assumed linearly

dependent on temperature in the bouyancy term only. This problem is formulated as an elliptic equation for a stream function coupled to a diffusion convection equation for the temperature and a hyperbolic equation for the propagation of the boundary. This problem is investigated in coordinate transformed domains similar to Methods 2 and 3 of Chapter 2, in both Cartesian and polar coordinates using finite differences.

Chapter 2 - A Subsidence Mound Problem

2.1 Introduction

The problem investigated in this chapter is the motion of a subsidence mound of saturated fluid spreading over an impervious surface in a porous medium as in Figure 1. This problem is of primary interest in groundwater hydrology where the motion of aquifers surfaces are to be determined. Apparently no work has appeared in the literature on this problem. Previous work has focussed on a different subsidence mound problem, where the decay of a mound in the groundwater surface as depicted in Figure 2 below, is of interest.

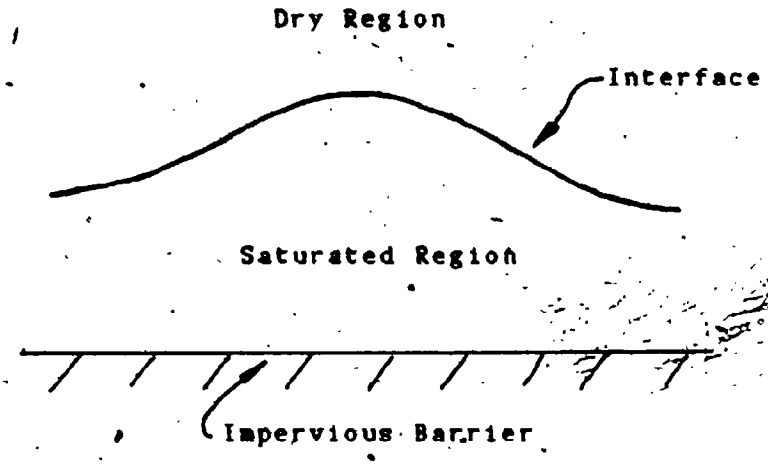

Figure 2 - Alternate Subsidence Mound Problem

Note that for the problem depicted in Figure 2, there is no contact between the interface and the impervious barrier and thus this problem is posed in an infinite or periodic domain. In the problem proposed in this thesis, in contrast, the interface contacts the impervious barrier and the domain is finite.

In this Chapter, a subsidence mound problem is formulated and solved using finite difference methods. A method which does not require iteration for calculating the new boundary position is developed. Additionally, a new similarity solution to the Dupuit approximation to this problem is presented and compared to the numerical solution to the full problem.

2.2 Equations for the Flow of Fluids Through a Porous Medium

The macroscopic equations for flow through a homogeneous and isotropic porous medium are given in Wooding (1957) as:

$$P \frac{\partial \rho}{\partial t} + \vec{\nabla} \cdot (\rho \vec{q}) = 0 \qquad (2.2.1)$$

$$\frac{1}{P} \frac{\partial \vec{q}}{\partial t} + \frac{1}{P^2} (\vec{q} \cdot \nabla) \vec{q} = -\nabla p + \rho \vec{g} - \frac{\mu}{k} \vec{q} \qquad (2.2.2)$$

where P is porosity, ρ is point density, μ is viscosity, k is permeability, $\vec{g}$ is a vector representing the force of gravity and $\vec{q}$ is the "seepage" velocity, that is, the volume of fluid passing through a unit area in a unit of time (i.e. $\vec{q} = P \vec{v}$ where $\vec{v}$ is the usual fluid velocity). Equation (2.2.1) is a statement of continuity for the fluid while equation (2.2.2) is a momentum balance. This is an extension of Darcy's Law, an empirical result established by Darcy in the mid 19'th century relating the quantity of fluid Q, of density ρ, passing down through a vertical column of porous material of cross-sectional area A and height h and the pressure differential Δp between the top and bottom of the column as follows:

$$Q = - \frac{k}{h} A (\Delta p + \rho g h) . \qquad (2.2.3)$$

where g is a constant representing the force of gravity and K is another constant (ref. Scheidegger(1974)). This relation is found to be applicable for liquids at low to moderate velocities and gases at moderate velocities.

For liquids of constant ρ and μ and porous media of constant k and P and at low velocities so that the inertial terms can be neglected, equations (2.2.1-2.2.2) become:

$$\vec{\nabla} \cdot \vec{q} = 0 \qquad (2.2.4)$$

$$\vec{q} = -\frac{k}{\mu} (\vec{\nabla} p - \rho \vec{g}) \qquad (2.2.5)$$

Since the curl of $\vec{q}$ vanishes we can introduce a potential,

$$\phi = \frac{k}{\mu} (p + \rho g z) \qquad (2.2.6)$$

where z is the vertical coordinate (elevation), such that:

$$\vec{q} = -\vec{\nabla} \phi \qquad (2.2.7)$$

Thus ϕ satisfies the Laplace equation:

$$\nabla^2 \phi = 0 \qquad (2.2.8)$$

The form of relations (2.2.1) and (2.2.5) may seem somewhat arbitrary, however similar equations have been derived by Whitaker (1977) by application of volume averaging to the usual hydrodynamic equations of fluid flow.

2.3 Boundary Conditions on the Moving Surface

The concept of a surface representing the division between the fully saturated region below and the dry region above is an idealization. In a typical groundwater situation there exists an intermediate region known as the capillary zone which may be several meters thick, where the moisture content decreases with elevation. In this zone capillary forces are greater than gravitational forces thereby holding some residual moisture in the pores. In the present thesis it is assumed that the thickness of this zone is much less than the characteristic length and that its effect is negligible.

It is assumed that for a two dimensional subsidence mound the equation of the moving surface in cartesian coordinates is:

$$z = f(x,t) \qquad (2.3.1)$$

On the moving surface two boundary conditions are required. The first is that the pressure is constant and equal to the atmospheric pressure. For convenience we take this to be:

$$p(x,f(x,t),t) = 0 \qquad (2.3.2)$$

or in terms of the potential

$$\phi(x, f(x,t), t) = \frac{k \rho g}{\mu} f(x,t) \qquad (2.3.3)$$

The second condition on the moving surface is the kinematic condition that particles of fluid on it remain there for all time. Taking the material derivative of (2.3.1) yields:

$$w = f_x u + f_t \quad \text{on } z = f(x,t) \qquad (2.3.4)$$

where u and w are the x and z components of the fluid velocity $\vec{v}$, respectively. Using the definition of the potential gives

$$f_t = \frac{1}{\rho} \left(f_x \phi_x + \phi_z \right)\Big|_{z=f} \qquad (2.3.5)$$

as the non-linear hyperbolic equation for moving the boundary. Finally since ϕ is known on the boundary, (2.3.3) can be differentiated with respect to x to obtain a relation between the derivatives of the potential on the boundary. That is,

$$\phi_x + \phi_z f_x = \frac{k \rho g f_x}{\mu} \quad \text{on} \quad z = f(x,t). \qquad (2.3.6)$$

This also gives a compatibility condition at the ends of the moving boundary. That is, if at one end, the moving boundary is in contact with a vertical impermeable barrier then:

$$\phi_x = 0 \qquad (2.3.7)$$

which implies (from (2.3.6))

$$\phi_x = \frac{k \rho g}{\mu} \quad \text{or} \quad f_x = 0 \qquad (2.3.8)$$

The first possibility is not physical since it would have the boundary moving down with a constant speed regardless of the rest of the problem. Thus the second condition must hold. Alternatively, if at one end, the moving boundary is in contact with a horizontal impermeable barrier then:

$$\phi_z = 0 \qquad (2.3.9)$$

which implies (from (2.3.6))

$$\phi_x = \frac{k \rho g f_x}{\mu} \qquad (2.3.10)$$

and thus:

$$f_e = \frac{k \rho g f_x^2}{P \mu} \qquad (2.3.11)$$

For the subsidence mound problem at hand, let the point at which the end of the moving boundary or toe, contacts the horizontal barrier be denoted by:

$$x = s(t) \tag{2.3.12}$$

Thus

$$f(s(t),t) = 0 \tag{2.3.13}$$

Differentiation with respect to time gives

$$f_t + f_x \dot{s} = 0 \tag{2.3.14}$$

Making use of (2.3.5) and (2.3.6) and noting that $\phi_x = 0$ at $x = s$ (since $w = 0$) yields the following equation for s:

$$\dot{s} = - \frac{f_t}{f_x} = - \frac{k \rho g f_x}{P \mu} \tag{2.3.15}$$

Clearly then, for the toe to be moving to the right, f_x must be negative there.

A final equation for this problem can be obtained from the conservation of mass of the fluid. That is,

$$\int_0^{s(t)} f(x,t)\,dx = \text{a constant} \qquad (2.3.16)$$

This relation will not be used explicitly in the numerical scheme since the information it contains is implicit in the continuity equation (2.2.4). It can, however, be used as a check on the numerical schemes adopted.

2.4 Statement of the Problem

The problem to be solved is depicted in Figure 3 below.

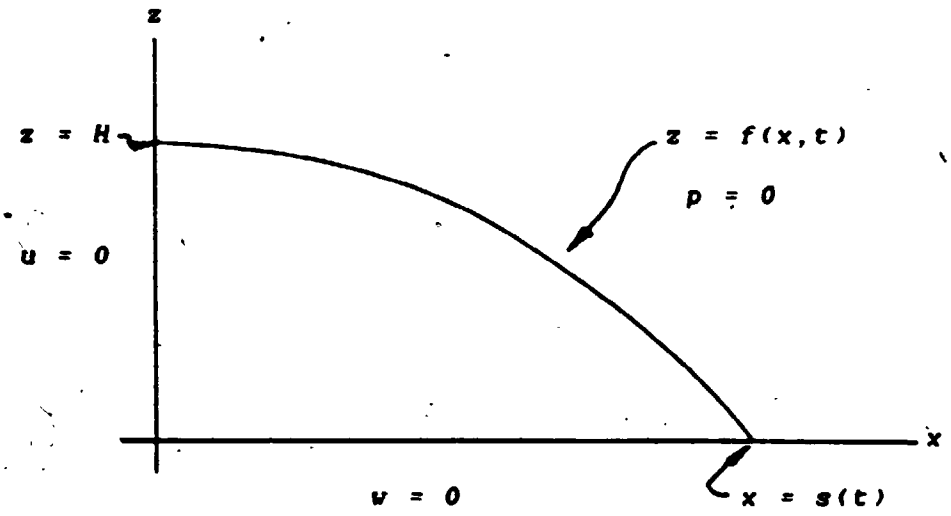

Figure 3 - The Subsidence Mound Problem as Formulated

Upon the introduction of the non-dimensional quantities

$$x' = \frac{x}{H} \ , \ z' = \frac{z}{H} \ , \ f' = \frac{f}{H} \ , \ s' = \frac{s}{H} \ ,$$

$$t' = \frac{k}{P} \frac{\rho g}{H \mu} t \ , \ p' = \frac{p}{\rho g H} \ , \ \vec{q}' = \frac{\mu P}{k \rho g} \vec{q} \ , \qquad (2.4.1)$$

and $\phi' = p' + z'$

where H is the initial height of the mound at the central line of symmetry, the field equation becomes (dropping the primes):

$$\nabla^2 \phi = 0 \qquad (2.4.2)$$

The new boundary conditions are:

$$\left.\begin{aligned} &\text{on } z = 0,\ \phi_z = 0, \\ &\text{on } x = 0,\ \phi_x = 0, \\ &\text{on } z = f(x,t),\ \phi = f \text{ and} \\ &\qquad f_t = f_x \phi_x - \phi_z = f_x^2 (1 - \phi_z) - \phi_z \end{aligned}\right\} \qquad (2.4.3)$$

with $f_x(0,t) = 0$ (symmetric mound)

and $f(s(t),t) = 0$,

and finally on $x = s(t)$, $\dot{s} = - f_x$

The initial conditions are:

$$f(x,0) \text{ and } s(0) \text{ given} \qquad (2.4.4)$$

Note that in the above formulation, no account of the actual microscopic physics of the situation along the moving surface and especially at its toe has been taken. Thus the complicated three phase interface which exists there is not modelled as such. Rather, the boundary

conditions used are merely those that are natural for the macroscopic model. That is, the macroscopic model implies that the flow is potential flow with no velocity across the impermeable barrier below and the potential equal to the elevation on the moving surface. The compatibility of the boundary conditions at the toe gives the relation between the speed of the toe and the slope of the moving surface there. This method of deriving boundary conditions based on the macroscopic model only is well accepted in groundwater flow problems, as in for example the seepage dam problem.

2.5 Review of Previous Work

Unsteady porous flow problems with a pheatic surface (moving surface of constant pressure) are discussed in texts on porous flow such as Bear (1972). After noting the difficulties in the analytic treatment of the problem, the Dupuit approximation is invoked. Under this approximation the flow is assumed to be essentially horizontal, that is the equipotentials are assumed to be vertical and the slope of the water table small. The continuity equation for this theory which is called the Boussinesq or porous media equation in two dimensions is:

$$\frac{\partial h}{\partial t} = \frac{\partial}{\partial x}\left(h \frac{\partial h}{\partial x}\right) \qquad (2.5.1)$$

where $z = h(x,t)$ is the equation of the pheatic surface and the saturated region is bounded below by a horizontal impervious barrier.

Many unsteady as well as steady problems including those with recharge and wells have been solved using this approximation. In fact, considerable effort has been expended to find efficient and accurate numerical schemes for Stefan problems like equation (2.5.1) on $0 < x < s(t)$ coupled to boundary conditions (2.3.12)-(2.3.14) (see for example Gurtin, MacCamy and Socolovski (1984) or Meek and Norbury (1984)).

Numerical methods have been used to directly tackle unsteady porous flow problems with a moving surface. Finite difference techniques were used by Todsen (1971) to solve ditch drainage and earth dam problems with accretion (water influx from above along the moving suface). A regular grid with interpolation along the boundary was used to solve the potential problem along with a second order accurate leap-frog scheme for calculating boundary motion. Smoothing was used to eliminate oscillations in the boundary motion. Guvanasen and Volker (1980) compare a finite difference scheme and three finite element schemes as well as experimental results for a drainage ditch problem with recharge. For their finite difference scheme they usé an explicit Euler method to move the boundary and found this to be inferior to a finite element approach which implicitly moved the boundary. Furthermore, they conclude that the smoothing applied by Todsen to improve stability resulted in greater deviation from the experimental results.

Rasmussen and Salhani (1981) examine a subsidence mound problem as in Figure 2, but with recharge and pumping. They compare three different methods, Rayleigh-Ritz, Kantorovich and finite differences with a coordinate transformation, for the variational formulation of the potential problem. A Crank-Nicolson scheme with iteration

was used to move the boundary. They found that satisfactory results could be obtained by all three methods and that the finite difference solution scheme for the coordinate transformed variational formulation (which results in a diagonally dominant system of linear equations) although more costly in terms of computing time was the recommended method.

To summarise, there are two major issues in the construction of a numerical scheme for these transient porous flow problems. The first is which method to choose for a potential problem that has a non-uniform domain. The wide variety of methods used in the past indicates that this choice is not that critical. The method for solving the resulting system of linear equations appears to be a greater factor in the outcome in terms of computational time. The second is which method to use for computing new boundary positions. Due to the non-linearity and the inability to write the boundary equations in a conservative form, appealing schemes such as those for the porous media equation are not applicable. Hence the schemes employed were apparently chosen for simplicity rather than analytic appeal. For this problem the consensus appears to be that implicit schemes are superior to explicit schemes and that finite difference schemes are effective.

2.6 A Similarity Solution of the Boussinesq Equation

As discussed in the previous section, if the Dupuit approximation is made the subsidence mound problem becomes:

$$h_t = (h\, h_x)_x \qquad \text{on} \quad 0 < x < s(t) \qquad (2.6.1a)$$

with $h_x(0,t) = 0$ and (2.6.1b)

$$h(s(t),t) = 0 \quad \text{and} \qquad (2.6.1c)$$

$$s'(t) = \frac{h_x(s(t),t)}{h_x(s(t),t)} \qquad (2.6.1d)$$

The following derivation of a similarity solution to the above one dimensional Stefan problem is similar to that in Meek and Norbury (1984) for a viscous fluid spreading over a horizontal flat plate.

Upon definition of the similarity variable

$$u = \frac{x}{t^b} \qquad (2.6.2)$$

and substitution of the trial solution

$$h(x,t) = t^c\, g(u) \quad \text{and} \quad s(t) = a\, t^d \qquad (2.6.3)$$

into (2.6.1a) one obtains:

$$ct^{c-1}g(u) - bt^{c-1}u\,g'(u) = t^{2(c-b)}g^{-2}(u) + t^{2(c-b)}g(u)g''(u) \qquad (2.6.4)$$

Clearly for a similarity solution to exist

$$c - 1 = 2(c-b) \text{ or } c = 2b - 1 \qquad (2.6.5)$$

In order for the boundary condition (2.6.1c) to be fixed at $x = s(t)$ for $g(u)$

$$u = \frac{s(t)}{t^b} = a\,t^{d-b} = \text{constant} \qquad (2.6.6)$$

which implies that

$$d = b \qquad (2.6.7)$$

Furthermore substitution into (2.6.1b)-(2.6.1d) yields:

$$g'(0) = 0 \quad \text{and} \quad g(a) = 0 \qquad (2.6.8)$$

Thus the problem for $g(u)$ is:

$$(2b-1)\, g(u) - b\, u\, g'(u) - g'^{2}(u) + g(u)\, g''(u) = 0 \qquad (2.6.9)$$

subject to the boundary conditions (2.6.8) above.

One solution to (2.6.9) is of the form

$$g(u) = \frac{1}{6}\,(A - u^{2}) \qquad (2.6.10)$$

when $b = \frac{1}{3}$ and where A is a parameter. Finally upon substitution into boundary conditions (2.6.8) obtains

$$A = a^{2} \qquad (2.6.11)$$

Thus a similarity solution to (2.6.1) is

$$\left.\begin{aligned} h(x,t) &= \frac{1}{6\, t^{1/3}}\left(a^{2} - \frac{x^{2}}{t^{2/3}}\right) \\ s(t) &= a\, t^{1/3} \end{aligned}\right\} \qquad (2.6.12)$$

with parameter a which can be used to match a parabolic initial profile and change the time origin so as to avoid the singulatity at $t = 0$. Note that an initially parabolic water table remains parabolic for all time and that fluid is conserved since

$$\int_0^{s(t)} h(x,t)\,dx = \frac{a^2}{9} \qquad (2.6.13)$$

This similarity solution to the Dupuit approximation to the problem is used later to compare to the numerical results for the full problem to get a quantitative estimate of the error induced by this widely used approximation.

2.7 Numerical Method

2.7.1 The Potential Problem

Three different finite difference approaches are taken to the potential problem. In the first, the x coordinate is transformed so that the leading edge of the toe is stationary in time, while in the second, the entire domain is fixed by applying a coordinate transformation to both x and z. In the third method the problem is reformulated in polar coordinates in terms of a stream function and a coordinate transformation fixing the entire domain is applied.

For Method 1 let

$$\xi = \frac{x}{s(t)} \quad , \quad \eta = z, \text{ and } \tau = t \qquad (2.7.1)$$

Then the transformed problem (2.4.2-2.4.4) becomes:

$$\phi_{\xi\xi} + s^2 \phi_{\eta\eta} = 0 \qquad (2.7.2a)$$

with $\phi_\xi = 0$ on $\xi = 0$,

$\phi_\eta = 0$ on $\eta = 0$, } (2.7.2b)

$\phi = f$ and

$$f_\tau = \frac{f_\xi}{s}\left(\frac{f_\xi}{s} - \frac{\xi\, f_\xi(1,\tau)}{s}\right) - \phi_\eta\left[1 + \left(\frac{f_\xi}{s}\right)^2\right]$$

on $\eta = f(\xi,\tau)$

with $f_\xi(0,\tau) = 0$ and $f(1,\tau) = 0$

and finally $\dot{s} = -\frac{f_\xi(1,\tau)}{s}$.

Note that the toe is fixed in time at $\xi = 1$ (see Figure 4 below).

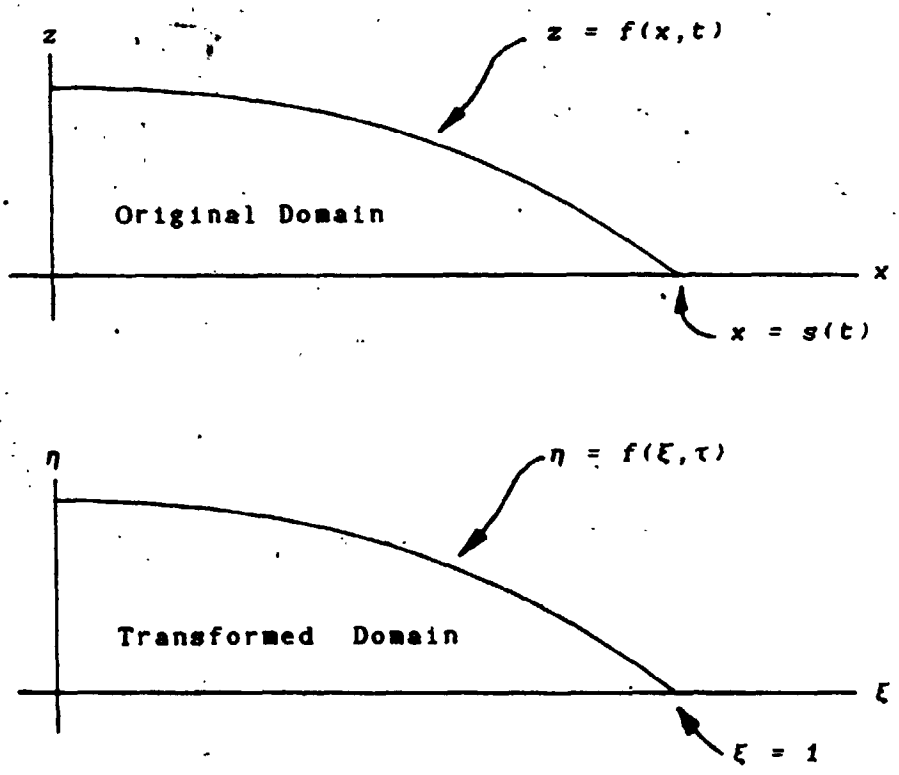

Figure 4 - The Original and Transformed Domains for Method 1

Employing a regular rectangular finite difference grid where subscripts l, j and superscript n denote a quantity evaluated at grid point $\xi_l = (l-1)h$, $\eta_j = (j-1)k$, and $\tau^n = \Delta\tau\, n$

yields the difference equation:

$$\left.\begin{aligned} & C^n_{0_{l,j}}\,\phi^n_{l,j} - C^n_{1_{l,j}}\,\phi^n_{l+1,j} - C^n_{2_{l,j}}\,\phi^n_{l,j+1} \\ & - C^n_{3_{l,j}}\,\phi^n_{l-1,j} - C^n_{4_{l,j}}\,\phi^n_{l,j-1} = RHS^n_{l,j} \end{aligned}\right\} \quad (2.7.3)$$

$$l = 1,2,\ldots,M \text{ and } j = 1,2,\ldots,NROWS_l$$

For grid points $l = 1,2,\ldots,M$ and $j = 1,2,\ldots,NROWS_l - 1$, where $NROWS_l$ = integer part of $\left\{ \frac{f_l}{k} \right\}$ and where the five point operator depicted in Figure 5 is used with $h = \frac{1}{M}$ and $k = \frac{1}{N}$. The coefficients are:

$$\left.\begin{aligned} & C^n_{0_{l,j}} = 2\left[\,1 + \left(\frac{s^n h}{k}\right)^2\,\right] \\ & C^n_{1_{l,j}} = C^n_{3_{l,j}} = +1 \\ & C^n_{2_{l,j}} = C^n_{4_{l,j}} = \left(\frac{s^n h}{k}\right)^2 \\ & RHS^n_{l,j} = 0 \end{aligned}\right\} \quad (2.7.4)$$

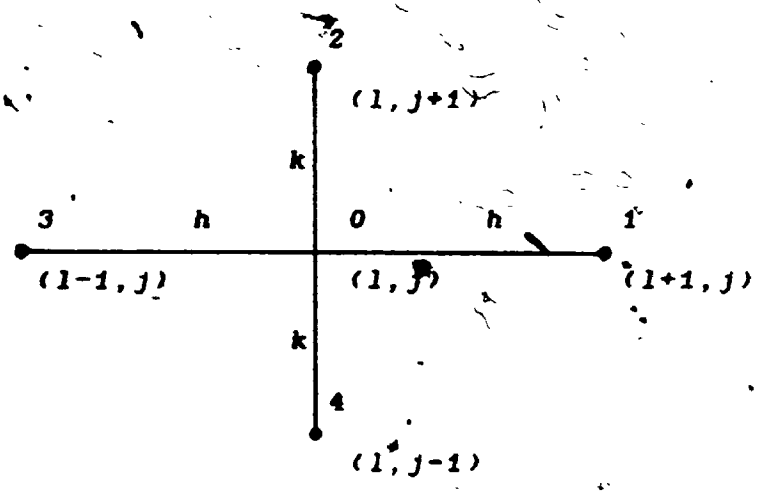

Figure 5 - Five Point Difference Molecule at an Interior Grid Point

For grid points adjacent to the moving boundary as in Figure 6 (i.e. $l = 1,2,\ldots M$ and $j = NROWS_1$) the coefficients are:

$$C_{0_{1,j}}^{n} = 2\left[\frac{1}{S_1} + \frac{1}{S_2}\left(\frac{s^n h}{k}\right)^2\right]$$

$$C_{1_{1,j}}^{n} = C_{2_{1,j}}^{n} = 0$$

$$C_{3_{1,j}}^{n} = \frac{2}{(S_2+1)} \qquad \left.\begin{array}{l}\\ \\ \\ \end{array}\right\} \quad (2.7.5)$$

$$C_{4_{1,j}}^{n} = \frac{2(s^n h)^2}{(S_2+1)k^2}$$

$$RHS_{1,j}^{n} = \frac{2}{(S_1+1)S_1}\eta_j + \frac{2(s^n h)^2}{(S_2+1)S_2 k^2} f_1$$

where S_1 and S_2 are calculated from the f_i as follows:

$$S_2 = \frac{(f_2 - \eta_2)}{k} \quad , \quad S_1 = \frac{(f_2 - \eta_2)}{(f_2 - f_{2-1})} \qquad (2.7.6)$$

and where $j = NROWS_1$.

Note that potential corresponding to point 1 of the difference molecule has been estimated using linear interpolation and that both it and the known potential (i.e. the height f_2) have been incorporated into the right hand side.

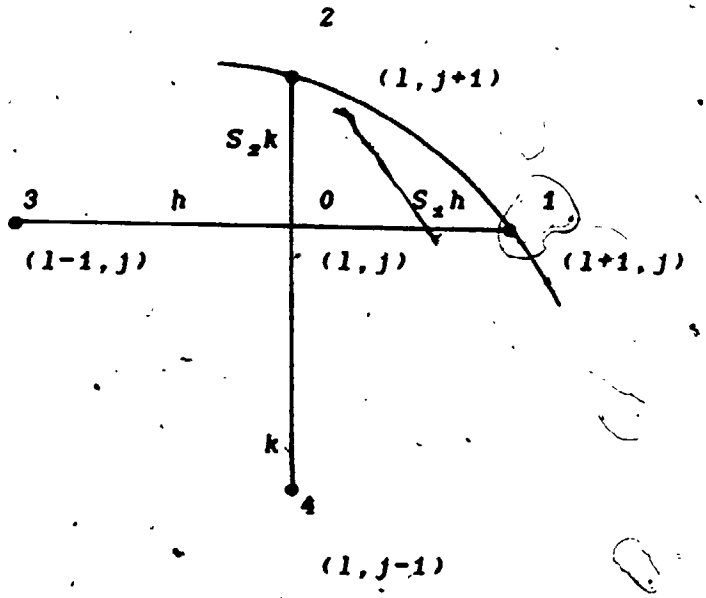

Figure 6 - Five Point Difference Molecule at a Grid Point Adjacent to the Boundary

In order to avoid situations where S_2 is extremely small, which may result in numerical errors during the solution of the linear system of equations for the potential, the corresponding difference molecule is not used when S_2 is less than a cutoff value (say 10^{-3}). Instead the top arm of the molecule below is extended up to the moving surface and the coefficients of this molecule are modified accordingly.

The boundary conditions along $\xi = 0$ and $\eta = 0$ are incorporated by using the difference equation (2.7.3) on these boundaries and eliminating the fictitious points outside the region using

$$\phi^n_{0,j} = \phi^n_{2,j} \quad \text{and} \quad \phi^n_{1,0} = \phi^n_{1,2} \qquad (2.7.7)$$

$$j = 1,2,\ldots,NROWS_1 \quad \text{and} \quad l = 1,2,\ldots,M$$

Note that the above difference equations (2.7.3) have a local trunction error of $\bar{O}(s^2 h^2 + k^2)$ assuming that the boundary position (i.e. the f_i's) is known exactly. The local truncation error at grid points adjacent to the boundary drops to $O(s h + k)$.

Clearly the system of linear equations described

above has non-negative coefficients $C^n_{k_{i,j}}$ and is diagonally dominant and hence satisfies a maximum principle since

$$C^n_{o_{i,j}} \geq \sum_{k=1}^{4} C^n_{k_{i,j}} \qquad (2.7.8)$$

with the strict inequality holding when one of the grid points lies on the moving boundary in which case the associated known potential enters into the right hand side. This property is important for two reasons. First, since the partial differential equation that is being modelled is elliptic and therefore satisfies the maximum principle it is desireable that the numerical scheme retain this property. Of even greater importance is that for approximating Laplace's equation this property can be used to infer an estimate of global error and thereby convergence of the finite difference method. Since the difference scheme corresponds to solving Laplace's equation on a rectangular grid of spacing sk by h and the following conditions are satisfied (assuming $sh = O(k)$):

(1) the boundary conditions are approximated with an error not exceeding $O(k^2)$

(2) the local truncation error of difference replacements at grid points adjacent to the boundary is at least $O(k)$

(3) the local truncation error at other grid points is at least $O(k^2)$

(4) the derivatives of ϕ up to the fourth order exist and are bounded in the region (this is assumed)

Then the global error between the exact solution of Laplace's equation and the numerical solution is $O(k^2)$ (Mitchel and Griffiths (1980)). Note that although condition (4) is assumed to hold this does not seem unreasonable if the boundary shape is smooth.

For Method 2 let

$$\xi = \frac{x}{s(t)} \quad , \quad \eta = \frac{y}{f(x,t)} \quad \text{and} \quad \tau = t \qquad (2.7.9)$$

The transformed problem (2.S.1) becomes:

$$\phi_{\xi\xi} - \frac{2\eta f}{f}\,\phi_{\xi\eta} + \frac{(s^2 + \eta^2 f_\xi^2)}{f^2}\,\phi_{\eta\eta}$$

$$- \frac{\eta\,(f\,f_{\xi\xi} - 2\,f_\xi^2)}{f^2}\,\phi_\eta = 0$$

with $\phi_\xi = 0$ on $\xi = 0$,

$$\left.\begin{array}{l} \phi_\eta = 0 \quad \text{on} \quad \eta = 0, \\ \phi = f \quad \text{and} \end{array}\right\} \qquad (2.7.10)$$

$$f_\tau = \frac{f_\xi}{s}\left(\frac{f_\xi}{s} - \frac{\xi\, f_\xi(1,\tau)}{s}\right) - \frac{\phi_\eta}{f}\left[1 + \left(\frac{f_\xi}{s}\right)^2\right]$$

on $\eta = 1$ and with $f_\tau(0,\tau) = 0$ and $f(1,\tau) = 0$

and finally $\dot{s} = -\frac{f_\xi(1,\tau)}{s}$

This transformation fixes the entire moving boundary at $\eta = 1$ as shown in Figure 7 below.

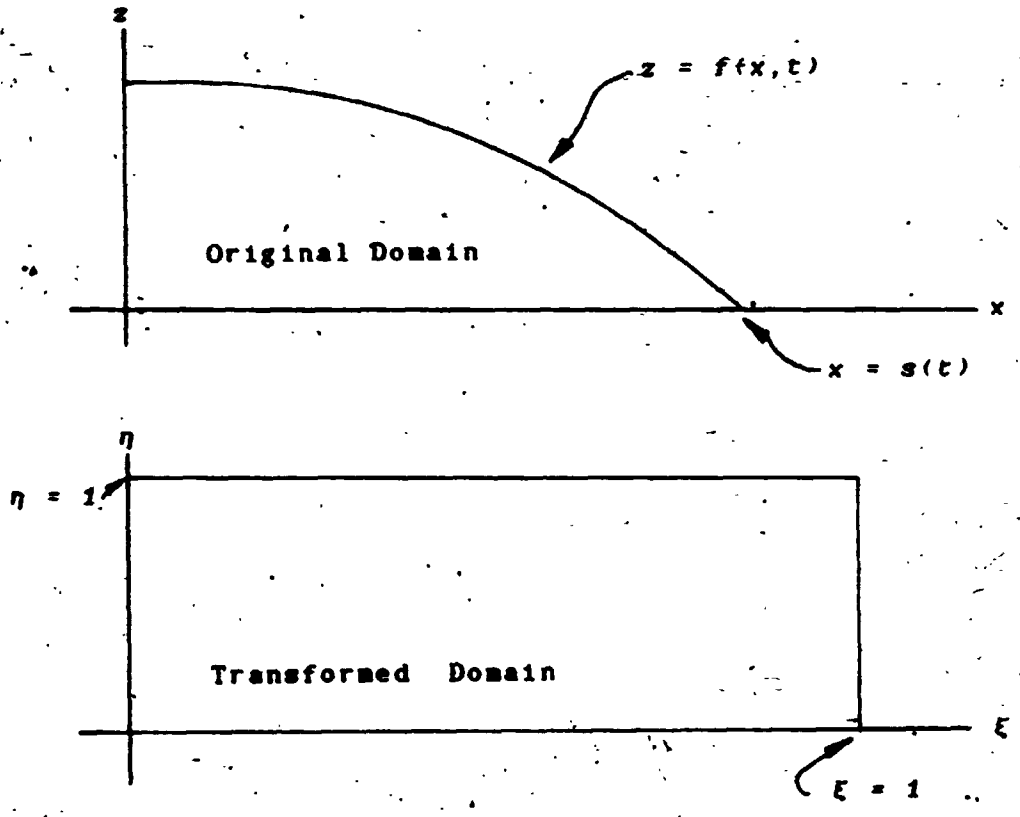

Figure 7 - The Original and Transformed Domains for Method 2

Using the regular finite difference mesh as before but using the nine point opperator as in Figure 8 leads to the difference equation:

$$C_{0_{i,j}}^{n} \phi_{i,j}^{n} - C_{1_{i,j}}^{n} \phi_{i-1,j}^{n} - C_{2_{i,j}}^{n} \phi_{i,j-1}^{n}$$

$$- C_{3_{i,j}}^{n} \phi_{i-1,j}^{n} - C_{4_{i,j}}^{n} \phi_{i,j-1}^{n} - C_{5_{i,j}}^{n} \phi_{i-1,j-1}^{n}$$

$$- C_{6_{i,j}}^{n} \phi_{i-1,j-1}^{n} - C_{7_{i,j}}^{n} \phi_{i-1,j-1}^{n} - C_{8_{i,j}}^{n} \phi_{i-1,j-1}^{n}$$

$$= RHS_{i,j}^{n} \qquad (2.7.11)$$

for $i = 1,2,\ldots,M$ and $j = 1,2,\ldots,N$

where the coefficients for the interior are evaluated as follows:

$$C_{0_{i,j}}^{n} = 2 \left(A_{i,j}^{n} + C_{i,j}^{n} + 2 B_{i,j}^{n} \left(\alpha_{2_{i,j}}^{n} - \alpha_{1_{i,j}}^{n} \right) \right)$$

$$C_{1_{i,j}}^{n} = C_{3_{i,j}}^{n} = A_{i,j}^{n} + 2 B_{i,j}^{n} \left(\alpha_{2_{i,j}}^{n} - \alpha_{1_{i,j}}^{n} \right)$$

$$C_{2_{i,j}}^{n} = C_{i,j}^{n} + 2 B_{i,j}^{n} \left(\alpha_{2_{i,j}}^{n} - \alpha_{1_{i,j}}^{n} \right) + D_{i,j}^{n}$$

$$C_{4_{i,j}}^{n} = C_{i,j}^{n} + 2 B_{i,j}^{n} \left(\alpha_{2_{i,j}}^{n} - \alpha_{1_{i,j}}^{n} \right) - D_{i,j}^{n}$$

$$C_{8_{i,j}}^{n} = C_{7_{i,j}}^{n} = 2 B_{i,j}^{n} \alpha_{1_{i,j}}^{n} \qquad (2.7.12)$$

$$C^n_{\alpha_{1,j}} = C^n_{\beta_{1,j}} = -2\, B^n_{1,j}\, \alpha^n_{2_{1,j}}$$

$$RHS^n_{1,j} = 0$$

where

$$A^n_{1,j} = 1$$

$$\left.\begin{aligned} B^n_{1,j} &= \frac{-\eta_j\left(f^n_{i+1} - f^n_{i-1}\right)}{2\,k\,f^n_i} \\ C^n_{1,j} &= \frac{(s^n h)^2 + \left(\eta_j\left(f^n_{i+1} - f^n_{i-1}\right)/2\right)^2}{(f^n_i k)^2} \\ D^n_{1,j} &= \frac{-\eta_j\left(f^n_i\left(f^n_{i+1} - 2f^n_i + f^n_{i-1}\right) - \left(f^n_{i+1} - f^n_{i-1}\right)^2/2\right)}{2\,k\,(f^n_i)^2} \end{aligned}\right\} \quad (2.7.13)$$

$$\left.\begin{aligned} \alpha^n_{1_{1,j}} &= \begin{cases} \frac{1}{2} & \text{if } B^n_{1,j} > 0 \\ 0 & \text{otherwise} \end{cases} \\ \alpha^n_{2_{1,j}} &= \begin{cases} \frac{1}{2} & \text{if } B^n_{1,j} < 0 \\ 0 & \text{otherwise} \end{cases} \end{aligned}\right\} \quad (2.7.14)$$

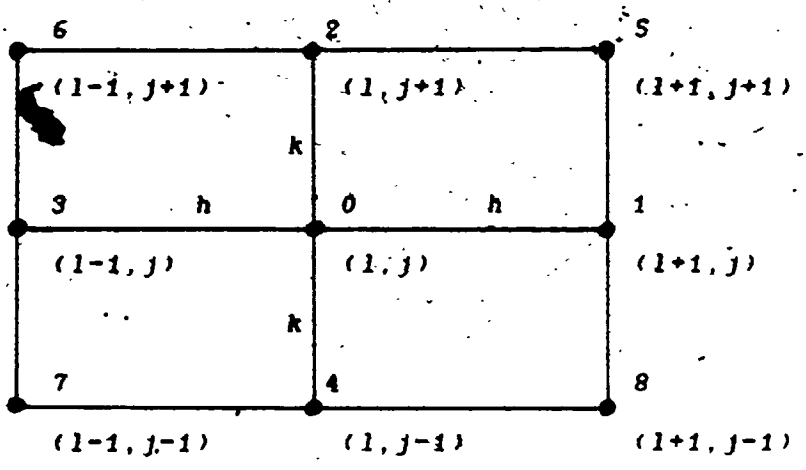

Figure 8 — Nine Point Difference Molecule

Again the difference equation is assumed to hold on the boundaries $\xi = 0$ and $\eta = 0$ where the fictitious points outside the region are eliminated using

$$\phi_{0,j} = \phi_{2,j}, \quad \phi_{1,0} = \phi_{1,2} \quad \text{and} \quad \phi_{0,0} = \phi_{2,2} \qquad (2.7.15)$$

and where second order one sided differences are used for the derivatives of f in the calculation of A, B, C and D. In addition for points adjacent to the moving boundary the known potentials on the moving boundary (i.e. f_1) are incorporated into the right hand side.

Note that the above difference equations have a local truncation error of $O(h^2 + k^2)$.

With the choice of the parameters α_1 and α_2 as above, which is required so that the coefficients $C^n_{5_{i,j}}$, $C^n_{6_{i,j}}$, $C^n_{7_{i,j}}$ and $C^n_{8_{i,j}}$ be non-negative, it is still not possible to guarantee the non-negativeness of the remaining coefficients of the linear system for the potential (see Appendix I). Thus the maximum principle is not necessarily satisfied by the numerical solution and hence in this case the global error cannot be easily evaluated and thus convergence is not guaranteed. Numerical convergence can be investigated and convergence inferred by comparing to the results of Method 1.

It is clear that this problem can also be mapped onto a quarter circle using a polar coordinate formulation. Unfortunately, solving Laplace's equation in a quarter circle gives a less accurate numerical solution when using finite differences based on polar coordinates than rectangular coordinates for an equivalent number of grid points (Mitchel and Griffith (1980)). However, as the results presented later indicate, the numerical method adopted for advancing the boundary is more robust in a polar coordinate formulation and this method is presented here. Additionally the problem is reformulated in terms of a stream function, providing another independent verification of the numerical results.

Let the moving boundary be denoted by:

$$r = R(\phi, t) \tag{2.7.16}$$

where r and ϕ are the radial distance from the origin and the angle measured counter clockwise from the x axis in the (x,z) plane respectively. Upon the introduction of a stream function Ψ such that

$$\begin{cases} \Psi_x = -\phi_z = w \\ \Psi_z = \phi_x = -u \end{cases} \quad \text{or} \quad \begin{cases} \frac{1}{r}\Psi_\phi = \phi_r \\ \Psi_r = -\frac{1}{r}\phi_\phi \end{cases} \tag{2.7.17}$$

the non-dimensional problem (2.4.2-2.4.4) becomes:

$$\frac{1}{r}\frac{\partial}{\partial r}\left(r\Psi_r\right) + \frac{1}{r^2}\Psi_{\phi\phi} = 0$$

with $\Psi = 0$ on $\phi = 0$, $\phi = \frac{\pi}{2}$ and $r = 0$

and on $r = R(\phi, t)$ $\Bigg\}$ (2.7.18)

$$-R\Psi_r + \frac{R_\phi}{R}\Psi_\phi = R_\phi \sin(\phi) + R\cos(\phi)$$

$$\text{and } R_\phi = -\left(\frac{R_\phi}{R}\Psi_r + \frac{1}{R}\Psi_\phi\right)$$

$$\text{with } R_\phi\left(\frac{\pi}{2}, t\right) = 0$$

Application of the coordinate transformation:

$$\xi = \phi \quad , \quad \eta = \frac{r}{R(\phi, t)} \quad \text{and} \quad \tau = t \qquad (2.7.19)$$

which fixes the moving boundary at $\eta = 1$ as shown in Figure 9 below, yields the transformed problem:

$$(1 + \sigma^2)\, \eta \frac{\partial}{\partial \eta} (\eta \Psi_\eta) - 2 \eta \sigma \Psi_{\eta\xi} + \Psi_{\xi\xi} - \frac{\partial \sigma}{\partial \xi} \Psi_\eta = 0$$

with $\Psi = 0$ on $\xi = 0$, $\xi = \frac{\pi}{2}$ and $\eta = 0$

and on $\eta = 1$

$$\left.\begin{aligned} & \\ \sigma \Psi_\xi - (1 + \sigma^2) \Psi_\eta = R_\tau \sin(\xi) + R \cos(\xi) & \end{aligned}\right\} (2.7.20)$$

and $R_\tau = -\frac{1}{R} \Psi_\xi$ with $R_\tau (\frac{\pi}{2}, \tau) = 0$

where $\sigma = \frac{R_\xi}{R}$

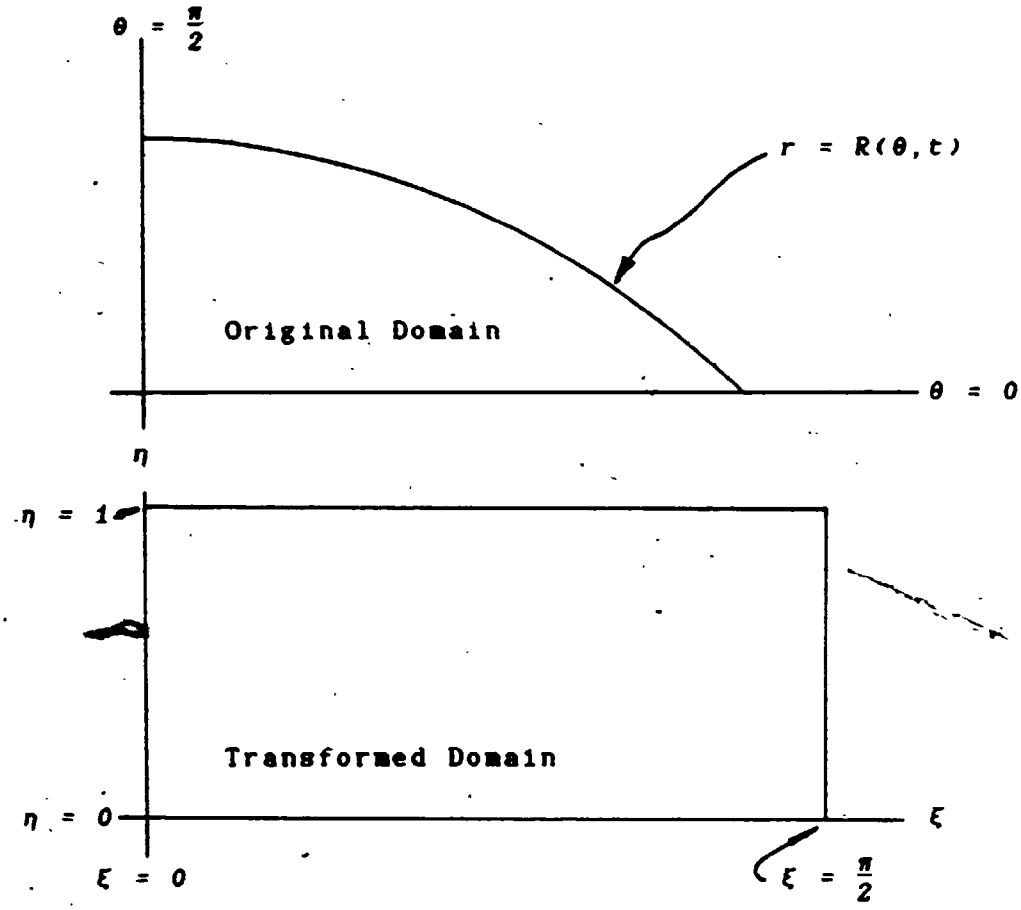

Figure 9 - The Original and Transformed Domains for Method 3

Employing a regular rectangular finite difference grid and a nine point difference operator, as before, except that

$$h = \frac{2}{\pi M} \tag{2.7.21}$$

yields the following equation for the stream function:

$$C^n_{0_{i,j}} \psi^n_{i,j} - C^n_{1_{i,j}} \psi^n_{i+1,j} - C^n_{2_{i,j}} \psi^n_{i,j+1}$$

$$- C^n_{3_{i,j}} \psi^n_{i-1,j} - C^n_{4_{i,j}} \psi^n_{i,j-1} - C^n_{5_{i,j}} \psi^n_{i+1,j+1}$$

$$- C^n_{6_{i,j}} \psi^n_{i-1,j+1} - C^n_{7_{i,j}} \psi^n_{i-1,j-1} - C^n_{8_{i,j}} \psi^n_{i+1,j-1}$$

$$= RHS^n_{i,j} \qquad (2.7.22)$$

for $i = 2,3,\ldots,M$ and $j = 2,3,\ldots,N$

where for interior grid points

$$C^n_{0_{i,j}} = 2 \left(A^n_{i,j} + \eta_j C^n_{i,j} + 2 B^n_{i,j} \left(\alpha^n_{2_{i,j}} - \alpha^n_{1_{i,j}} \right) \right)$$

$$C^n_{1_{i,j}} = C^n_{3_{i,j}} = A^n_{i,j} + 2 B^n_{i,j} \left(\alpha^n_{2_{i,j}} - \alpha^n_{1_{i,j}} \right)$$

$$C^n_{2_{i,j}} = \eta_{j+1/2} C^n_{i,j} + 2 B^n_{i,j} \left(\alpha^n_{2_{i,j}} - \alpha^n_{1_{i,j}} \right) + D^n_{i,j}$$

$$C^n_{4_{i,j}} = \eta_{j-1/2} C^n_{i,j} + 2 B^n_{i,j} \left(\alpha^n_{2_{i,j}} - \alpha^n_{1_{i,j}} \right) - D^n_{i,j}$$

$$C^n_{5_{i,j}} = C^n_{7_{i,j}} = 2 B^n_{i,j} \alpha^n_{1_{i,j}} \qquad (2.7.23)$$

$$C^n_{6_{i,j}} = C^n_{8_{i,j}} = - 2 B^n_{i,j} \alpha^n_{2_{i,j}}$$

$$RHS^n_{i,j} = 0$$

where

$$A^n_{i,j} = 1$$

$$B^n_{i,j} = \frac{-\eta_i}{4}\left(\Sigma^n_{i+1/2} + \Sigma^n_{i-1/2} \right)$$

$$C^n_{i,j} = \eta_j \left(\frac{h}{k} \right)^2 \left(1 + \frac{1}{2} \left(\left(\Sigma^n_{i+1/2} \right)^2 + \left(\Sigma^n_{i-1/2} \right)^2 \right) \right) \qquad (2.7.24)$$

$$D^n_{i,j} = \frac{-\eta_i}{2}\left(\frac{h}{k} \right)\left(\Sigma^n_{i+1/2} - \Sigma^n_{i-1/2} \right)$$

$$\alpha^n_{1\,i,j} = \begin{cases} \frac{1}{2} & \text{if } B^n_{i,j} > 0 \\ 0 & \text{otherwise} \end{cases}$$

$$\qquad (2.7.25)$$

$$\alpha^n_{2\,i,j} = \begin{cases} \frac{1}{2} & \text{if } B^n_{i,j} < 0 \\ 0 & \text{otherwise} \end{cases}$$

$$\left.\begin{aligned} \text{and } \Sigma^n_{i+1/2} &= \frac{2\left(R^n_{i+1} - R^n_i \right)}{h\left(R^n_{i+1} + R^n_i \right)} \\ \Sigma^n_{i-1/2} &= \frac{2\left(R^n_i - R^n_{i-1} \right)}{h\left(R^n_i + R^n_{i-1} \right)} \end{aligned}\right\} \qquad (2.7.26)$$

The above differencing is somewhat different than the standard central differencing employed in Method 2 but is similar to that suggested by Strikwerda and Geer (1980) for their jet problem, and is found to more accurately conserve mass.

The difference equation (2.7.22) is used for all points inside the region and the boundary condition on $\eta = 1$ is discretized as follows in order to form a complete system for the unknown stream function values:

$$- B^n_{i,N+1} \left(\psi^n_{i+1,N+1} - \psi^n_{i-1,N+1} \right)$$

$$- C^n_{i,N+1} \left(3\,\psi^n_{i,N+1} - 4\,\psi^n_{i,N} + \psi^n_{i,N-1} \right)$$

$$= R^n_i \, B^n_{i,N+1} \sin(E_i) + R^n_i \cos(E_i) \qquad (2.7.27)$$

for $i = 2,3,\ldots,M$

Note that due to the boundary conditions

$$\psi^n_{i,j} = \psi^n_{M+1,j} = 0 \quad \text{for } j = 1,2,\ldots,N+1$$

$$\psi^n_{i,1} = 0 \qquad \text{for } i = 2,3,\ldots,M$$

Also, note that the local truncation error of the above difference equations is $O(h^2 + k^2)$.

2.7.2 The Movement of the Boundary

As has already been discussed, the difficulty in formulating a numerical scheme for the boundary equations stems from the inability to write them in a conservative form. As a result, simple implicit schemes were used. To discuss these, the formulation of finite difference schemes for time dependent problems is briefly reviewed.

Numerical schemes for time dependent partial differential equations are usually formulated by separate temporal and spacial discretization. The resulting scheme is then analyzed for stability and convergence (if possible). For the time discretization, numerical schemes for ordinary differential equation are typically adapted. Two classes of such finite difference methods are the linear multistep and the one-leg multistep. For the model ordinary differential equation

$$u_t = F(u,t) \tag{2.7.28}$$

the linear k-step method gives:

$$\rho(E)\, u^n = \Delta t\, \sigma(E)\, F(u^n, t^n) \tag{2.7.29}$$

while the one-leg k-step method gives:

$$\rho(E)\, u^n = \Delta t\, F(\sigma(E)u^n, \sigma(E)t^n) \qquad (2.7.30)$$

where $\rho(E)$ and $\sigma(E)$ are polynomials of degree less than or equal to k in the shift operator E defined as

$$E\, u^n = u^{n+1} - u^n \qquad (2.7.31)$$

For linear problems both the above methods give the same numerical scheme, however for non-linear problems the linear stability analysis is much simpler using the second scheme. The only one step methods which are second order accurate in time are the Trapezoidal formula

$$u^{n+1} - u^n = \frac{\Delta t}{2} \left(F(u^{n+1}, t^{n+1}) + F(u^n, t^n) \right) \qquad (2.7.32)$$

and the Implicit mid-point rule

$$u^{n+1} - u^n = \Delta t\, F\left(\frac{u^{n+1} + u^n}{2}, \frac{t^{n+1} + t^n}{2} \right) \qquad (2.7.33)$$

both of which have been called Crank-Nicolson when applied to partial differential equations with central differencing used for the spatial derivatives.

Rasmussen and Salhani (1981) used central differences for the boundary slope and the trapezoidal formula above to move the boundary of their subsidence mound problem. This scheme required iteration since the calculation of

derivatives of the potential at the advanced time requires the knowledge of the boundary positions at that time.

Loh (1985) also used central differences for the slope of the boundary but used the implicit midpoint formulation to move the position of a large amplitude surface wave in viscous incompressible flow. Again iteration was required since the calculation of fluid velocities on the moving surface at the advanced time required the knowledge of the surface location at that time.

Let the boundary equations in either of the first two tranformed schemes ((2.7.2) or (2.7.10)) be represented by:

$$\vec{u}_\tau = \vec{F}(\vec{u}, \vec{u}_\xi, \phi_\eta, \tau) \qquad (2.7.3a)$$

where $\vec{u} = (f, s)^T$. Application of the trapezoidal formula yields:

$$\vec{u}_1^{n+1} - \vec{u}_1^n = \frac{\Delta\tau}{2}\left[\vec{F}(\vec{u}_1^{n+1}, D_2\vec{u}_1^{n+1}, D_3\phi_{1,M+1}^{n+1}, \tau^{n+1}) + \vec{F}(\vec{u}_1^n, D_2\vec{u}_1^n, D_3\phi_{1,M+1}^n, \tau^n)\right] \qquad (2.7.3b)$$

where D_1, D_2 and D_3 are appropriate difference replacements for the respective derivatives. This scheme requires iteration since the calculation of ϕ^{n+1} requires

the knowledge of $\vec{u}^{n-1}$. One way of solving (2.7.35) is to use the following predictor-corrector scheme

$$\vec{u}_i^{*} = \vec{u}_i^{n} + \Delta\tau\, \vec{F}\left(\vec{u}_i^{n},\ D_2\vec{u}_i^{n},\ D_1\phi_{i,N-1}^{n},\ \tau^{n} \right) \qquad (2.7.36a)$$

$$\vec{u}_i^{n-1} = \frac{1}{2}\left\{ \vec{u}_i^{n} + \vec{u}_i^{*} + \Delta\tau\, \vec{F}\left(\vec{u}_i^{*},\ D_2\vec{u}_i^{*},\ D_1\phi_{i,N-1}^{*},\ \tau^{n-1} \right) \right\} \qquad (2.7.36b)$$

with iteration on the corrector until convergence. That is, the starred values at which the function $\vec{F}$ is evaluated are replaced by the last iterates of the values at time $(n+1)$. However it is possible to obtain the same second-order in time/space accuracy (in terms of local truncation error), by performing only a single iteration of the corrector (see Appendix 2).

Thus the method of time stepping can be summarized in the following procedure:

(1) Set $\tau = 0$ and $n = 0$

(2) Calculate $\phi_{i,j}^{n}$ by solving the linear system for the potential using u_i^{n} as the boundary

(3) Predict u_i^{*} using (2.7.36a)

(4) Calculate $\phi_{i,j}^{*}$ by solving the linear system for the potential using u_i^{*} as the boundary

(5) Correct u_i^{n-1} using (2.7.36b)

(6) Calculate $\phi_{i,j}^{n-1}$ by solving the linear system for the potential using u_i^{n-1} as the boundary

(7) Set $\tau = \tau + \Delta\tau$ and $n = n + 1$

(8) If $\tau < \tau_{MAX}$ go to step (3)

where it may be necessary to iterate on steps (5) and (6) until convergence replacing $\phi^n_{i,j}$ and u^n_i inside $\hat{F}$ in (2.7.36b) with the latest iterates $\phi^{n+1}_{i,j}$ and u^{n+1}_i respectively and then applying relaxation to obtain the next iterates.

Using a second order backwards difference for D_1 and using second order central differences for D_2 and D_3 gives a Crank Nicolson scheme while using first order forwards and backwards differences respectively (or vice-versa) gives a MacCormack scheme. Both of these are second order accurate in time/space. Similar predictor-corrector schemes have been used to solve non-linear hyperbolic equations such as Burger's equation as in, for example, MacCormack (1978) where linear stability is also analyzed (for Burger's equation). The numerical results presented later investigate the stability and numerical convergence of the various methods above for propagating the boundary.

Similarly, the boundary equation for Method 3 can be discretized using the predictor-corrector:

$$- R^*_i = R^n_i - \Delta\tau \frac{\left(\phi^n_{i+1,N+1} - \phi^n_{i-1,N+1} \right)^2}{2\, h\, R^n_i} \qquad (2.7.37a)$$

$$R_i^{n+1} = \frac{1}{2}\left(R_i^n + R_i^* - \Delta\tau \frac{\left(\Psi^*_{i+1,M+1} - \Psi^*_{i-1,M+1} \right)}{2\,h\,R_i^*} \right) \qquad (2.7.37b)$$

for $i = 2,3,4,\ldots,(M+1)$ and for the first R (at $\xi = 0$)

$$R_1^* = R_1^n - \Delta\tau \frac{2\,h\,R_1^n}{\left(-3\,R_1^n + 4\,R_2^n - R_3^n\right)} \qquad (2.7.38a)$$

$$R_1^{n+1} = \frac{1}{2}\left(R_1^n + R_1^* - \Delta\tau \frac{2\,h\,R_1^*}{\left(-3\,R_1^* + 4\,R_2^* - R_3^*\right)} \right) \qquad (2.7.38b)$$

Note that the boundary condition on Ψ along the moving boundary (i.e. $\eta = 1$) has been incorporated in the derivation of the above scheme.

There is, however, one obvious limitation to this predictor-corrector scheme used to move the boundary. If the time step becomes too large, given a spacial discretization, one of the predicted boundary heights (i.e. f_i^* 's) will become negative and the method will break down. This usually happens to f_M^* , the height of the moving boundary adjacent to the toe in Methods 1 and 2. This is not a problem in the polar formulation of Method 3.

2.7.3 The Solution of the Linear Equations for the Potential and the Stream Function

Both methods for the potential problem as well as the method for the stream function require the solution of large sparse systems of linear equations. To reduce the storage requirements due to fill-in when direct methods are employed iterative methods are the natural choice. Moreover, since these problems must be solved at each time step, good first approximations to the unknowns (i.e. the potential or stream function values) are available (after the initial time) resulting in few iterations and low CPU time per time step.

When selecting iterative methods, two factors come into play. The first is the choice of basic iteration method and the second is the choice of acceleration method. In this context, the basic iterative method can be thought of as a pre-conditioning to the acceleration method, both of which can be chosen independent of each other.

This area is currently of much interest in the literature. A review of the basic iterative methods for symmetric systems resulting from the application of finite differences to Poisson's equation are given by Colgan (1982). Reviews of current work on non-symmetric systems

are given by Elman (1984) and Young et al (1984). The state of this field is summarized by Elman in the above paper, when after listing many of the latest proposed methods for non-symmetric systems he remarks, "None of these ideas have been stringently tested, though, and little is known about convergence rates".

The basic iterative method chosen for this work is called Block or Line Symmetric Successive Overrelaxation (BSSOR). That is, the equations along a vertical line in the grid are considered as a tridiagonal system for the new iterates of the potential along that line in terms of the last iterates of the potentials along the adjacent lines. Relaxation is then applied to the new values along the line. One complete iteration consists of one forward sweep from left to right along the lines followed by a backwards sweep from right to left. As indicated below, this results in a symmetric iteration matrix if the original equations are symmetric and allows the use of conjugate gradient acceleration.

Consider the linear system for the potential (i.e. system (2.7.3) or (2.7.11) with the appropriate boundary conditions) ordered in a natural way along the lines in the domain from bottom to top and left to right as (suppressing the time dependence superscript n):

$$A\vec{x} = \vec{b} \quad \text{or} \tag{2.7.39}$$

$$\begin{bmatrix} B_1 & C_1 & & & \\ A_2 & B_2 & C_2 & 0 & \\ & A_3 & B_3 & C_3 & \\ & & & & \\ 0 & & & A_{M-1}B_{M-1}C_{M-1} & \\ & & & A_M & B_M \end{bmatrix} \begin{bmatrix} \phi_1 \\ \phi_2 \\ \phi_3 \\ \cdot \\ \cdot \\ \phi_{M-1} \\ \phi_M \end{bmatrix} = \begin{bmatrix} b_1 \\ b_2 \\ b_3 \\ \cdot \\ \cdot \\ b_{M-1} \\ b_M \end{bmatrix}$$

(2.7.39)

where $A_k = \begin{bmatrix} C_{3_{k,1}} & -C_{6_{k,1}} & & & \\ -C_{7_{k,2}} & C_{3_{k,2}} & -C_{6_{k,2}} & 0 & \\ & & & & \\ 0 & & -C_{7_{k,j-1}} & C_{3_{k,j-1}} & -C_{6_{k,j-1}} \\ & & & -C_{7_{k,j}} & C_{3_{k,j}} \end{bmatrix}$

$$B_k = \begin{bmatrix} C_{0_{k,1}} & -C_{2_{k,1}} & & & \\ -C_{4_{k,2}} & C_{0_{k,2}} & -C_{2_{k,2}} & 0 & \\ & & & & \\ 0 & & -C_{4_{k,j-1}} & C_{0_{k,j-1}} & -C_{2_{k,j-1}} \\ & & & -C_{4_{k,j}} & C_{0_{k,j}} \end{bmatrix}$$

(2.7.40)

and $C_k = \begin{bmatrix} C_{1_{k,1}} & -C_{S_{k,1}} & & & \\ -C_{e_{k,2}} & C_{1_{k,2}} & -C_{S_{k,2}} & & 0 \\ & \cdot & \cdot & \cdot & \\ & & \cdot & \cdot & \cdot \\ & 0 & & -C_{e_{k,j-1}} & C_{1_{k,j-1}} & -C_{S_{k,j-1}} \\ & & & & -C_{e_{k,j}} & C_{1_{k,j}} \end{bmatrix}$

$$b_k = \begin{bmatrix} RHS_{k,1} \\ RHS_{k,2} \\ \cdot \\ \cdot \\ RHS_{k,j-1} \\ RHS_{k,j} \end{bmatrix}, \qquad \phi_k = \begin{bmatrix} \phi_{k,1} \\ \phi_{k,2} \\ \cdot \\ \cdot \\ \phi_{k,j-1} \\ \phi_{k,j} \end{bmatrix}$$

and $j = NROWS_k$. The BSSOR method can be written as it is actually implemented in a program as (for one iteration) :

$$\left.\begin{aligned} B_k\, T_k^{p+1/2} &= b_k - A_k\, \phi_{k-1}^{p+1/2} - C_k\, \phi_{k+1}^{p} \\ \phi_k^{p+1/2} &= \omega\, T_k^{p+1/2} + (1-\omega)\, \phi_k^{p} \end{aligned}\right\} \quad k = 1,2,\ldots M$$

(2.7.41)

$$\left.\begin{aligned} B_k\, T_k^{p+1} &= b_k - A_k\, \phi_{k-1}^{p+1/2} - C_k\, \phi_{k+1}^{p+1} \\ \phi_k^{p+1} &= \omega\, T_k^{p+1} + (1-\omega)\, \phi_k^{p+1/2} \end{aligned}\right\} \quad k = M, M-1, \ldots 1$$

where the superscript p denotes the iteration number (not time).

Similarly the equations for the stream function of Method 3 (i.e. (2.7.22) and (2.7.27)) can be written in the block tridiagonal form of (2.7.39) and solved iteratively using BSSOR as above.

The BSSOR method can also be written as a method of successive substitution, a form which lends itself to the application of an acceleration method, as:

$$x^{p+1} = G\, x^{p} + k, \qquad (2.7.42)$$

where the iteration matrix $G = (I - Q^{-1}A)$,

$$Q = \frac{1}{\omega (2 - \omega)} (D + \omega E) D^{-1} (D + \omega F) \qquad (2.7.43)$$

and $k = Q^{-1} b$

Here

$$D = \begin{bmatrix} B_1 & & & \\ & B_2 & 0 & \\ & & \ddots & \\ 0 & & & B_N \end{bmatrix}, \quad E = \begin{bmatrix} 0 & & & \\ A_2 & 0 & & 0 \\ & A_3 & 0 & \\ & & \ddots & \\ 0 & & A_N & 0 \end{bmatrix} \qquad (2.7.44)$$

and $$F_1 = \begin{bmatrix} 0 & C_1 & & \\ & 0 & C_2 & 0 \\ & & & \\ & & 0 & C_{M-1} \\ 0 & & & 0 \end{bmatrix}$$

Finally the equations can be written as the preconditioned system:

$$Q^{-1}A\,x = k \qquad (2.7.45)$$

Note that if A is symmetric positive definite then so is Q for $0 < \omega < 2$ (see Colgan (1982)). Thus in the case of Method 1 for the potential, which results in a positive definite A and Q, the well established method of Conjugate Gradient acceleration, CG, is employed (Colgan (1982) or Mitchel and Griffiths (1978)).

CG acceleration has been adapted to problems where A is not symmetric but the preconditioning matrix Q is equal to the symmetric part of A (Concus and Goulub (1976) and Widlund (1978)). This is not the case for the Q resulting from BSSOR applied to the equations for the potential in Method 2 and stream function in Method 3. Furthermore, if A is split such that Q is the symmetric part of A the system $Q\,x = d$ is not easy to solve (as it should be to

apply CG in this case) since Q would have a block tridiagonal structure similar to A. Consequently, a more general acceleration procedure is required.

Saad's Incomplete Orthogonalization Method (without correction); IOM, was chosen as the acceleration method in Method 2 for the potential and in Method 3 for the stream function (Saad (1981) and (1984)). IOM is one of many proposed iteration methods that can be used as acceleration methods that is refered to by Elman in his comment above.

Saad derived this acceleration method by modifying Arnoldi's method. To discuss the basic ideas in this method the concept of a projection process onto a Krylov subspace must be defined. A projection process onto the Krylov subspace

$$K_m = \text{span}\left\{ r_o , A r_o , (A)^2 r_o , \ldots , (A)^{m-1} r_o \right\} \qquad (2.7.46)$$

with basis $V_m = \left\{ v_1 , v_2 , v_3 , \ldots , v_m \right\}$

seeks a solution x_m to (2.7.39) such that

$$\begin{cases} x_m \in K_m \\ b - A x_m \perp v_j \quad \text{for} \quad j = 1,2,3,\ldots,m \end{cases} \qquad (2.7.47)$$

where $r_o = A x_o - b$ is the residual of x_o, the initial estimate for x. Note that x_m is a Galerkin approximation to x.

If x_m is written as :

$$x_m = x_o + V_m y_m \qquad (2.7.48)$$

then the conditions that x_m be orthogonal to the residual $r_m = A x_m - b$ implies that

$$V_m^T (b - A x_m) = 0 \qquad (2.7.49)$$

so that

$$y_m = (V_m^T A V_m)^{-1} V_m^T r_o \qquad (2.7.50)$$

The idea of Arnoldi's method is to construct the v_i's using a recurrence relation and to impose conditions on them such that $(V_m^T A V_m)^{-1}$ is relatively easy to compute. More specifically, in the case of the preconditioned system (2.7.46), A is replaced by $Q^{-1} A$ and r_o by $Q^{-1} r_o$. Thus the appropriate Krylov subspace is

$$K_m = \text{span}\left\{ Q^{-1}r_o \, , \; Q^{-1}A\, r_o \, , \; (Q^{-1}A)^2 r_o \, , \; \ldots \right.$$

$$\left. (Q^{-1}A)^{m-1} r_o \right\} \qquad (2.7.51)$$

Consider the recurrence relation

$$h_{j+1,j} v_{j+1} = Q^{-1}A\, v_j - \sum_{i=1}^{j} h_{i,j}\, v_i \qquad (2.7.52)$$

where

$$v_1 = \frac{Q^{-1}r_o}{\| Q^{-1}r_o \|} \qquad (2.7.53)$$

and $h_{i,j}$ are chosen such that

$$v_i^T v_{j+1} = 0 \text{ and } \| v_{j+1} \| = 1 \text{ for } i = 1,2,3,\ldots,j \qquad (2.7.54)$$

That is

$$h_{i,j} = v_i^T Q^{-1} A\, v_j \qquad (2.7.55)$$

If H_m is the upper Hessenberg matrix with elements $h_{i,j}$ then

$$V_m^T Q^{-1} A\, V_m - H_m = 0 \qquad (2.7.56)$$

Thus the solution given in (2.7.48) can be calculated

from

$$y_m = (V_m^T Q^{-1} A V_m)^{-1} V_m^T Q^{-1} r_0 = H_m^{-1} \| Q^{-1} r_0 \| e_1$$

(2.7.57)

where $e_1 = (1, 0, 0, \ldots, 0)^T$

That is, after the upper Hessenburg matrix H_m is formed the linear system for y_m is solved (for example using LU decomposition).

This method requires the storage of m v's which for large m may lose orthogonality due to round off errors. Additionally the residual is not available until x_m is calculated. Saad addresses these problems by changing the algorithm so that each v_{j+1} is orthogonal only to the previous p v's, incorporating a restart procedure so that after the calculation of m v's (with m fixed and determined by the storage available) x_m is updated and x_0 is set equal to x_m after which the entire procedure is restarted and by giving an estimate for the residual norm at each step.

Saad's method can also be applied when A is symmetric such as in the case of Method 1 for the potential. In this case, Q is also symmetric and hence H_m is symmetric and thus tridiagonal. As a result the v_j's satisfy a three

term recurrence relation. Thus p need only be 2 and the inversion of H_m can be performed using a tridiagonal solver. In the next section results are presented that compare the use of CG and IOM to Method 1 for the potential in order to establish the efficiency of IOM.

2.8 Discussion of Numerical Results

In this section an example problem is used to compare the two different methods for the potential problem and the method for the stream function in detail. In addition the various methods for moving the boundary are investigated. Graphic results are then presented for various representative problems and compared to the similarity solution derived in Section 2.6 .

For the first example consider the parabolic initial profile:

$$f(x,0) = 1 - \left(\frac{x}{s(0)} \right)^2 \qquad (2.8.1)$$

$$s(0) = 1$$

The results for $f(0,t)$ and $s(t)$ at various times are given in Tables 1, 2 and 3 for Methods 1, 2 and 3 respectively. Note that these variables are indicative of the degree of similarity between the various numerical results and are common to all the calculations. The (a) parts of the tables compare the results with and without iteration on the predictor-corrector for moving the boundary using central differences for the boundary slope (i.e. Crank Nicolson) while the (b) parts show the same comparison using first order derivatives (backward in the predictor and forward in the corrector) for the boundary slope

(i.e. MacCormack). Additionally note that the exact value of the area under the mound should be $^2/_3$ units for all time and that the CPU times given are for the Control Data Corporation Cyber 170/835 computer.

The following parameters were used in the calculations:

(1) The equations for the potential or stream function were iterated on until the 2-norm of the Q residual was less than 10^{-5} .

(2) The relaxation factor used for the BSSOR iteration was 1.6 .

(3) In the IOM acceleration the maximum number of v's was 8 and each v_{j+1} was held orthogonal to the last 4 v's (i.e. $m = 8$ and $p_o = 4$).

(4) For the methods that require iteration on the corrector this was carried out until the maximum relative change between two successive iterates was less than 10^{-3} using a relaxation factor of .5 (i.e. underrelaxation).

Inspection of Tables 1,2 and 3 reveals some general trends on the methods for calculating new boundary positions. Clearly iterating on the corrector does not significantly alter the results of any method. In fact very few iterations were performed especially after the first few time steps. Furthermore, the Crank Nicolson scheme for the moving boundary slope is more robust than

Table 1a - Example 1 : Method 1 Results

Boundary moved using Crank Nicolson with iteration

$\Delta\tau$=.05

	h=.1, k=.1,	h=.05, k=.05,	h=.025, k=.025
f(0,.25)	.834492	.835034	pred f<0
s(.25)	1.286929	1.285185	
f(0,.5)	.715002	.716087	
s(.5)	1.488194	1.487726	
f(0,1.0)	.572463	.574246	
s(1.0)	1.797603	1.798831	
f(0,2.0)	.446129	.448304	
s(2.0)	2.239848	2.242442	
area(2.0)	.653319	.658403	
CPU time	12 secs	51 secs	

$\Delta\tau$=.025

	h=.1, k=.1,	h=.05, k=.05,	h=.025, k=.025
f(0,.25)	.834562	.835133	.835347
s(.25)	1.288538	1.286914	1.286599
f(0,.5)	.714994	.716357	.716943
s(.5)	1.489833	1.489364	1.489732
f(0,1.0)	.572561	.574774	-
s(1.0)	1.798894	1.800580	-
f(0,2.0)	.446446	.448953	-
s(2.0)	2.241466	2.244476	-
area(2.0)	.654332	.659989	-
CPU time	16 secs	78 secs	212 secs

Boundary moved using Crank Nicolson without iteration

$\Delta\tau$=.05

	h=.1, k=.1,	h=.05, k=.05,	h=.025, k=.025
f(0,.25)	.834472	corr f<0	pred f<0
s(.25)	1.282338		
f(0,.5)	.715194		
s(.5)	1.487102		
f(0,1.0)	.572843		
s(1.0)	1.797350		
f(0,2.0)	.446503		
s(2.0)	2.240393		
area(2.0)	.654110		
CPU time	11 secs		

$\Delta\tau$=.025

	h=.1, k=.1,	h=.05, k=.05,	h=.025, k=.025
f(0,.25)	.834719	.835183	pred f<0
s(.25)	1.288831	1.286709	
f(0,.5)	.715288	.716501	
s(.5)	1.490324	1.489761	
f(0,1.0)	.572888	.575004	
s(1.0)	1.799772	1.801086	
f(0,2.0)	.446735	.449159	
s(2.0)	2.242342	2.245173	
area(2.0)	.655001	.660505	
CPU time	19 secs	75 secs	

Table 1b - Example 1 : Method 1 Results (continued)

Boundary moved using MacCormack with iteration

Δτ=.05

	h=.1, k=.1,	h=.05, k=.05,	h=.025, k=.025
f(0,.25)	.835043	pred f<0	pred f<0
s(.25)	1.287671		
f(0,.5)	.716276		
s(.5)	1.489050		
f(0,1.0)	.578168		
s(1.0)	1.805064		
f(0,2.0)	.454243		
s(2.0)	2.261873		
area(2.0)	.673719		
CPU time	14 secs		

Δτ=.025

	h=.1, k=.1,	h=.05, k=.05,	h=.025, k=.025
f(0,.25)	.831974	.835010	pred f<0
s(.25)	1.288844	1.287181	
f(0,.5)	.711945	.716268	
s(.5)	1.490235	1.489671	
f(0,1.0)	.571658	.574512	
s(1.0)	1.799450	1.800739	
f(0,2.0)	.446468	.448913	
s(2.0)	2.242047	2.244701	
area(2.0)	.654787	.660052	
CPU time	17 secs	85 secs	

Boundary moved using MacCormack without iteration

Δτ=.05

	h=.1, k=.1,	h=.05, k=.05,	h=.025, k=.025
f(0,.25)	.835096	pred f<0	pred f<0
s(.25)	1.280797		
f(0,.5)	.716397		
s(.5)	1.484508		
f(0,1.0)	.574426		
s(1.0)	1.795635		
f(0,2.0)	.448052		
s(2.0)	2.240144		
area(2.0)	.656643		
CPU time	11 secs		

Δτ=.025

	h=.1, k=.1,	h=.05, k=.05,	h=.025, k=.025
f(0,.25)	.835060	.835361	pred f<0
s(.25)	1.288201	1.285316	
f(0,.5)	.716143	.716828	
s(.5)	1.489982	1.488631	
f(0,1.0)	.574263	.575311	
s(1.0)	1.799802	1.800323	
f(0,2.0)	.448182	.449449	
s(2.0)	2.243510	2.244845	
area(2.0)	.657654	.660923	
CPU time	16 secs	78 secs	

Table 2a - Example 1 : Method 2 Results

Boundary moved using Crank Nicolson with iteration

$\Delta\tau = .05$

	h=.1, k=.1,	h=.05, k=.05,	h=.025, k=.025
f(0,.25)	.835415	.835387	pred f<0
s(.25)	1.288387	1.284573	
f(0,.5)	.717611	.717257	
s(.5)	1.491969	1.488671	
f(0,1.0)	.577206	.576580	
s(1.0)	1.805749	1.802538	
f(0,2.0)	.451853	.451215	
s(2.0)	2.252478	2.249241	
area(2.0)	.667503	.665729	
CPU time	36 secs	170 secs	

$\Delta\tau = .025$

	h=.1, k=.1,	h=.05, k=.05,	h=.025, k=.025
f(0,.25)	.835531	.835504	.835515
s(.25)	1.290244	1.286902	1.286022
f(0,.5)	.717851	.717506	.717446
s(.5)	1.493772	1.490782	1.489943
f(0,1.0)	.577536	.576944	-
s(1.0)	1.807461	1.804510	-
f(0,2.0)	.452208	.451610	-
s(2.0)	2.254178	2.251183	-
area(2.0)	.668538	.666897	-
CPU time	62 secs	285 secs	714 secs

Boundary moved using Crank Nicolson without iteration

$\Delta\tau = .05$

	h=.1, k=.1,	h=.05, k=.05,	h=.025, k=.025
f(0,.25)	.835410	.835351	pred f<0
s(.25)	1.285788	1.275391	
f(0,.5)	.717778	.717348	
s(.5)	1.491467	1.483642	
f(0,1.0)	.577494	.576693	
s(1.0)	1.806015	1.799614	
f(0,2.0)	.452127	.451212	
s(2.0)	2.253086	2.247352	
area(2.0)	.668114	.665237	
CPU time	-	-	

$\Delta\tau = .025$

	h=.1, k=.1,	h=.05, k=.05,	h=.025, k=.025
f(0,.25)	.835544	.835513	.835503
s(.25)	1.290478	1.286689	1.276241
f(0,.5)	.717900	.717548	.717437
s(.5)	1.494164	1.490876	1.485822
f(0,1.0)	.577618	.577013	-
s(1.0)	1.807870	1.804712	-
f(0,2.0)	.452298	.451681	-
s(2.0)	2.254588	2.251426	-
area(2.0)	.666879	.667077	-
CPU time	64 secs	275 secs	642 secs

Table 2b - Example 1 : Method 2 Results (continued)

Boundary moved using MacCormack with iteration

$\Delta\tau$=.05

	h=.1, k=.1,	h=.05, k=.05,	h=.025, k=.025
f(0,.25)	.836604	pred f<0	pred f<0
s(.25)	1.283694		
f(0,.5)	.719697		
s(.5)	1.489430		
f(0,1.0)	.579479		
s(1.0)	1.804845		
f(0,2.0)	.453884		
s(2.0)	2.253460		
area(2.0)	.671129		
CPU time	32 secs		

$\Delta\tau$=.025

	h=.1, k=.1,	h=.05, k=.05,	h=.025, k=.025
f(0,.25)	.836465	.835882	pred f<0
s(.25)	1.289986	1.286227	
f(0,.5)	.719467	.718087	
s(.5)	1.493936	1.490470	
f(0,1.0)	.579437	.577569	
s(1.0)	1.808146	1.804500	
f(0,2.0)	.454000	.452163	
s(2.0)	2.256077	2.251604	
area(2.0)	.671923	.667906	
CPU time	57 secs	275 secs	

Boundary moved using MacCormack without iteration

$\Delta\tau$=.05

	h=.1, k=.1,	h=.05, k=.05,	h=.025, k=.025
f(0,.25)	.836604	pred f<0	pred f<0
s(.25)	1.283694		
f(0,.5)	.719597		
s(.5)	1.489430		
f(0,1.0)	.579479		
s(1.0)	1.804845		
f(0,2.0)	.453884		
s(2.0)	2.253460		
area(2.0)	.671129		
CPU time	32 secs		

$\Delta\tau$=.025

	h=.1, k=.1,	h=.05, k=.05,	h=.025, k=.025
f(0,.25)	.836465	.835882	pred f<0
s(.25)	1.289986	1.286227	
f(0,.5)	.719467	.718087	
s(.5)	1.493936	1.490470	
f(0,1.0)	.579437	.577569	
s(1.0)	1.808146	1.804500	
f(0,2.0)	.454000	.452163	
s(2.0)	2.256077	2.251604	
area(2.0)	.671923	.667906	
CPU time	57 secs	275 secs	

Table 3 - Example 1 : Method 3 Results

Boundary moved with iteration

$\Delta\tau = .05$

	$h=\pi/20$, $k=.1$,	$h=\pi/40$, $k=.05$,	$h=\pi/80$, $k=.025$
f(0,.25)	.828261	.830985	.831485
s(.25)	1.305288	1.295317	1.293498
f(0,.5)	.707161	.708481	.708262
s(.5)	1.518523	1.504826	1.501940
f(0,1.0)	.567440	.563884	-
s(1.0)	1.851519	1.827363	-
f(0,2.0)	.448812	.440307	-
s(2.0)	2.341152	2.289824	-
area(2.0)	.718158	.680169	-
CPU time	30 secs	-	290 secs

$\Delta\tau = .025$

	$h=\pi/20$, $k=.1$,	$h=\pi/40$, $k=.05$,	$h=\pi/80$, $k=.025$
f(0,.25)	.828202	.830936	.831451
s(.25)	1.304621	1.295042	1.293173
f(0,.5)	.707103	.708428	.708215
s(.5)	1.518192	1.504624	1.501671
f(0,1.0)	.567328	.563777	-
s(1.0)	1.851289	1.827157	-
f(0,2.0)	.448732	.440248	-
s(2.0)	2.340964	2.289639	-
area(2.0)	.718059	.680085	-
CPU time	52 secs	318 secs	424 secs

Boundary moved without iteration

$\Delta\tau = .05$

	$h=\pi/20$, $k=.1$	$h=\pi/40$, $k=.05$	$h=\pi/80$, $k=.025$
f(0,.25)	.828391	.831103	.831598
s(.25)	1.304232	1.294646	1.291760
f(0,.5)	.707355	.708648	.708429
s(.5)	1.518073	1.504571	1.501573
f(0,1.0)	.567488	.563933	-
s(1.0)	1.851273	1.827177	-
f(0,2.0)	.448906	.440301	-
s(2.0)	2.340966	2.289654	-
area(2.0)	.718075	.680097	-
CPU time	30 secs	160 secs	259 secs

$\Delta\tau = .025$

	$h=\pi/20$, $k=.1$,	$h=\pi/40$, $k=.05$,	$h=\pi/80$, $k=.025$
f(0,.25)	.828208	.830942	.831454
s(.25)	1.304459	1.294949	1.293106
f(0,.5)	.707106	.708431	.708217
s(.5)	1.518130	1.504592	1.501644
f(0,1.0)	.567328	.563778	-
s(1.0)	1.851263	1.827139	-
f(0,2.0)	.448731	.440248	-
s(2.0)	2.340949	2.289625	-
area(2.0)	.718053	.680080	-
CPU time	57 secs	322 secs	423 secs

the MacCormack-scheme allowing larger time steps for a given space step. Note that reversing the one sided differences for the slope of the moving boundary to forward in the predictor and backward in the corrector in the MacCormack scheme resulted in even greater restriction on the time step.

Closer inspection of the results indicate an approximately three decimal figure agreement in the mound centre height and a four decimal figure agreement in the toe location for various grid sizes and time steps within and between the results of Methods 1 and 2 for the potential. Method 2 conserves mass about one decimal figure better than Method 1 while the latter is about three times faster in terms of CPU time. It appears that for both these methods, using a *10 x 10* spacial grid with a time step of *.05* gives results with acceptable numerical convergence.

The results using Method 3 for the stream function differ somewhat from the other methods. The agreement between these results and those of Methods 1 and 2 is only about two and one half decimal figures for both the mound height and the toe location and deteriorate as time progresses. The agreement within Method 3 between the results of various grid and time step sizes is better at about three and one half decimal figures but also shows

deterioration in time. Finally, although not reported in the tables, the results for Method 3 display a non-monotonic behaviour of the mound height (computed from the R_j 's) in approximately the fourth decimal place. This type of behaviour was not evident in the results of either of the other methods. It appears that this lack of accuracy is due to spatial errors since there is very good agreement when different time steps are used for a given spacial grid. Conservation of mass is also much less adhered to using this method than the others. The predictor-corrector scheme for moving the boundary is, however, very robust in this formulation. The problem of predicted negative boundary positions did not arise, due to the fact that the radial distance from the origin to the moving boundary being large. Finally it appears that a 20×20 spacial grid with a time step of .05 is required in order to obtain acceptable numerical convergence when using this method.

Although not reported in the tables Method 1 for the potential was also implemented using the IOM instead of the CG method for accelerating the convergence of the BSSOR iterations. The results indicated that CG is approximately twice as fast as IOM (using CPU time as a measure and using $p = 2$ and $m = 8$ in IOM). The additional time advantage of Method 1 over Method 2 for the potential is probably due to the fact that for

identical grid sizes the fixed grid of Method 1 has less grid points inside the boundary. Initially it has about one third less grid points inside the boundary. This decreases to only about one quarter of the grid points inside the boundary at a non-dimensional time of two. This also possibly explains the better conservation of mass when using Method 2 for the potential.

The deteriorating accuracy apparent in Method 3 for the stream function can be explained by the lack of spacial resolution at the toe of the moving boundary. Since the speed of the toe is inversely proportional to its slope it is essential to adequately calculate this slope. As the toe advances the size of the grid at the toe increases (see Figure 10 below) and the slope of the toe increases (in polar coordinates) thus lowering the accuracy of the calculated slope.

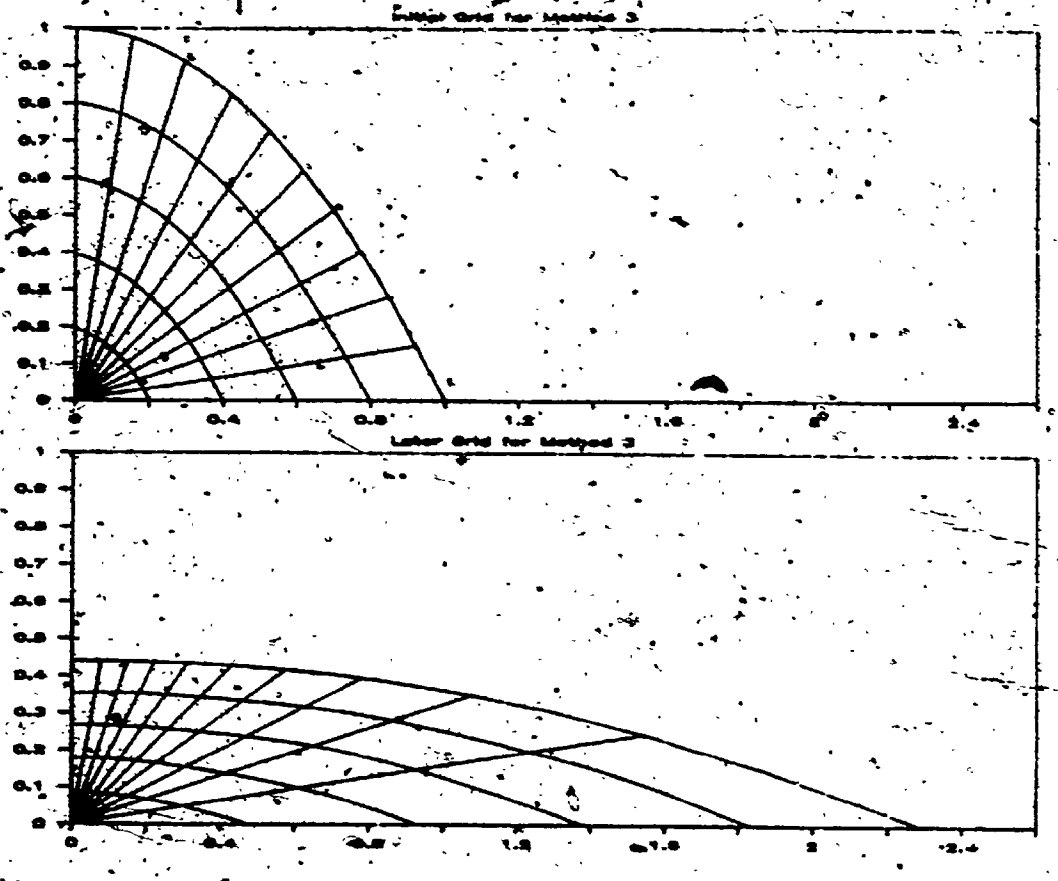

Figure 10 - The Grids for Method 3 at Two Different Times

The subsidence mound is plotted at different times in steps of .5 units from the results of Methods 1,2 and 3, for the given initial conditions in Figure 11 following. Figure 12 shows the results of Method 2 (using the Crank Nicolson based predictor-corrector to move the boundary with a time step of $\Delta\tau = .05$ and a 10×10 spatial grid) and the similarity solution to the Dupuit approximation to the problem (see Section 2.6). Note that for this mound initially of aspect ratio 1 (height to width ratio) there is not much similarity between the solutions.

Figure 11 — Comparison of Methods

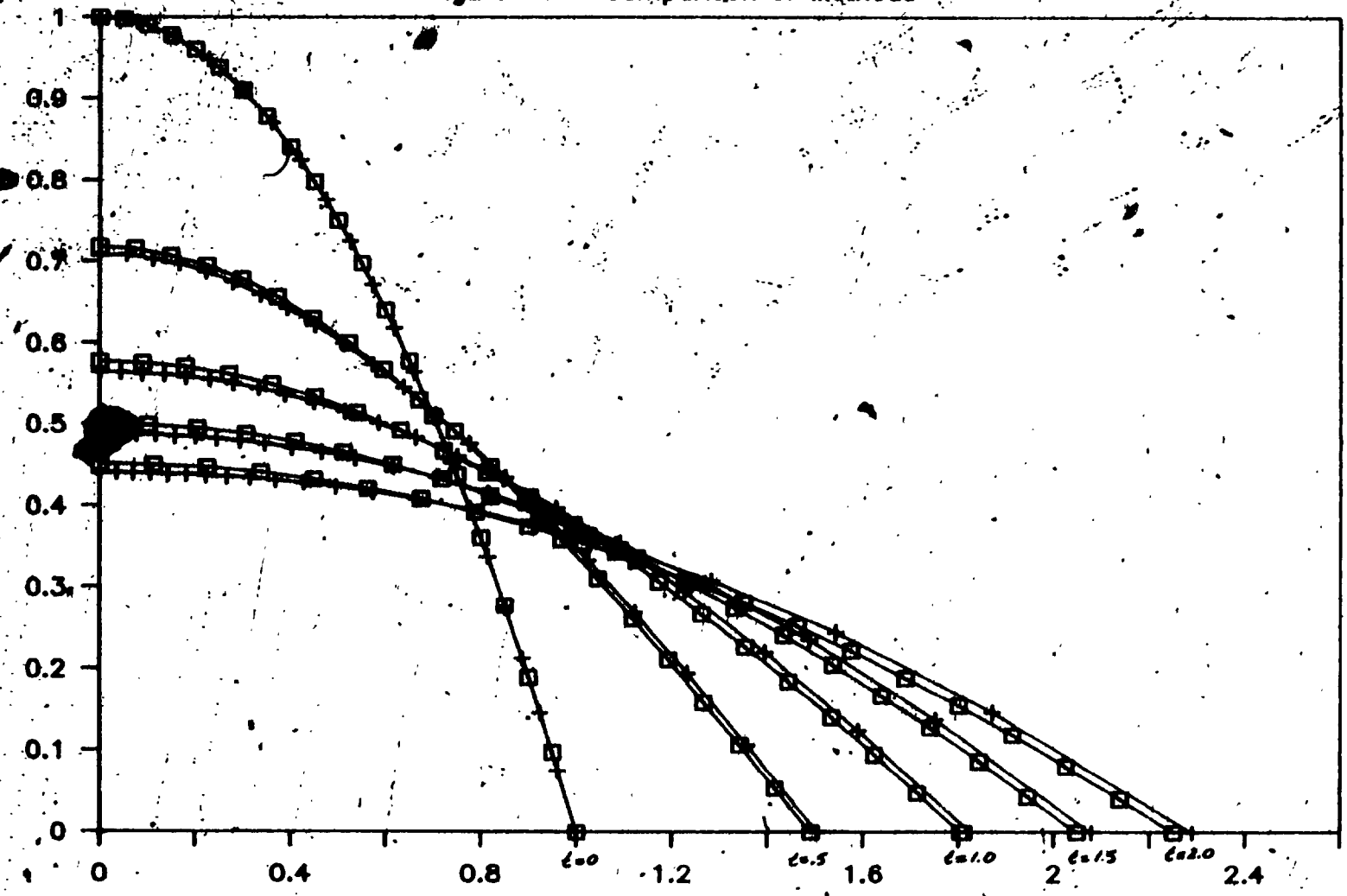

Figure 12 - Numerical vs Similarity Solution s(0)=1

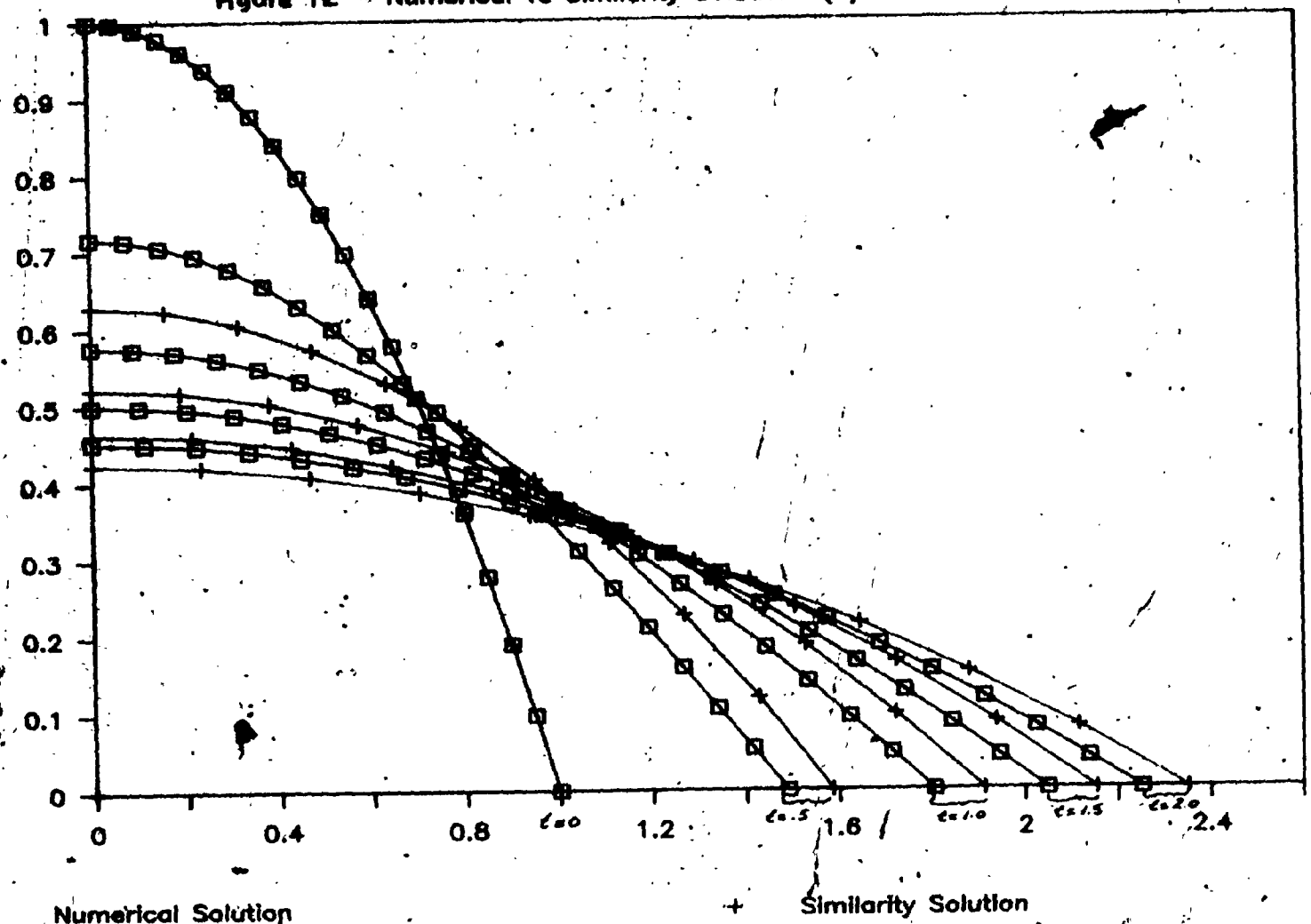

Figures 13, 14 and 15 show the same comparison for the same problem except that $s(0)$ is 2, 4 and 8 and at time intervals of 1, 2 and 4 units respectively (using the Crank Nicolson based predictor-corrector with time steps of $\Delta\tau$ = .1 , .2 and .5 respectively and a 10 x 10 spacial grid). Note that as the initial aspect ratio decreases the solutions look more and more alike. In particular for $s(0)$ equal to 8 the decaying mound profiles are virtually identical. This implies that the Dupuit approximation that the flow is essentially horizontal is extremely good in this case. This can be explained by the fact that for mounds of large aspect ratios, a small drop in the moving surface location in the main part of the mound requires a much larger spreading motion in the toe region in order to conserve mass. As a result the vertical fluid velocities are much smaller than the horizontal ones. It is concluded that the Dupuit approximation is indeed an excellent approximation for groundwater mound problems since in these applications the aspect ratios are typically even larger than 8.

Lastly the results for the initial profiles (using the Crank Nicolson based predictor-corrector with a 10 x 10 spacial grid):

Figure 13 – Numerical vs Similarity Solution s(0)=2

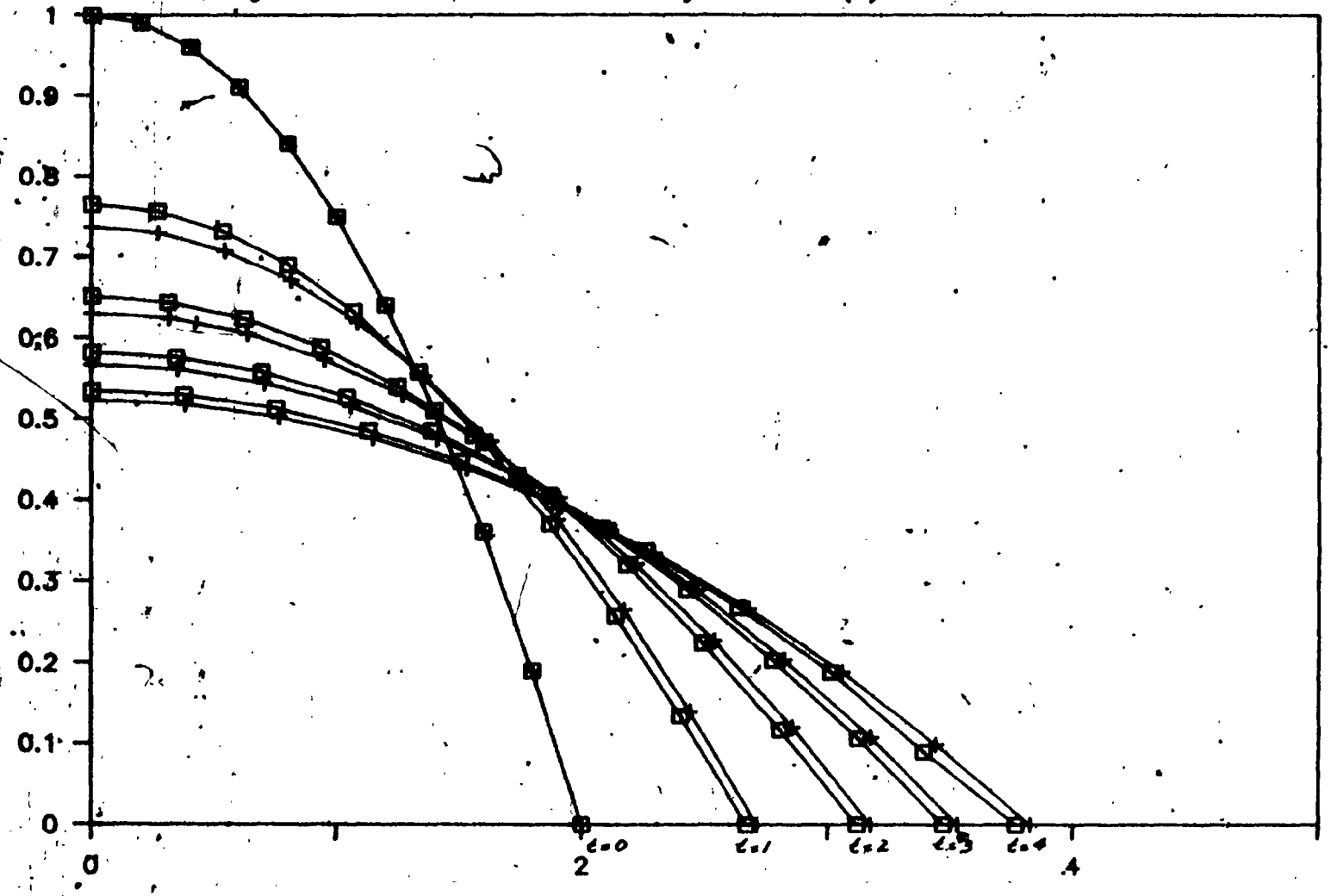

□ Numerical Solution + Similarity Solution

Figure 14 – Numerical vs Similarity Solution s(0)=4

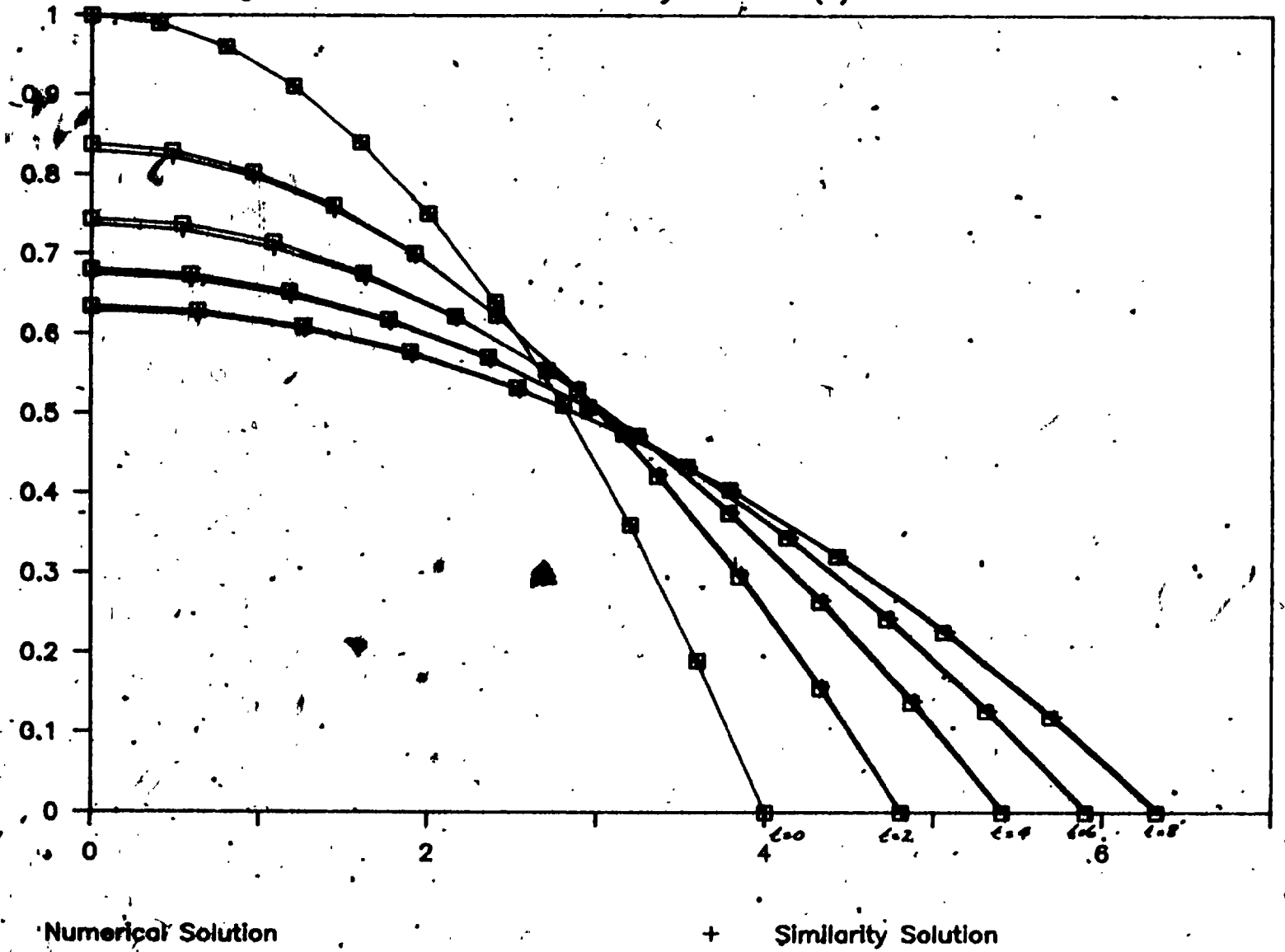

Figure 15 – Numerical vs Similarity Solution s(0)=8

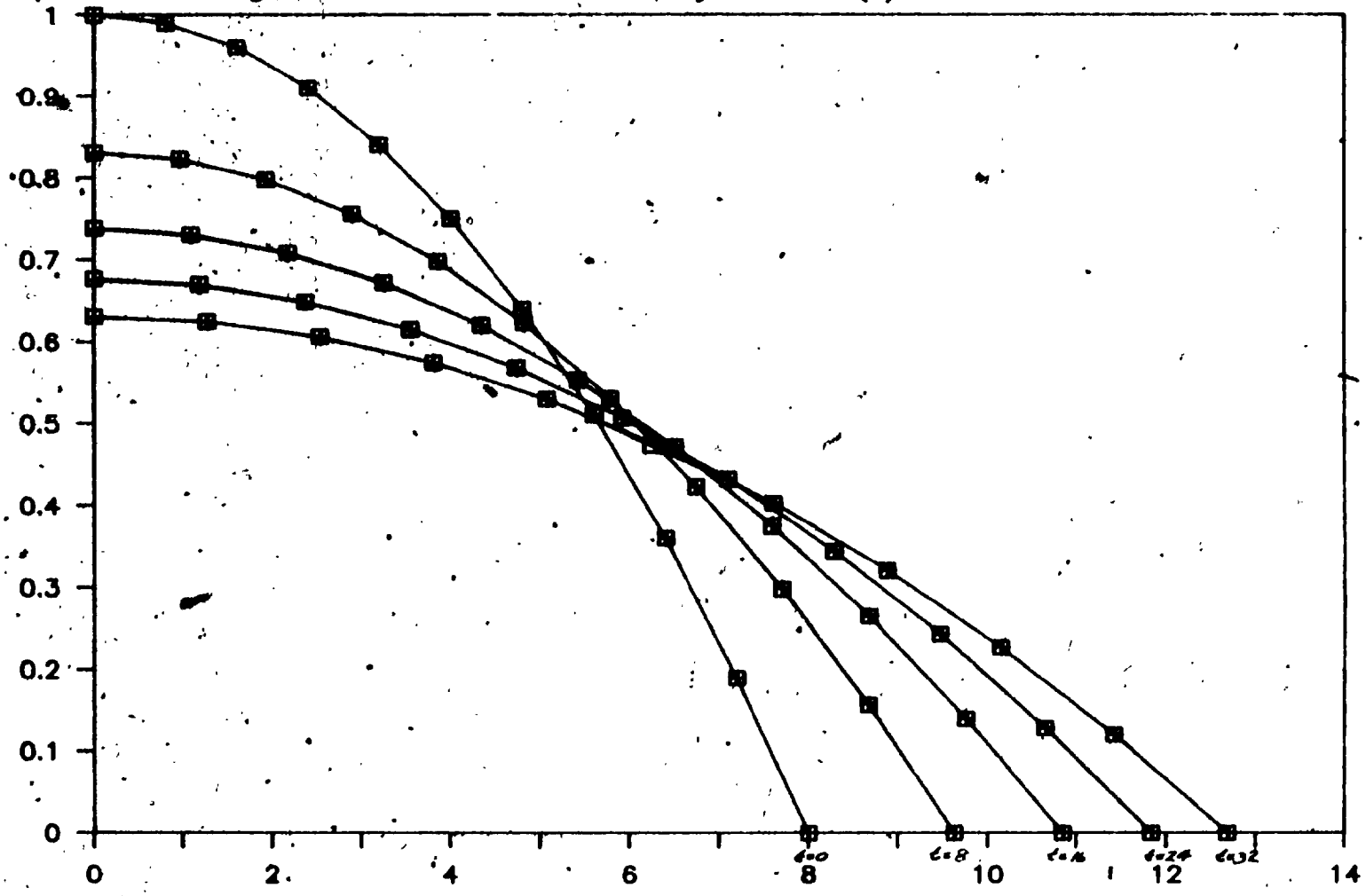

□ Numerical Solution + Similarity Solution

Figure 16 – Cubic Initial Mound s(0)=1

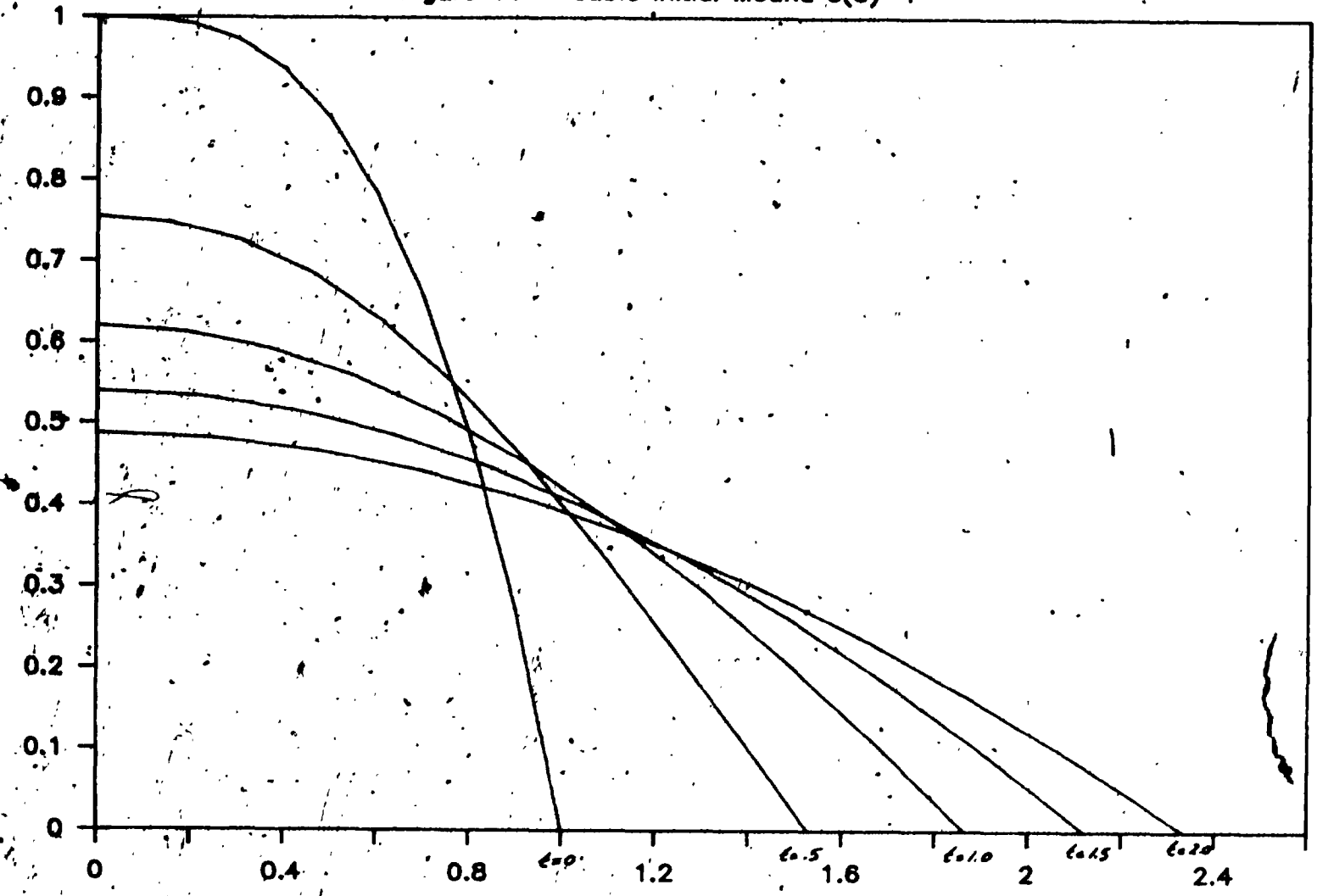

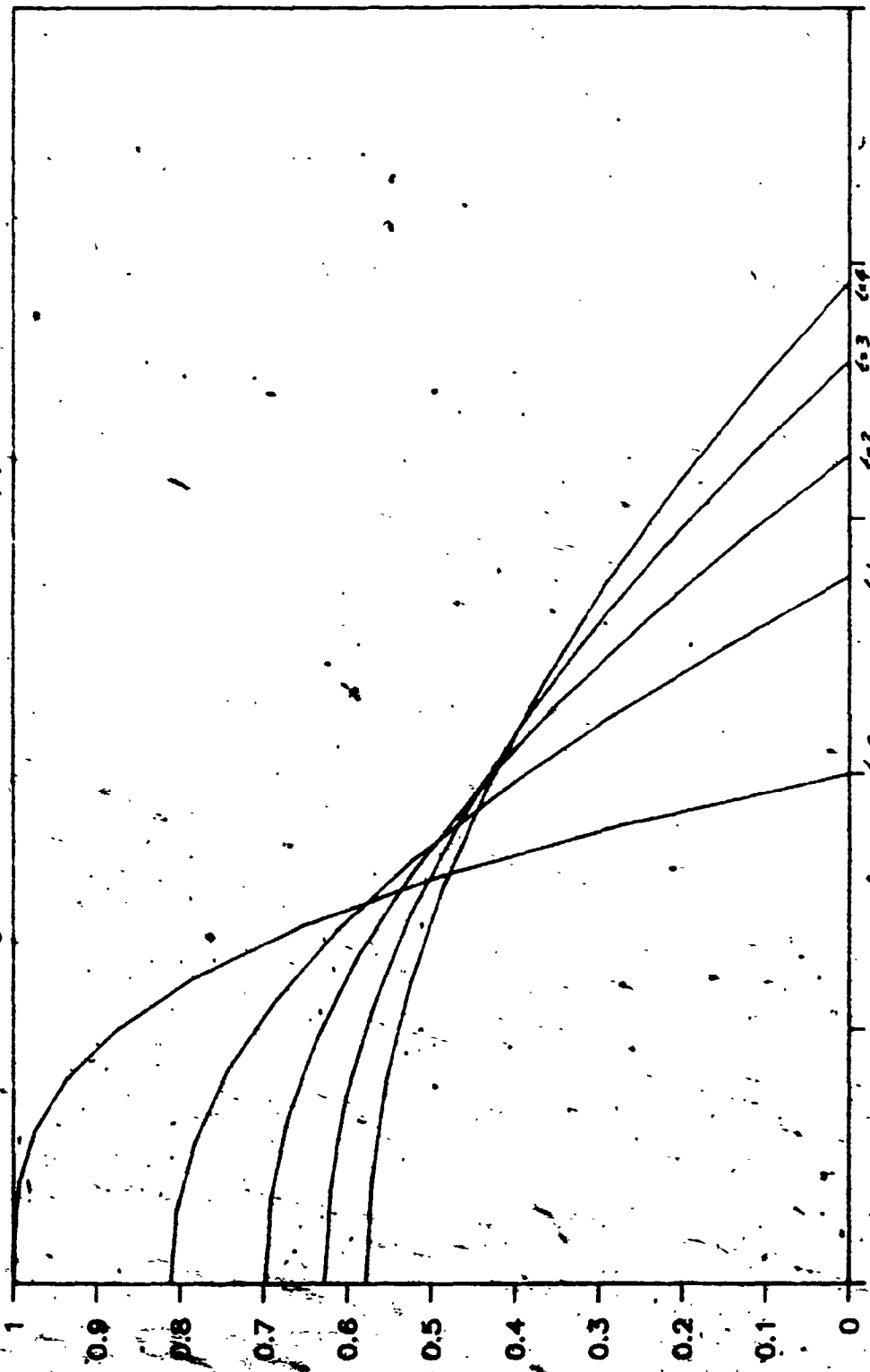

Figure 17 – Cubic Initial Mound s(0)=2

Figure 18 – Humped Initial Mound e(0)=1

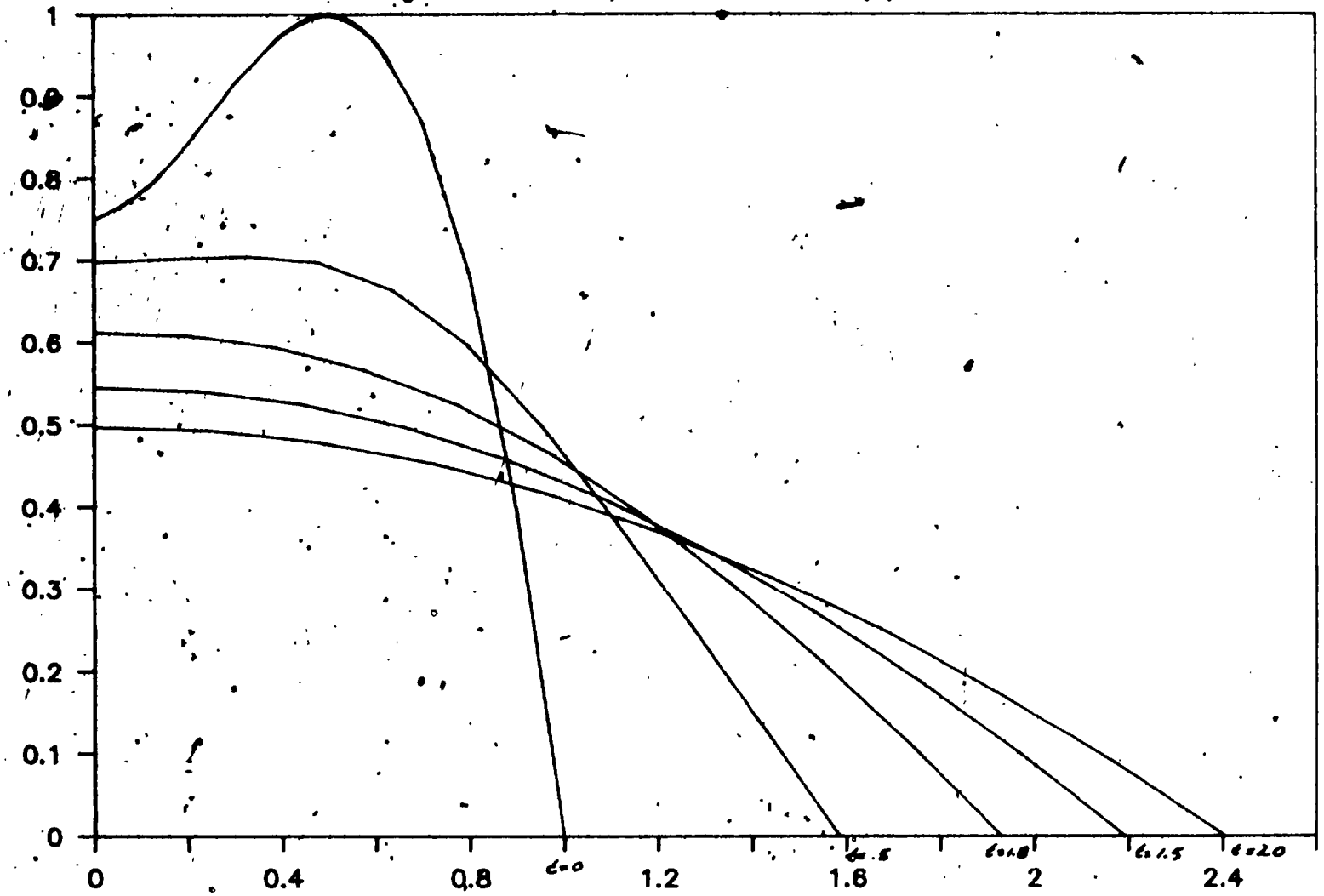

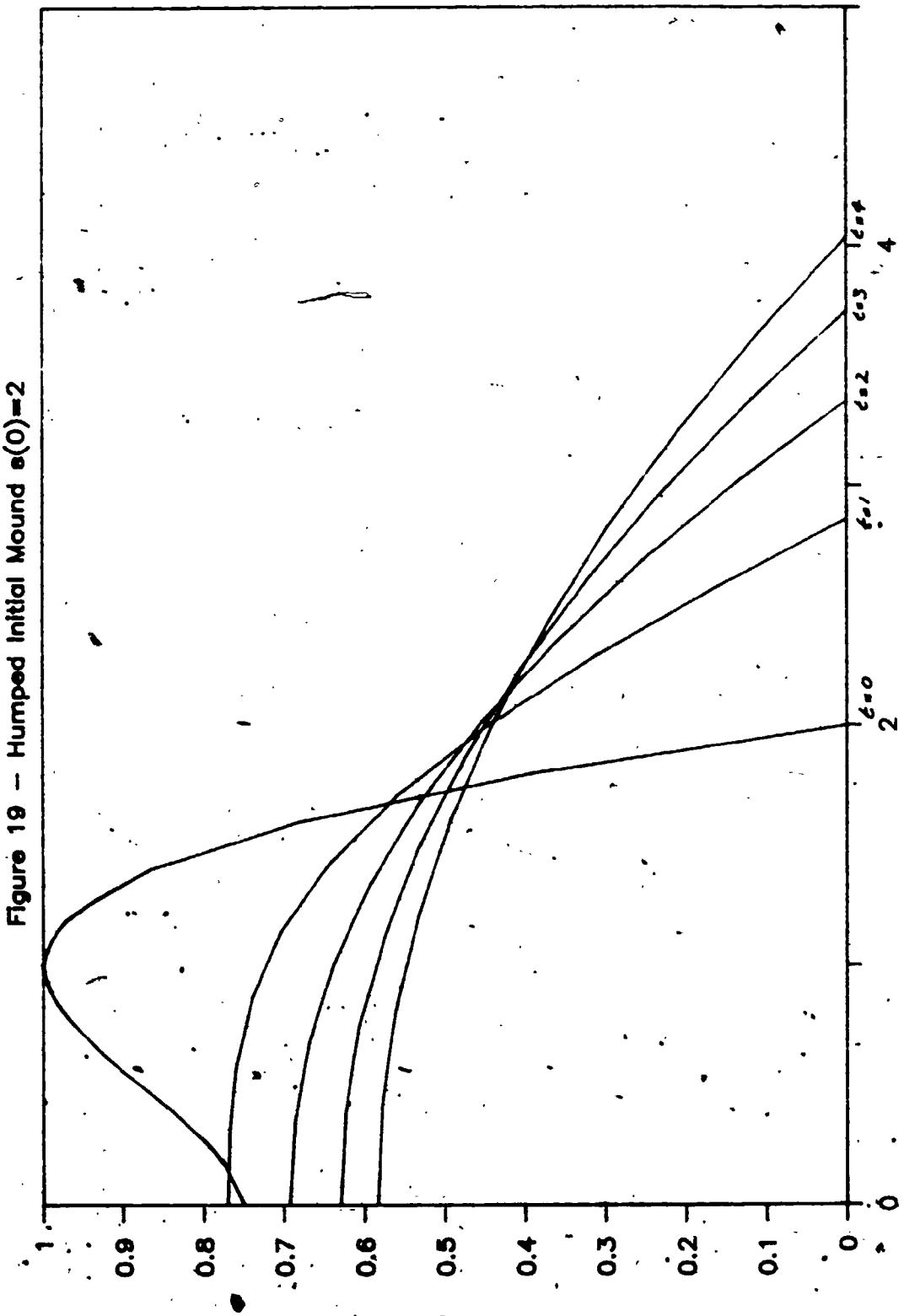

Figure 19 – Humped Initial Mound s(0)=2

$$f(x,0) = 1 - \left(\frac{x}{s(0)} \right)^3 \qquad (2.8.2)$$

$$f(x,0) = .75 + \left(\frac{x}{s(0)} \right)^2 \left[3.25 + \frac{x}{s(0)} \left(\frac{x}{s(0)} - 5 \right) \right] \qquad (2.8.3)$$

with $s(0) = 1$ and $s(0) = 2$ at time itervals of .5 and 1.0 respectively are given in Figures 16 to 19 respectively. Note that after a short time period the profiles of all these mounds look very similar to the profiles of the initially parabolic mound with the same $s(0)$ condition. This is especially noteworthy of the initial profile (2.8.3) which has a substantial 'hump' that quickly dissipates.

2.9 Conclusions

The predictor-corrector scheme for calculating new boundary positions, proposed in this Chapter is effective and does not require iteration. When the slope of the moving boundary is calculated using central differences (i.e. Crank Nicolson) the predictor-corrector scheme allows for the use of larger time steps for a given spatial grid as compared to using alternate one sided differences (i.e. MacCormack).

The two methods for the potential appear to have the same global accuracy. Since the global accuracy of Method 1 is second order in space this must also be the case for Method 2.

The stream function, transformed polar coordinate formulation of Method 3 is less accurate but more robust in terms of the time step selection, for a given number of spatial grid points than either of the other methods. This inaccuracy appears to be due to the lower spatial grid resolution near the toe of the moving boundary.

The Dupuit approximation is excellent for subsidence mound problems where the aspect ratio (i.e. width to height ratio) is large.

Employing a regular rectangular finite difference grid where subscripts l, j and superscript n denote a quantity evaluated at grid point $\xi_l = (l-1)h$, $\eta_j = (j-1)k$, and $\tau^n = \Delta\tau\, n$

yields the difference equation:

$$\left.\begin{aligned} & C_{0_{l,j}}^n \phi_{l,j}^n - C_{1_{l,j}}^n \phi_{l-1,j}^n - C_{2_{l,j}}^n \phi_{l,j+1}^n \\ & - C_{3_{l,j}}^n \phi_{l-1,j}^n - C_{4_{l,j}}^n \phi_{l,j-1}^n = RHS_{l,j}^n \end{aligned}\right\} \quad (2.7.3)$$

$l = 1, 2, \ldots, M$ and $j = 1, 2, \ldots, NROWS_l$

For grid points $l = 1, 2, \ldots, M$ and $j = 1, 2, \ldots, NROWS_l - 1$, where $NROWS_l$ = integer part of $\left\{ \frac{f_l}{k} \right\}$ and where the five point operator depicted in Figure 5 is used with $h = \frac{1}{M}$ and $k = \frac{1}{N}$. The coefficients are:

$$\left.\begin{aligned} C_{0_{l,j}}^n &= 2\left(1 + \left(\frac{s_l^n h}{k}\right)^2\right) \\ C_{1_{l,j}}^n &= C_{3_{l,j}}^n = +1 \\ C_{2_{l,j}}^n &= C_{2_{l,j}}^n = \left(\frac{s_l^n h}{k}\right)^2 \\ RHS_{l,j}^n &= 0 \end{aligned}\right\} \quad (2.7.4)$$

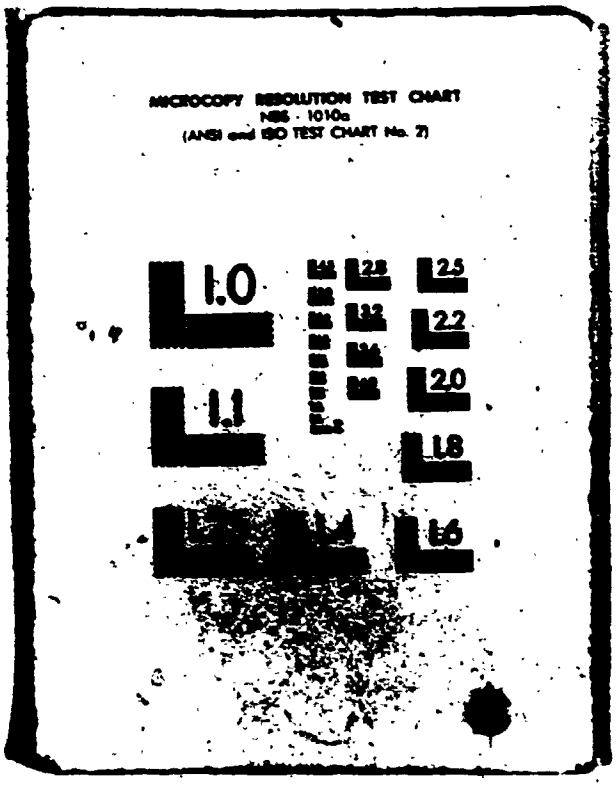
MICROCOPY RESOLUTION TEST CHART
NBS - 1010a
(ANSI and ISO TEST CHART No. 2)
1.0
1.1
2.5
2.2
2.0
1.8
1.6

Chapter 3 - A Heated Subsidence Mound Problem

3.1 Introduction

In this Chapter the effects of adding heat through the moving boundary on the subsidence mound problem of Chapter 2 are investigated. Again, the applications of interest come from groundwater hydrology where the storage of heat in geothermal reservoirs is of interest and from petroleum engineering where the in situ heating of oil in tar sands is of interest. The latter is an extremely complicated situation where steam, water and oil are all present in various regions of the oil reservoir. One approach to the oil recovery problem is exemplified in Douglas (1985) where the saturations of the various components in the assumed homogeneous mixture are the variables. Basic physical laws as well as empirical relations are then used to formulate a system of partial differential equations for the saturations and temperature in a known and fixed domain. The goal of these studies is to accurately predict well recovery rates.

The approach taken in this study, however, is one where the moving boundary nature of the problem is retained while other aspects of the problem are simplified. Thus to the subsidence mound problem from Chapter 2 are added density dependence on temperature in

the bouyancy term (Bousinesq approximation) as well as viscosity dependence on temperature. These dependecies introduce coupling between the equations for continuity momentum and energy conservation. For convenience the boundary condition on temperature on the moving boundary is that the temperature is known there. This is an attempt to approximate the phase change in the steam/water which releases energy at a fixed temperature.

The problem is formulated in terms of a stream function and normalized temperature in both Cartesian and polar coordinates and the moving domain is fixed via the coordinate transformations of Chapter 2. Finite difference methods are used to solve the resulting system of nonlinear coupled partial differential equations and the results of both approaches are compared.

3.2 Equations for the Flow of Heated Fluids Through a Porous Medium

To obtain the macroscopic equations for heated flow through a porous medium, in the spirit of the type of model in Chapter 2 an energy balance equation is required in addition to (2.2.1) and (2.2.2). The desired equations are given in Combarnous and Bories (1975) as :

$$P \frac{\partial \rho}{\partial t} + \vec{\nabla} \cdot (\rho \vec{q}) = 0 \qquad (3.2.1)$$

$$\frac{\rho}{P} \frac{\partial \vec{q}}{\partial t} + \frac{\rho}{P^2} (\vec{q} \cdot \vec{\nabla}) \vec{q} = \vec{\nabla} p + \rho \vec{g} - \frac{\mu}{k} \vec{q} \qquad (3.2.2)$$

$$\frac{\partial}{\partial t} ((\rho c)^* T) + \vec{\nabla} \cdot ((\rho c)^f \vec{q} T) = \vec{\nabla} \cdot (\lambda^* \vec{\nabla} T) \qquad (3.2.3)$$

where T is temperature, $\alpha_2 \equiv (\rho c)^f$ and $(\rho c)^s$ are the heat capacities of the fluid and solid respectively, $\alpha_1 \equiv (\rho c)^*$ is the effective heat capacity of the solid/fluid which is defined as:

$$(\rho c)^* \equiv (\rho c)^s (1 - P) + (\rho c)^f P \qquad (3.2.4)$$

and λ^* is the effective thermal conductivity. Again an equation similar to (3.2.3) can be derived using the volume averaging process as shown in Cheng (1978).

The simplifying assumptions made in this work are that the porous medium has constant porosity, permeability and heat capacity and that the fluid has constant heat capacity and that the effective thermal conductivity is constant. The equations of state are assumed to be:

$$\rho = \rho_o (1 - \beta (T - T_o)) \qquad (3.2.5)$$

$$\frac{1}{\mu} = \frac{1}{\mu_o} \left(\frac{T - T_o}{\Delta T} \right)^m \qquad (3.2.6)$$

where β is the coefficient of thermal expansion of the fluid and ΔT is a reference temperature difference used to fit to experimental data. Model (3.2.6) is taken as an approximation for the viscosity of oil with m about 3 to 4 (see Butler, McNab and Lo (1979)).

Furthermore, variations in density are neglected except in the bouyancy term $\rho \vec{g}$ (this is called Boussinesq flow) and as in Chapter 2, the filtration velocity, $\vec{q}$, is assumed to be small and vary little in time or space. Thus equations (3.2.1) and (3.2.2) become:

$$\vec{\nabla} \cdot \vec{q} = 0 \qquad (3.2.7)$$

$$\vec{q} = - \frac{k}{\mu} (\vec{\nabla} p - \rho \vec{g}) \qquad (3.2.8)$$

A potential ϕ can be introduced, as in Chapter 2, such that:

$$\phi = -\frac{k}{\mu_o}(p + \rho_o g z) \qquad (3.2.9)$$

However, since the curl of $\vec{q}$ does not vanish, the potential does not satisfy Laplace's equation.

The boundary conditions for the heated subsidence mound problem are the same as those for the unheated problem of Chapter 2 with the additional boundary conditions on temperature, namely:

on $z = 0$, $w = 0$ and $\theta_z = 0$ (insulated bottom)

on $x = 0$, $u = 0$ and $\theta_x = 0$ (symmetric mound)

on $z = f(x,t)$ $\phi = \frac{k \rho_o g}{\mu_o} f(x,t)$; $\theta = \theta_{sb}$ (given)

(3.2.10)

and $f_t = w - f_x u$ with $f(s(t),t) = 0$

and $f_x(0,t) = 0$

and finally on $x = s(t)$ $\dot{s} = -\frac{u}{f_x}$

Similarly the initial conditions are that $f(x,0)$, $s(0)$ and $\theta(x,z,0)$ all given.

As in Chapter 2, no microscopic details of the physical situation at the multiphase interface that comprizes the moving boundary have been included. Thus the boundary conditions at the toe of the moving boundary are derived from macroscopic, zero heat flux and no flow conditions. Additionally, the condition that the temperature is a given fixed constant along the moving boundary is a first approximation to the physical situation during the in situ heating of heavy oils. In this case, most of the heat release is due to a phase change in steam/water releasing heat at a relatively fixed temperature. Thus, for example, no account is made in the current model for pressure changes, chemical reactions or an energy balance across the moving boundary.

3.3 Statement of the Problem

The problem to be solved is depicted in Figure 20 below.

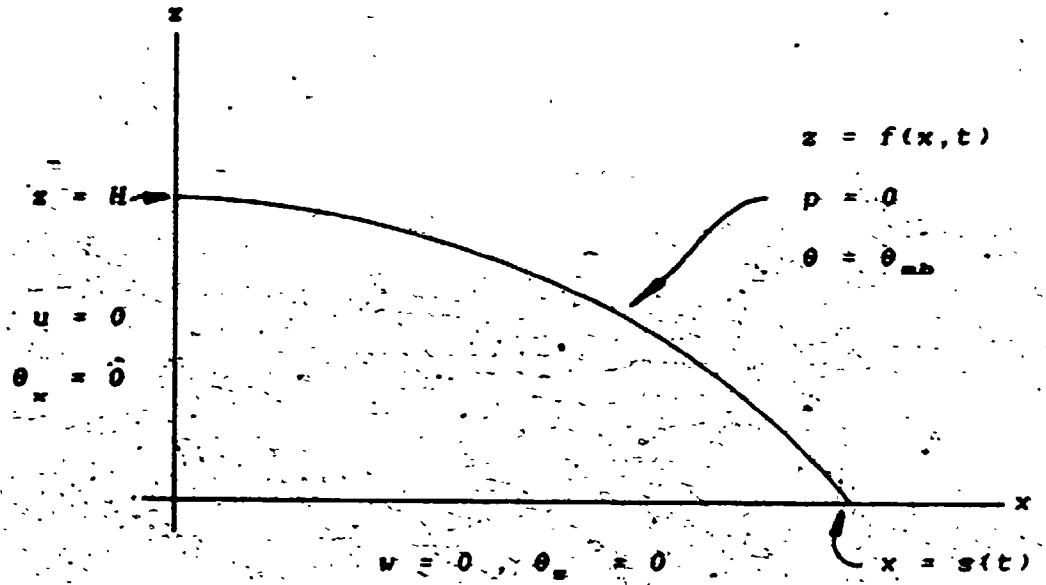

Figure 20 - The Heated Subsidence Mound Problem

Upon the introduction of the non-dimensional quantities:

$$x' = \frac{x}{H} \quad , \quad z' = \frac{z}{H} \quad , \quad f' = \frac{f}{H} \quad , \quad s' = \frac{s}{H}$$

$$t' = \frac{\lambda}{H^2 a_1 Ra}\, t \quad , \quad p' = \frac{1}{\rho_0 g H}\, p \quad , \quad \vec{q}' = \frac{a_1 H}{\lambda Ra}\, \vec{q} \quad , \qquad (3.3\text{-}1)$$

$$\phi' = p' + z' \quad , \quad \rho' = \frac{\rho}{\rho_0} \quad , \quad \mu' = \frac{\mu}{\mu_0} \quad , \quad \theta = \frac{T - T_0}{\Delta T}$$

where H is the initial height of the mound at the central line of symmetry, θ is the non-dimensional temperature and the Rayleigh number, Ra, is defined as:

$$Ra = \frac{\alpha_2 k \rho_0 g \beta \Delta T H}{\mu_0 \lambda} \qquad (3.3.2)$$

The non-dimensional field equations are (dropping the primes):

$$\left.\begin{aligned} &\vec{\nabla} \cdot \vec{q} = 0 \\ &\vec{q} = -\frac{\alpha_1}{\alpha_2}\,\theta^m \left(\frac{\vec{\nabla}\phi}{\beta\,\Delta T} - \theta\,\hat{k} \right) \\ &\frac{\partial \theta}{\partial t} = \frac{1}{Ra}\,\nabla^2\theta + \vec{\nabla} \cdot \left(\theta^{m+1} \left(\frac{\vec{\nabla}\phi}{\beta\,\Delta T} - \theta\,\hat{k} \right) \right) \end{aligned}\right\} \qquad (3.3.3)$$

where $\hat{k}$ is a unit vector in the z direction.

Upon the introduction of a stream function ψ, such that:

$$\left.\begin{aligned} &\psi_z = -\frac{\alpha_2}{\alpha_1} P u = \frac{1}{\beta \Delta T}\,\theta^m \phi_x \\ &\psi_x = \frac{\alpha_2}{\alpha_1} P v = -\theta^m \left(\frac{1}{\beta \Delta T}\,\phi_z - \theta \right) \end{aligned}\right\} \qquad (3.3.4)$$

the above field equations become:

$$\left.\begin{aligned} \psi_{xx} + \psi_{zz} - \frac{m}{\theta}\left(\psi_x \theta_x + \psi_z \theta_z \right) &= \theta^m \theta_x \\ \frac{\partial \theta}{\partial t} &= \frac{1}{Ra}\left(\theta_{xx} + \theta_{zz} \right) + \theta_x \psi_z - \theta_z \psi_x \end{aligned}\right\} \quad (3.3.5)$$

The boundary conditions become:

on $z = 0$, $\psi = 0$ and $\theta_z = 0$

on $x = 0$, $\psi = 0$ and $\theta_x = 0$

on $z = f(x,t)$, $\theta = \theta_{mb}$, $\psi_z - f_x \psi_x = f_x \theta_{mb}^m \left(\frac{1}{\beta \Delta T} - \theta_{mb} \right)$

$$\text{and} \quad f_t = \frac{\alpha_1}{\alpha_2 P}\left(\psi_{xx} + f_x \psi_z \right) \quad (3.3.6)$$

with $f(s(t),t) = 0$ and $f_x(0,t) = 0$

and finally on $x = s(t)$,

$$\dot{s} = - \frac{\alpha_1}{\alpha_2 P} f_x(s(t),t)\, \theta_{mb} \left(\frac{1}{\beta \Delta T} - \theta_{mb} \right)$$

Thus the equations involve the four non-dimensional parameters: Ra, $\frac{\alpha_1}{\alpha_2 P}$, $\beta\, \Delta T$ and m .

Note that a different normalization could be used that would result in the Rayleigh number, Ra, appearing with the convective terms in the temperature equation.

This is not done here since the interest, in this study lies with moderate Rayleigh number (i.e. $Ra > 1$) and as a result $\frac{1}{Ra}$ should appear in the equations (see Roache (1972)).

As in Chapter 2, the above problem can be reformulated in terms of polar coordinates, (r,ϕ), as follows:

$$\left.\begin{aligned} \frac{1}{r}\frac{\partial}{\partial r}\left(r\,\psi_r \right) + \frac{1}{r^2}\,\psi_{\phi\phi} - \frac{m}{\theta}\left(\psi_r\,\theta_r + \frac{1}{r^2}\,\psi_\phi\,\theta_\phi \right) \\ = \theta^m \left(\cos(\phi)\,\theta_r - \frac{\sin(\phi)}{r}\,\theta_\phi \right) \end{aligned}\right\} (3.3.7)$$

$$\frac{\partial\theta}{\partial t} = \frac{1}{Ra}\left(\frac{1}{r}\frac{\partial}{\partial r}\left(r\,\theta_r \right) + \frac{1}{r^2}\,\theta_{\phi\phi} \right) + \frac{1}{r}\left(\psi_\phi\,\theta_r - \psi_r\,\theta_\phi \right)$$

$$\left.\begin{aligned} &\text{with on } \phi = 0\,,\ \psi = 0 \text{ and } \theta_\phi = 0 \\ &\quad \text{on } \phi = \frac{\pi}{2}\,,\ \psi = 0 \text{ and } \theta_\phi = 0 \\ &\quad \text{on } r = 0\,,\ \psi = 0\,,\ \theta_\phi = 0 \text{ and } \theta_r = 0 \\ &\text{and on } r = R(\phi,t)\,,\ \theta = \theta_{mb}\,, \end{aligned}\right\} (3.3.8)$$

$$\frac{R_\phi}{R}\,\psi_\phi - R\,\psi_r = \theta_{mb}^m\left(\frac{1}{\beta\Delta T} - \theta_{mb} \right)\left(R_\phi \sin(\phi) + R\cos(\phi) \right)$$

$$\text{and } R_\tau = -\frac{\alpha_1}{\alpha_2 P}\,\frac{1}{R}\left(R_\phi\,\psi_r + \psi_\phi \right)$$

$$\text{with } R_\phi\left(\frac{\pi}{2}, t \right) = 0.$$

Finally, the initial conditions are that $R(\phi,0)$, $\theta(r,\phi,0)$ and θ_{wb} are all given.

3.4 Review of Previous Work

The problem presented in this chapter has apparently not been studied in the past. This problem differs from past work that computations with the combination of a Bousinesq fluid with temperature dependent density and viscosity and a moving interface with heat influx into the fluid along it have not been reported.

Although in the present heated subsidence mound problem convection may not be that important due to the fact that the heating is from above, the classical problem of convection in a porous slab is somewhat related in terms of computational methods. Numerous studies using the type of model descibed in section 3.2 appear in the literature with regards to this convection in a porous slab problem. Most of this work has focussed on the hydro-thermal aquifier applications where the onset on convection and steady-state convection patterns are of interest. Reviews by Combarnous and Bories (1975) and Cheng (1978) discuss both approximate analytic and numerical results.

Several recent numerical studies on steady-state and transient convection patterns as a result of several different heating configurations inside a porous slab of various aspect ratios highlight some relevant numerical

difficulties.

Hickox and Gartling (1981) used a Galerkin finite element approach to solve for the steady state convection pattern in a closed porous box with end to end temperature difference. They used a Bousinesq fluid with a linearly temperature dependent density. Successive substitution was used to iterate between the pressure and temperature equations. As the Rayleigh number was increased convergence was achieved by increasing the convergence criteria tolerence (e.g. to 10^{-2} for Ra = 200). Numerical results are reported for Rayleigh numbers from 25 to 200 and aspect ratios from .1 to .5 .

Prasad and Kulacki (1984a) used a conservative finite difference approach to solve the same problem and one with constant heat flux along one wall (1984b) for Rayleigh numbers from 100 to 10,000. They used point succesive substitution with a relaxations scheme to obtain convergence to .1 percent.

Loh and Rasmussen (1984) also solve a similar end to end heated porous slab problem but with a free surface. They used a coordinate transformation to map the domain into a box and used standard second order finite differences with a successive substitution iterative scheme with overrelaxation to obtain solutions for

Rayleigh numbers from less than 1 to 1,000. They concluded that the free surface had little effect on the problem and that the steady-state free surface was almost flat.

Gary and Kassoy (1981) studied the transient convection patterns in a porous slab heated from below and filled with a Bousinesq fluid. They used a finite difference Poisson solver to solve for stream function and compared an Alternating Direction Implicit, ADI, method and a Runge-Kutta-Fehlberg, RKF, method for calculating the temperatures. They also tried various schemes for dealing with the time dependent coupling terms between the equations. They concluded that the ADI method was more efficient than the RKF method for computing steady-state solutions while the reverse was true for oscillatory solutions. They reported that fourth order spatial derivatives were more efficient for a given accuracy. Additionally they found a predictor-corrector scheme for the coupling terms to be more stable than an extrapolated scheme. Finally they reported various different steady-state solutions for a Rayleigh number of 40 depending upon the initial conditions.

Horne and O'Sullivan (1978) also studied the transient convection in a porous slab heated from below. They attempted to use a fluid closely matching the physical

properties of water and thus incorporate both a quadratic dependence of density on temperature and an inverse cubic dependence of viscosity on temperature. They reformulate the problem into one involving eliptic equations for pressure and stream function and a parabolic equation for the temperature with all the coupling terms in Jacobian form. This allowed them to use Arakawa's finite difference scheme which semi-conserves the kinetic energy of the fluid. Fourth order spatial differences were used throughout their calculations. They reported various oscillatory and regular oscillatory convection patterns for Rayleigh numbers from 50 to 180.

Greydanus (1983) studied the transient convection in a closed porous slab heated from below using the same governing equations as the present study. He performed a linear stability analysis and found the critical Rayleigh numbers for the onset of convective instabilities to be approximately 280 and 417 for values of the parameter m in the viscosity temperature relationship of 3 and 4 respectively. He attempted to calculate the steady state convection patterns using a central difference based finite difference scheme for the stream function and temperature equations. Fourth order spatial differences were used throughout. An SOR scheme for solving for the stream function values was combined with an ADI scheme for the temperature values with iteration between the two

equations. It was found that there were difficulties in obtaining convergence to steady state, especially at large Rayleigh numbers and when finer grids were used.

In summary it appears that finite differences methods can be effectively used to solve transient convection problems, at least for moderate Rayleigh numbers. Second order differences in space and time can be used but fourth order spatial derivatives may be more efficient. ADI methods appear to be effective for calculating steady state solutions. Finally, successive substitution with relaxation is the usual method for handling the coupling between the various equations.

For the heated subsidence mound problem, the interest lies in the transient behaviour of the boundary. In Chapter 2 it was found that the coordinate transformation is an effective way of dealing with the moving boundary. Thus it is intended to solve the problem in a coordinate transformed domain, using the equations as derived in the next section. The major problems not dealt with in Chapter 2 are the addition of a parabolic field equation for temperature equation and the coupling terms between the field equations. Due to the appearance of time and space dependent coefficients and a mixed second derivative term in the transformed temperature equation, the schemes used by the above researchers are not applicable. The method of

successive substitution with relaxation is, however, applicable to handling the coupling between the various equations and, as presented later is effective.

3.5 Numerical Method

3.5.1 Coordinate Transformation

The strategy in the development of a numerical scheme for this problem was to attempt to use methods similar to those for the unheated problem of Chapter 2. In particular, the coordinate transformation which was used to fix the moving boundary was adopted. Thus as in Section 2.7.1, set

$$\xi = \frac{x}{s(t)} \quad , \quad \eta = \frac{z}{f(x,t)} \quad \text{and} \quad \tau = t \qquad (3.5.1)$$

The transformed problem becomes:

$$\psi_{\xi\xi} - \frac{2\,\eta\,f_\xi}{f}\,\psi_{\xi\eta} + \frac{s^2 + \eta^2 f_\xi^2}{f^2}\,\psi_{\eta\eta} +$$

$$\left(- \frac{\eta\,(f\,f_{\xi\xi} - 2\,f_\xi^2)}{f^2} + \frac{m}{\theta}\left(\frac{\eta\,f_\xi}{f}\,\theta_\xi - \frac{s^2 + \eta^2 f_\xi^2}{f^2}\,\theta_\eta \right) \right) \psi_\eta +$$

$$+ \frac{m}{\theta}\left(\frac{\eta\,f_\xi}{f}\,\theta_\eta - \theta_\xi \right) \psi_\xi = s\left(\theta_\xi - \frac{\eta\,f_\xi}{f}\,\theta_\eta \right) \theta^m$$

(3.5.2a)

$$\frac{\partial\theta}{\partial\tau} = \frac{1}{Ra}\left(\frac{1}{s^2}\theta_{\xi\xi} - \frac{2\eta}{s^2 f}f_\xi\theta_{\xi\eta} + \frac{s^2+\eta^2 f_\xi^2}{s^2 f^2}\theta_{\eta\eta}\right)$$

$$+\left(-\frac{\eta\,(f f_{\xi\xi} - 2f_\xi^2)}{Ra\, s^2 f^2} - \frac{1}{s f}\psi_\xi + \frac{\alpha_1\eta}{\alpha_2 P s f}\psi_\xi\Big|_{\eta=1}\right)\theta_\eta$$

$$+\left(\frac{1}{s f}\psi_\eta - \frac{\alpha_1\xi}{\alpha_2 P s^2}f_\xi\Big|_{\substack{\xi=1\\ \eta=1}}\theta_{mb}^{m}\left(\frac{1}{B\Delta T} - \theta_{mb}\right)\right)\theta_\xi$$

(3.5.2b)

with $\psi = 0$ and $\theta_\xi = 0$ on $\xi = 0$,

$\psi = 0$ and $\theta_\eta = 0$ on $\eta = 0$,

$\psi = 0$ and $\theta = \theta_{mb}$ on $\xi = 1$,

and on $\eta = 1$, $\theta = \theta_{mb}$,

$$\left.\begin{aligned}(-s^2 + f_\xi^2)\psi_\eta - f f_\xi\psi_\xi &= s f f_\xi\theta_{mb}^{m}\left(\frac{1}{B\Delta T} - \theta_{mb}\right)\\ \end{aligned}\right\}$$ (3.5.3)

and $$f_\xi = \frac{\alpha_1}{\alpha_2 P}\left\{\frac{1}{s}\psi_\xi - \frac{\xi}{s^2}f_\xi f_\xi\Big|_{\xi=1}\theta_{mb}^{m}\left(\frac{1}{B\Delta T} - \theta_{mb}\right)\right\}$$

with $f_\xi(0,\tau) = 0$ and $f(1,\tau) = 0$

and finally $$\dot{s} = -\frac{\alpha_1}{\alpha_2 P s^2}f_\xi(1,\tau)\theta_{mb}^{m}\left(\frac{1}{B\Delta T} - \theta_{mb}\right)$$

The additional difficulties introduced into the equations by the coordinate transformation are the appearance of mixed derivative terms and time dependent coefficients for the Laplacian terms.

Similarly, in the polar coordinate formulation the moving boundary is fixed using transformation (2.7.19), that is,

$$\xi = \phi \ , \quad \eta = \frac{r}{R(\phi, t)} \quad \text{and} \quad \tau = t \tag{3.5.4}$$

The transformed problem is:

$$\eta \left(1 + \sigma^2 \right) \frac{\partial}{\partial \eta} \left(\eta \, \psi_\eta \right) - 2 \, \eta \, \sigma \, \psi_{\xi\eta} + \psi_{\xi\xi} - \eta \, \frac{\partial \sigma}{\partial \xi} \, \psi_\eta$$

$$- \frac{m}{\theta} \left(\left\{ \left(1 + \sigma^2 \right) \theta_\eta - \eta \, \sigma \, \theta_\xi \right) \psi_\eta + \left\{ - \eta \, \sigma \, \theta_\eta + \theta_\xi \right\} \psi_\xi \right)$$

$$= \eta \, R \, \theta^m \left\{ \eta \left(\cos(\xi) + \sigma \sin(\xi) \right) \theta_\eta - \sin(\xi) \, \theta_\xi \right\}$$

(3.5.5a)

$$\frac{\partial \theta}{\partial \tau} = \frac{1}{Ra} \left(\frac{1}{\eta R} \right)^2 \left\{ \eta \left(1 + \sigma^2 \right) \frac{\partial}{\partial \eta} \left(\eta \, \theta_\eta \right) - 2 \, \eta \, \sigma \, \theta_{\xi\eta} + \theta_{\xi\xi} \right)$$

$$+ \frac{1}{\eta \, R^2} \left[\left(- \frac{1}{Ra} \frac{\partial \sigma}{\partial \xi} - \frac{\alpha_1}{\alpha_2 P} \, \psi_\xi \Big|_{\eta=1} + \psi_\xi \right) \theta_\eta - \psi_\eta \, \theta_\xi \right]$$

(3.5.5b)

where σ is as defined in Section (2.7.1) and

with on $\xi = 0$, $\Psi = 0$ and $-\eta\,\sigma\,\theta_{\eta} + \theta_{\xi} = 0$,

on $\xi = \frac{\pi}{2}$, $\Psi = 0$ and $\theta_{\xi} = 0$,

on $\eta = 0$, $\Psi = 0$, $\theta_{\xi} = 0$ and $\theta_{\eta} = 0$,

and on $\eta = 1$, $\theta = \theta_{mb}$, (3.5.6)

$$\sigma\,\Psi_{\xi} - (1 + \sigma^2)\,\Psi_{\eta} = R\,\theta_{mb}^{m}\left(\frac{1}{\beta\Delta T} - \theta_{mb}\right)\left(\sigma\,\sin(\xi) + \cos(\xi)\right)$$

and $R_{\xi} = -\frac{\alpha_s}{\alpha_g P}\left(\frac{1}{R}\right)\Psi_{\xi}$ with $R_{\xi}\left(\frac{\pi}{2}, \tau\right) = 0$

Again, the coordinate transformation has introduced mixed derivative terms as well as time dependence in the Laplacian's coefficients..

3.5.2 The Stream Function Equation

The finite difference schemes for the stream function equation are similar to those used for Method 2 for the potentials in transformed Cartesian coordinates and Method 3 for the stream function in transformed polar coordinates in Chapter 2.

That is, in transformed Cartesian coordinates, employing a nine point difference molecule at interior points of a rectangular grid identical to that in Section 2.7.1, yields the following difference equation for the stream function:

$$C_{0_{i,j}}^{n}\,\psi_{i,j}^{n} - C_{1_{i,j}}^{n}\,\psi_{i+1,j}^{n} - C_{2_{i,j}}^{n}\,\psi_{i,j+1}^{n}$$

$$- C_{3_{i,j}}^{n}\,\psi_{i-1,j}^{n} - C_{4_{i,j}}^{n}\,\psi_{i,j-1}^{n} - C_{5_{i,j}}^{n}\,\psi_{i+1,j+1}^{n}$$

$$- C_{6_{i,j}}^{n}\,\psi_{i-1,j+1}^{n} - C_{7_{i,j}}^{n}\,\psi_{i-1,j-1}^{n} - C_{8_{i,j}}^{n}\,\psi_{i+1,j-1}^{n}$$

$$= RHS_{i,j}^{n} \qquad (3.5.7)$$

$i = 2,3,4,\ldots,M$ and $j = 2,3,4,\ldots,N$

where the coefficients are:

$$C^n_{0_{i,j}} = 2\left(A^n_{i,j} + C^n_{i,j} + 2 B^n_{i,j} \left(\alpha^n_{2_{i,j}} - \alpha^n_{1_{i,j}} \right) \right)$$

$$C^n_{1_{i,j}} = A^n_{i,j} + 2 B^n_{i,j} \left(\alpha^n_{2_{i,j}} - \alpha^n_{1_{i,j}} \right) + E^n_{i,j}$$

$$C^n_{2_{i,j}} = C^n_{i,j} + 2 B^n_{i,j} \left(\alpha^n_{2_{i,j}} - \alpha^n_{1_{i,j}} \right) + D^n_{i,j}$$

$$C^n_{3_{i,j}} = A^n_{i,j} + 2 B^n_{i,j} \left(\alpha^n_{2_{i,j}} - \alpha^n_{1_{i,j}} \right) - E^n_{i,j}$$

$$C^n_{4_{i,j}} = C^n_{i,j} + 2 B^n_{i,j} \left(\alpha^n_{2_{i,j}} - \alpha^n_{1_{i,j}} \right) - D^n_{i,j}$$

$$C^n_{5_{i,j}} = C^n_{7_{i,j}} = 2 B^n_{i,j} \alpha^n_{2_{i,j}} \qquad \Big\} (3.5.8)$$

$$C^n_{6_{i,j}} = C^n_{8_{i,j}} = -2 B^n_{i,j} \alpha^n_{2_{i,j}}$$

$$RHS^n_{i,j} = e^n \left(\theta^n_{i,j} \right)^{n+1} \left(h^2 T_{c_{i,j}} + h k B^n_{i,j} T_{n_{i,j}} \right)$$

where $A^n_{i,j}$, $B^n_{i,j}$, $C^n_{i,j}$, $\alpha^n_{1_{i,j}}$ and $\alpha^n_{2_{i,j}}$ are as defined in (2.7.13) and (2.7.14) and

$$D^n_{i,j} = \frac{-n_1 \left(f^n_i \left(f^n_{i+1} - 2 f^n_i + f^n_{i-1} \right) - \left(f^n_{i+1} - f^n_{i-1} \right)^2 / 2 \right)}{2 k \left(f^n_i \right)^2}$$

$$- m \left(B^n_{i,j} T_{c_{i,j}} + C^n_{i,j} T_{n_{i,j}} \right)$$

$$E^n_{i,j} = -m\left(B^n_{i,j} T_{\eta}{}^n_{i,j} + A^n_{i,j} T_{\xi}{}^n_{i,j} \right) \qquad (3.5.9)$$

$$T_{\xi}{}^n_{i,j} = \frac{1}{h}\left(\frac{\theta^n_{i+1,j} - \theta^n_{i,j}}{\theta^n_{i+1,j} + \theta^n_{i,j}} + \frac{\theta^n_{i,j} - \theta^n_{i-1,j}}{\theta^n_{i,j} + \theta^n_{i-1,j}} \right)$$

$$T_{\eta}{}^n_{i,j} = \frac{1}{k}\left(\frac{\theta^n_{i,j+1} - \theta^n_{i,j}}{\theta^n_{i,j+1} + \theta^n_{i,j}} + \frac{\theta^n_{i,j} - \theta^n_{i,j-1}}{\theta^n_{i,j} + \theta^n_{i,j-1}} \right)$$

To complete the system of equations for the stream function values the boundary condition on $\eta = 1$ is discretized as follows:

$$B^n_{i,N+1}\left(\Psi^n_{i+1,N+1} - \Psi^n_{i-1,N+1} \right)$$

$$+ C^n_{i,N+1}\left(3\,\Psi^n_{i,N+1} - 4\,\Psi^n_{i,N} + \Psi^n_{i,N-1} \right)$$

$$= 2\,h\,s^n\,B^n_{i,N+1}\left(\frac{1}{\beta\Delta T} - \theta^n_{i,N+1} \right)\left(\theta^n_{i,N+1} \right)^m \qquad (3.5.10)$$

$$i = 2,3,4,\ldots,M$$

Similarly, the stream function equation in transformed polar coordinates is discretized using a nine point difference molecule on the grid introduced in Section

2.7.1 yielding equation (3.5.7) above where

$$C^n_{o_{i,j}} = 2 \left(A^n_{i,j} + \eta_j C^n_{i,j} + 2 B^n_{i,j} \left(\alpha_{2_{i,j}} - \alpha^n_{1_{i,j}} \right) \right)$$

$$C^n_{1_{i,j}} = A^n_{i,j} + 2 B^n_{i,j} \left(\alpha^n_{2_{i,j}} - \alpha^n_{1_{i,j}} \right) + E^n_{i,j}$$

$$C^n_{2_{i,j}} = \eta_{j-1/2} C^n_{i,j} + 2 B^n_{i,j} \left(\alpha^n_{2_{i,j}} - \alpha^n_{1_{i,j}} \right) + D^n_{i,j}$$

$$C^n_{3_{i,j}} = A^n_{i,j} + 2 B^n_{i,j} \left(\alpha^n_{2_{i,j}} - \alpha^n_{1_{i,j}} \right) - E^n_{i,j}$$

$$C^n_{4_{i,j}} = \eta_{j-1/2} C^n_{i,j} + 2 B^n_{i,j} \left(\alpha^n_{2_{i,j}} - \alpha^n_{1_{i,j}} \right) - D^n_{i,j}$$

$$C^n_{5_{i,j}} = C^n_{7_{i,j}} = 2 B^n_{i,j} \alpha^n_{1_{i,j}} \qquad (3.5.11)$$

$$C^n_{6_{i,j}} = C^n_{8_{i,j}} = -2 B^n_{i,j} \alpha^n_{2_{i,j}}$$

$$RHS^n_{i,j} = h \eta_j R^n_i \left(\theta^n_{i,j} \right)^{m-1} \left(-h \sin(\xi_i) T^n_{\xi_{i,j}} \right.$$

$$\left. + \left(-k B^n_{i,j} \sin(\xi_i) + h \eta_j \cos(\xi_i) \right) T^n_{\eta_{i,j}} \right)$$

where $A^n_{i,j}$, $B^n_{i,j}$, $C^n_{i,j}$, $\alpha^n_{1_{i,j}}$ and $\alpha^n_{2_{i,j}}$ are as defined in (2.7.24) and (2.7.25) and

$$D^n_{1,j} = \frac{-\eta_1}{2}\left(\frac{h}{k}\right)\left(\Sigma^n_{1+1/2} - \Sigma^n_{1-1/2}\right)$$

$$\left. - \frac{m}{2}\left(h\, B^n_{1,j}\, T^n_{\xi_{1,j}} + k\, \eta_1\, C^n_{1,j}\, T^n_{\eta_{1,j}}\right)\right\} \quad (3.5.12)$$

$$E^n_{1,j} = -\frac{m}{2}\left(k\, B^n_{1,j}\, T^n_{\eta_{1,j}} + h\, T^n_{\xi_{1,j}}\right)$$

and where $\Sigma^n_{1+1/2}$ and $\Sigma^n_{1-1/2}$ are as defined in (2.7.27).

Again the above difference equation is used at all grid points in the interior of the domain and the boundary condition on $\eta = 1$ is discretized as follows in order to form a complete system for the unknown stream function values:

$$-k\, B^n_{1,N+1}\left(\psi^n_{1+1,N+1} - \psi^n_{1-1,N+1}\right)$$

$$-k\, C^n_{1,N+1}\left(3\,\psi^n_{1,N+1} - 4\,\psi^n_{1,N} + \psi^n_{1,n-1}\right)$$

$$= h\left(\left(R^n_{1+1} - R^n_{1-1}\right)\sin(\xi_1) + 2\,h\,R^n_1\cos(\xi_1)\right)$$

$$\left(\frac{1}{\beta\Delta T} - \theta^n_{1,N+1}\right)\left(\theta^n_{1,N+1}\right)^m \quad (3.5.13)$$

$$1 = 2,3,4,\ldots,M$$

Note that the local truncation error of all the above difference equations for the stream function is $O(h^2 + k^2)$

The system of linear equations for the stream functions have a similar structure to those in Chapter 2 for the potential of Method 2 and stream function of Method 3. Consequently, a similar IOM iterative proceedure with BSSOR preconditioning is used to obtain the solutions.

3.5.3 The Temperature Equation

The choice of finite difference schemes for the parabolic temperature equation is much more complex than that for the stream function equation. The desireable properties of such a scheme in the current context, are that it be second order accurate in time and space, unconditionally stable in a linear sense and that it be an alternating direction implicit, ADI, like. Relevant papers on this subject have been published by Warming and Beam who have derived a general two step ADI scheme for a second order parabolic partial differential equation with mixed derivative term and time and space dependent coefficients (but no convective terms) (see Beam and Warming (1980)) and a related scheme for mixed parabolic/hyperbolic systems that can be written in a conservative form (see Warming and Beam (1978a,b)). They also show that no one step unconditionally stable, second order in space and time, ADI scheme exits when there is a mixed derivative term present in the partial differential equation.

Briefly, the difficulty in formulating such ADI schemes lies in the splitting of the mixed derivative term in an ADI manner. Beam and Warming resolve this by treating this term explicitly. Unfortunately the temperature equation at hand can apparently not be written

in the form required to use their mixed - parabolic-hyperbolic scheme. Additionally the analysis required to prove the stability of their general two step scheme extended to include convective terms is extremely complex as the location of the roots of a quadratic with complex coefficients must be established (see Chan (1984) for more details on the application of a theory that gives equivalent conditions on a polynomial of reduced order - employing this theory to the present case, with first derivative terms, apparently does not give simple conditions on the relevant parameters). Furthermore, both schemes require that the time dependent coefficients be evaluated at an intermediate time between the current and advanced time levels. However, since in the present case, these coefficients depend on the boundary position and stream function which are unknown at times other than previous time levels, this poses a great difficulty. Under certain choices of the relevant parameters, this intermediate time will correspond to the advanced time level and as a result this method could be used with iteration. In any case, since these schemes are two step, a one step ADI scheme with lower accuracy is recommended for the first time step.

An alternative to ADI schemes is to use a basic time differencing scheme such as the Crank Nicholson schemes discussed in Section 2.7.2 without attempting to split the

spatial operators. As pointed out in Section 2.7.2 the only second order in time one step methods are the implicit mid-point rule and trapezoidal formula. If the former is used in conjunction with second order central differences for the spatial derivatives the resulting scheme is unconditionally stable in the linear sense. Since the coefficients of the spatial derivatives must be evaluated in the middle of the time interval and are coupled to the stream function and boundary equations, this method cannot be used. On the other hand if the trapezoidal formula was used, the coefficients would be required only at the current and advanced time levels, however the unconditional linear stability of the scheme has not be established.

Due to the above considerations, and the desire for simplicity the backward Euler method, a one step scheme was chosen for the temporal derivative in the temperature equation. Note that this method is first order accurate in time. It is easy to verify that this scheme in conjunction with second order central differences for the spatial derivatives is unconditionally stable in the linear sense (due to the parabolicity of the spatial operator). This scheme requires the solution of a large banded system of linear equations similar in structure to that for the stream function. Thus the same iterative method of solution (i.e. BSSOR preconditioned IOM) is used to solve

for the normalized temperatures. Note that the number of computations required for each BSSOR iteration that is required by the IOM method is approximately equivalent to that required for one ADI step. Thus since the IOM method is used to solve for the stream function, using the current method for solving for the temperature approximately doubles the computations required for finding the stream function alone while using an ADI method for the temperature equation would add approximately the cost of one additional BSSOR iteration. As a result it is expected that for this problem, incorporating an ADI method (if parameter values could be found so that it be unconditionally stable) be would roughly cut CPU time in half.

When the backward Euler method is used for the temporal derivative in the normalized temperature equation (first order accurate in time) and the spatial derivatives are discretized using nine point difference molecules similar to those used for the stream function equation (second order accurate in space)the resulting difference equation for the normalized temperatures is:

$$C_{o_{i,j}}^{n+1}\,\theta_{i,j}^{n+1} - C_{1_{i,j}}^{n+1}\,\theta_{i+1,j}^{n+1} - C_{2_{i,j}}^{n+1}\,\theta_{i,j+1}^{n+1}$$

$$- C_{3_{i,j}}^{n+1}\,\theta_{i-1,j}^{n+1} - C_{4_{i,j}}^{n+1}\,\theta_{i,j-1}^{n+1} - C_{5_{i,j}}^{n+1}\,\theta_{i+1,j+1}^{n+1}$$

$$- C_{6_{i,j}}^{n+1}\,\theta_{i-1,j+1}^{n+1} - C_{7_{i,j}}^{n+1}\,\theta_{i-1,j-1}^{n+1} - C_{8_{i,j}}^{n+1}\,\theta_{i+1,j-1}^{n+1}$$

$$= RHS_{i,j}^{n} \qquad (3.5.14)$$

$i = 1,2,3,\ldots,M$ and $j = 1,2,3,\ldots,N$

where the coefficients for the transformed Cartesian coordinates version are:

$$C_{o_{i,j}}^{n+1} = 1 + \frac{\Delta\tau}{h^2}\left(\frac{2}{Ra\,(s^{n+1})^2}\right)\left(A_{i,j}^{n+1} + C_{i,j}^{n+1}\right)$$

$$C_{1_{i,j}}^{n+1} = \frac{\Delta\tau}{h^2}\left(\frac{1}{Ra\,(s^{n+1})^2}\,A_{i,j}^{n+1} + E_{i,j}^{n+1}\right)$$

$$C_{2_{i,j}}^{n+1} = \frac{\Delta\tau}{h^2}\left(\frac{1}{Ra\,(s^{n+1})^2}\,C_{i,j}^{n+1} + D_{i,j}^{n+1}\right)$$

$$C_{3_{i,j}}^{n+1} = \frac{\Delta\tau}{h^2}\left(\frac{1}{Ra\,(s^{n+1})^2}\,A_{i,j}^{n+1} - E_{i,j}^{n+1}\right)$$

$$C_{4_{i,j}}^{n+1} = \frac{\Delta\tau}{h^2}\left(\frac{1}{Ra\,(s^{n+1})^2}\,C_{i,j}^{n+1} - D_{i,j}^{n+1}\right)$$

$$C_{5_{i,j}}^{n+1} = C_{7_{i,j}}^{n+1} = \frac{\Delta\tau}{h^2}\left(\frac{1}{2\,Ra\,(s^{n+1})^2}\right)B_{i,j}^{n+1} \qquad (3.5.15)$$

$$C_{6_{i,j}}^{n+1} = C_{8_{i,j}}^{n+1} = -\frac{\Delta\tau}{h^2}\left(\frac{1}{2\,Ra\,(s^{n+1})^2}\right)B_{i,j}^{n+1}$$

$$RHS_{i,j}^{n} = \theta_{i,j}^{n}$$

where $A^{n+1}_{i,j}$, $B^{n+1}_{i,j}$ and $C^{n+1}_{i,j}$ are as defined in (2.7.13) and

$$D^{n+1}_{i,j} = \frac{1}{Ra\ (s^{n+1})^2}$$

$$\left(\frac{-\eta_j \left(f^n_i \left(f^n_{i+1} - 2 f^n_i + f^n_{i-1} \right) - \left(f^n_{i+1} - f^n_{i-1} \right)^2 / 2 \right)}{2\ k\ (f^n_i)^2} \right)$$

$$+ \frac{h^2}{s^{n+1} f^{n+1}_i} \left(- S_{\xi^{n+1}_{i,j}} + \frac{\alpha_1}{\alpha_2 P}\ \eta_j\ S_{\xi^{n+1}_{i,M+1}} \right)$$

$$E^{n+1}_{i,j} = \frac{h^2}{s^{n+1} f^{n+1}_i} S_{\eta^{n+1}_{i,j}} - \frac{\alpha_1}{\alpha_2 P}\ h\ \xi_i \qquad \Big\} \text{(3.5.16)}$$

$$\left(\frac{\left(3 f^{n+1}_{M+1} - 4 f^{n+1}_M + f^{n+1}_{M-1} \right)}{2\ (s^{n+1})^2} \right)$$

$$\left(\frac{1}{B\Delta T} - \theta^{n+1}_{i,M+1} \right) \left(\theta^{n+1}_{i,M+1} \right)^{\alpha}$$

$$S_{\xi^{n+1}_{i,j}} = \frac{\psi^{n+1}_{i+1,j} - \psi^{n+1}_{i-1,j}}{2\ h}$$

$$S_{\eta^{n+1}_{i,j}} = \frac{\psi^{n+1}_{i,j+1} - \psi^{n+1}_{i,j-1}}{2\ k}$$

To complete the system of equations for the new normalized temperatures the boundary conditions on $\eta = 0$ and $\xi = 0$ are discretized and incorporated into the above equations as follows:

on $\eta = 0$, $B^{n+1}_{i,1} = 0$, $D^{n+1}_{i,1} = 0$, $S_{\xi^{n+1}_{i,1}} = 0$,

$$S_{\eta^{n+1}_{i,1}} = \frac{(-3\,\psi^{n+1}_{i,1} + 4\,\psi^{n+1}_{i,2} - \psi^{n+1}_{i,3})}{2\,k} \qquad \text{(5.5.17a)}$$

and $\theta^{n+1}_{i,0} = \theta^{n+1}_{i,2}$ for $i = 1,2,3,\ldots,M$

on $\xi = 0$, $B^{n+1}_{i,j} = 0$, $E^{n+1}_{i,j} = 0$, $S_{\eta^{n+1}_{i,j}} = 0$,

$$S_{\xi^{n+1}_{i,j}} = \frac{(-3\,\psi^{n+1}_{i,1} + 4\,\psi^{n+1}_{2,1} - \psi^{n+1}_{3,1})}{2\,h} \qquad \text{(3.5.17b)}$$

and $\theta^{n+1}_{0,j} = \theta^{n+1}_{2,j}$ for $j = 1,2,3,\ldots,N$

Similarly in transformed polar coordinates the coefficients of equation (3.5.14) are:

$$C_{\sigma_1}^{n+1}{}_{,j} = 1 + \frac{\Delta\tau}{h^2}\left\{\frac{2}{Re\,(\eta_j R_1^{n+1})^2}\right\}\left(A_{1,j}^{n+1} + \eta_j C_{1,j}^{n+1}\right)$$

$$C_{\tau_1}^{n+1}{}_{,j} = \frac{\Delta\tau}{h^2}\left\{\frac{1}{Re\,(\eta_j R_1^{n+1})^2} A_{1,j}^{n+1} + E_{1,j}^{n+1}\right\}$$

$$C_{\varepsilon_1}^{n+1}{}_{,j} = \frac{\Delta\tau}{h^2}\left\{\frac{1}{Re\,(\eta_j R_1^{n+1})^2} \eta_{j+1/2} C_{1,j}^{n+1} + D_{1,j}^{n+1}\right\}$$

$$C_{\theta_1}^{n+1}{}_{,j} = \frac{\Delta\tau}{h^2}\left\{\frac{1}{Re\,(\eta_j R_1^{n+1})^2} A_{1,j}^{n+1} - E_{1,j}^{n+1}\right\}$$

$$C_{\phi_1}^{n+1}{}_{,j} = \frac{\Delta\tau}{h^2}\left\{\frac{1}{Re\,(\eta_j R_1^{n+1})^2} \eta_{j-1/2} C_{1,j}^{n+1} - D_{1,j}^{n+1}\right\}$$

$$C_{\theta_1}^{n+1}{}_{,j} = C_{\tau_1}^{n+1}{}_{,j} = \frac{\Delta\tau}{h^2}\left\{\frac{1}{2\,Re\,(\eta_j R_1^{n+1})^2}\right\} B_{1,j}^{n+1} \qquad (3.5.18)$$

$$C_{\phi_1}^{n+1}{}_{,j} = C_{\theta_1}^{n+1}{}_{,j} = -\frac{\Delta\tau}{h^2}\left\{\frac{1}{2\,Re\,(\eta_j R_1^{n+1})^2}\right\} B_{1,j}^{n+1}$$

$$RHS_{1,j}^{n} = \theta_{1,j}^{n}$$

where $A_{1,j}^{n+1}$, $B_{1,j}^{n+1}$ and $C_{1,j}^{n+1}$ are as defined in (2.7.24) and

$$D_{1,j}^{n+1} = -\frac{1}{Re\,\eta_j\,(R_1^{n+1})^2}\left\{\frac{h}{2k}\right\}\left(\Sigma_{1+1/2}^{n+1} - \Sigma_{1-1/2}^{n+1}\right)$$

$$+ \frac{1}{\eta_j\,(R_1^{n+1})^2} S_{\varepsilon_{1,j}}^{n+1} - \frac{\alpha_1}{\alpha_2 P}\left\{\frac{1}{(R_1^{n+1})^2}\right\}\eta_j S_{\varepsilon_{1,m+1}}^{n+1}$$

$$E_{1,j}^{n+1} = -\frac{1}{\eta_j\,(R_1^{n+1})^2} S_{\eta_{1,j}}^{n+1} \qquad \Big\} (3.5.19)$$

$$S_{\xi_{i,j}}^{n+1} = \frac{\psi_{i+1,j-1}^{n+1} - \psi_{i-1,j-1}^{n+1}}{2h}$$

$$S_{\eta_{i,j}}^{n+1} = \frac{\psi_{i,j+1}^{n+1} - \psi_{i,j-1}^{n+1}}{2k}$$

and where $\Sigma_{i-1/2}^{n+1}$ and $\Sigma_{i-1/2}^{n+1}$ are as defined in (2,7.27').

To complete the system of equations for the new normalized temperatures the boundary conditions on $\xi = 0$ and $\xi = \frac{\pi}{2}$ are discretized and incorporated into the above equations as follows:

On $\xi = 0$, $\xi_{i,j}^{n+1} = 0$ & $S_{\eta_{i,j}}^{n+1} = 0$,

$$S_{\xi_{i,j}}^{n+1} = \frac{(-3\psi_{1,j}^{n+1} + 4\psi_{2,j}^{n+1} - \psi_{3,j}^{n+1})}{2h} \qquad (3.5.20)$$

and, since $-\eta\alpha\theta_\eta + \theta_\xi = 0$, $\theta_{0,j}^{n+1}$ is eliminated from the difference equation using:

$$-B_{i,j}^{n+1}(\theta_{0,j}^{n+1} - \theta_{2,j}^{n+1}) + \frac{1}{k^2}(\theta_{i,j+1}^{n+1} - \theta_{i,j-1}^{n+1}) = 0$$

$$j = 2, 3, 4, \ldots, N \qquad (3.5.21)$$

Finally taking $\frac{\partial}{\partial \eta}$ of the boundary condition on θ above gives:

$$\theta_{\xi\eta} = \sigma \frac{\partial}{\partial \eta} (\eta \theta_{\eta}) \qquad (3.5.22)$$

which allows $\theta_{\xi\eta}$ to be eliminated from the governing partial differential equation. Thus

$$C^{n+1}_{i,j} = \eta_j \left\{ \frac{h}{k} \right)^2 \left\{ 1 - \frac{1}{(2 h R_1^{n+1})^2} \right.$$

$$\left. (- 3 R_1^{n+1} + 4 R_2^{n+1} - R_3^{n+1})^2 \right\}$$

$$D^{n+1}_{i,j} = - \frac{1}{Re \eta_j (R_1^{n+1})^2} \left(\frac{1}{2 k h} \right)$$

$$\left(2 R_1^{n+1} - 5 R_2^{n+1} + 4 R_3^{n+1} - R_4^{n+1} \right)$$

$$+ \frac{1}{\eta_j (R_1^{n+1})^2} S_{\xi i,j}^{n+1} - \frac{\alpha_1}{\alpha_2 P} \left(\frac{1}{(R_1^{n+1})^2} \right) \eta_j S_{\xi i,j}^{n+1}$$

$$j = 2, 3, 4, \ldots, N \qquad (3.5.23)$$

and the coefficients become;

$$C_{o_1}^{n+1}{}_{,j} = 1 + \frac{\Delta\tau}{h^2}\left(\frac{2}{Ra\,(\eta_j R_1^{n+1})^2}\right)\left(A_{1,j}^{n+1} + \eta_j C_{1,j}^{n+1}\right)$$

$$C_{2_1}^{n+1}{}_{,j} = -2\left(\frac{\Delta\tau}{h^2}\right)\left(\frac{1}{Ra\,(\eta_j R_1^{n+1})^2}\, A_{1,j}^{n+1}\right)$$

$$C_{3_1}^{n+1}{}_{,j} = \frac{\Delta\tau}{h^2}\left[\frac{1}{Ra\,(\eta_j R_1^{n+1})^2}\,\eta_{j+1/2}\, C_{1,j}^{n+1} + D_{1,j}^{n+1} + \frac{1}{k^2 B_{1,j}^{n+1}}\left(\frac{\Delta\tau}{h^2}\right)\left(\frac{1}{Ra\,(\eta_j R_1^{n+1})^2}\, A_{1,j}^{n+1}\right)\right]$$

$$C_{4_1}^{n+1}{}_{,j} = \frac{\Delta\tau}{h^2}\left[\frac{1}{Ra\,(\eta_j R_1^{n+1})^2}\,\eta_{j-1/2}\, C_{1,j}^{n+1} - D_{1,j}^{n+1} - \frac{1}{k^2 B_{1,j}^{n+1}}\left(\frac{\Delta\tau}{h^2}\right)\left(\frac{1}{Ra\,(\eta_j R_1^{n+1})^2}\, A_{1,j}^{n+1}\right)\right]$$

$$C_{5_1}^{n+1}{}_{,j} = C_{6_1}^{n+1}{}_{,j} = C_{7_1}^{n+1}{}_{,j} = C_{8_1}^{n+1}{}_{,j} = C_{9_1}^{n+1}{}_{,j} = 0$$

$$RHS_{1,j}^{n} = \theta_{1,j}^{n} \qquad (3.5.24)$$

On $\xi = \frac{\pi}{2}$, $B_{M+1,j}^{n+1} = 0$; $E_{M+1,j}^{n+1} = 0$, $S_{\eta_{M+1,j}}^{n+1} = 0$,

$$S_{\xi_{M+1,j}}^{n+1} = \frac{\left(3\,\psi_{M+1,1}^{n+1} - 4\,\psi_{M,1}^{n+1} + \psi_{M-1,1}^{n+1}\right)}{2\,h}$$

and $\theta_{M+1,0}^{n+1} = \theta_{M+1,2}^{n+1}$

$j = 2, 3, 4, \ldots, N \qquad (3.5.25)$

Finally an equation is required for the temperature at the origin $r = 0$ or $\eta = 0$ where the normalized temperatute equation has a singularity. Using a second order backward difference formula for the zero temperature flux condition gives:

$$\theta^{n+1}_{1,1} = \frac{4\,\theta^{n+1}_{2,2} - \theta^{n+1}_{2,3}}{2\,k} \qquad (3.5.26)$$

$$1 = 1, 2, 3, \ldots, M+1$$

where $P = \frac{M}{2} + 1$ (assuming M is even).

Note that as previously mentioned an iteration scheme between the stream function, normalized temperature and boundary position equations will be required in order to calculate the temperatures at the advanced time level. The details of this overall iteration will be discussed later.

3.S.4 Movement of the Boundary

Since the backward Euler method was chosen for the temperature equation, and due to the coupling between this equation and the equation for moving the boundary, the backward Euler method was also employed for the latter equation. Thus in the case of transformed Cartesian coordinates the difference equation used is:

$$f_I^{n+1} = f_I^n + \Delta\tau \left(\frac{\alpha_1}{\alpha_2 P} \right) \left(\frac{1}{s^{n+1}} S_{\xi_I}^{n+1} - \frac{\xi_I}{(2\,h\,s^{n+1})^2} \right.$$

$$\left(f_{I+1}^{n+1} - f_{I-1}^{n+1} \right)\left(3\,f_{M+1}^{n+1} - 4\,f_M^{n+1} + f_{M-1}^{n+1} \right)$$

$$\left. \left(\frac{1}{\beta\Delta T} - \theta_{I,M+1}^{n+1} \right) \left(\theta_{I,M+1}^{n+1} \right)^m \right)$$

for $I = 1,2,3,4,\ldots M$ (3.S.27a)

$$s^{n+1} = s^n - \Delta\tau \left(\frac{\alpha_1}{\alpha_2 P} \right)\left(\frac{1}{2\,h\,(s^{n+1})^2} \right)$$

$$\left(3\,f_{M+1}^{n+1} - 4\,f_M^{n+1} + f_{M-1}^{n+1} \right)$$

$$\left(\frac{1}{\beta\Delta T} - \theta_{I,M+1}^{n+1} \right) \left(\theta_{I,M+1}^{n+1} \right)^m$$

(3.S.27b)

with $f_{M+1}^{n+1} = 0$, $S_{\xi_I}^{n+1}$ as defined in (S.S.17) and a second order forward difference used in place of the central difference for f_ξ when $I = 1$

In the case of transformed polar coordinates the difference equation used is:

$$R_i^{n+1} = R_i^n - \Delta\tau \left(\frac{\alpha_i}{\alpha_2 P} \right) \left(\frac{1}{R_i^{n+1}} \right) S_{\xi_i}^{n+1}$$

$$\text{for } i = 2,3,4,\ldots,M+1 \qquad (3.5.28a)$$

where $S_{\xi_i}^{n+1}$ is as defined in (3.5.20). For R_i^{n+1} the boundary condition on the derivatives of the stream function on moving surface (i.e. equation (3.5.6b)) is incorporated into the equation giving:

$$R_i^{n+1} = R_i^n - \Delta\tau \left(\frac{\alpha_i}{\alpha_2 P} \right) \left(\frac{R_i^{n+1}}{3 R_{i,M+1}^{n+1} - 4 R_2^{n+1} + R_3^{n+1}} \right)$$

$$\left(\frac{1}{B\Delta T} - \theta_{i,M+1}^{n+1} \right) \left(\theta_{i,M+1}^{n+1} \right)^m$$

(3.5.28b)

Note again that an iteration scheme will be required to solve the above equations.

3.S.S Overview of the Numerical Proceedure,

Due to the coupling between the various difference equations involved in solving for the variables in either of the two transformed scheme set up in this chapter an iteration scheme is required. Amongst the numerous possible schemes the following procedure was adopted (where the second superscript denotes iteration number):

(1) Set $\tau = 0$ and $n = 0$

(2) Calculate $\psi^n_{i,j}$ by solving the linear system for the stream function using f^n_i and s^n (or R^n_i) and $\theta^n_{i,j}$ in calculating the coefficients

(3) Set $f^{n+1,0}_i = f^n_i$ and $s^{n+1,0} = s^n$ (or $R^{n+1,0}_i = R^n_i$), $\psi^{n+1,0}_{i,j} = \psi^n_{i,j}$ and $\theta^{n+1,0}_{i,j} = \theta^n_{i,j}$ and $p = 0$.

(4) Calculate f^{n+1}_i and s^{n+1} (or R^{n+1}_i) using $f^{n+1,p}_i$ and $s^{n+1,p}$ (or $R^{n+1,p}_i$), $\psi^{n+1,p}_{i,j}$ and $\theta^{n+1,p}_{i,j}$ in the right hand side of (3.S.27) (or (3.S.28))

(5) Set $f^{n+1,p+1}_i = \omega f^{n+1}_i + (1 - \omega) f^{n+1,p}_i$ and $s^{n+1,p+1} = \omega s^{n+1} + (1 - \omega) s^{n+1,p}$ (or $R^{n+1,p+1}_i = \omega R^{n+1}_i + (1 - \omega) R^{n+1,p}_i$)

(6) Calculate $\theta_{i,j}^{n+1}$ by solving the linear system for the temperature using $f_i^{n+1,p+1}$ and $s^{n+1,p+1}$ (or $R_i^{n+1,p+1}$) and $\psi_{i,j}^{n+1,p}$ in calculating the coefficients

(7) Set $\theta_{i,j}^{n+1,p+1} = \omega\, \theta_{i,j}^{n+1} + (1 - \omega)\, \theta_{i,j}^{n+1,p}$

(8) Calculate $\psi_{i,j}^{n+1,p+1}$ by solving the linear system for the stream function using $f_i^{n+1,p+1}$ and $s^{n+1,p+1}$ (or $R_i^{n+1,p+1}$) and $\theta_{i,j}^{n+1,p+1}$ in calculating the coefficients

(9) If the last two iterates of $f_i^{n+1,p+1}$ and $s^{n+1,p+1}$ (or $R_i^{n+1,p+1}$) and $\theta_{i,j}^{n+1,p+1}$ have a relative difference greater than ε then set $p = p + 1$ and go to step (4)

(10) Set $\tau = \tau + \Delta\tau$ and $n = n + 1$

(11) If $\tau > \tau_{max}$ go to step (13)

(12) Set $f_i^{n+1,0} = 2 f_i^n - f_i^{n-1}$ and $s^{n+1,0} = 2 s^n - s^{n-1}$ (or $R_i^{n+1,0} = 2 R_i^n - R_i^{n-1}$) $\psi_{i,j}^{n+1,0} = 2 \psi_{i,j}^n - \psi_{i,j}^{n-1}$ and $\theta_{i,j}^{n+1,0} = 2 \theta_{i,j}^n - \theta_{i,j}^{n-1}$ and go to step (4)

(13) Stop

3.6 Discussion of Numerical Results

In this section an example problem is used to compare, in detail, the two different methods developed in this chapter. In addition, graphic results are then presented for various representative problems for which the effect of different free parameters values are studied.

For the first example consider the parabolic initial profile and quadratic temperature distribution:

$$f(x,0) = 1 - \left(\frac{x}{s(0)} \right)^2 \qquad (3.6.1)$$

$$s(0) = 1$$

$$\theta(0,x,z) = 1 - K \left(1 - \left(\frac{x}{s(0)} \right)^2 \right) \left(1 - \frac{s^2(0) - z^2}{s^2(0) - x^2} \right)$$

$$\theta(t,x,f(x,t)) = 1$$

where

$$K = .9,\ m = 3,\ Ra = 10,\ \beta\Delta T = .1 \text{ and } \frac{\alpha_1}{\alpha_2 P} = 5$$

The results for $f(0,t)$ and $s(t)$ at various times are given in Table 4. These variables are indicative of the degree of similarity between the results of the various numerical methods and are common to all the calculations. The (a) part of the table compares the results for various time steps and spatial grid for the transformed rectangular

coordinate version (Method 1) while the (b) parts show the same comparisons for the transformed polar coordinate version (Method 2). Note that the areas reported in Table 4 in only indicative of the amount of thermal expansion experienced by the fluid and does not imply any inherent accuracy or lack thereof, in the numerical schemes. Also note that the CPU times given are for the Control Data Corporation Cyber 170/135 computer.

The following parameters were used in the calculations:

(1) The linearized equations for the stream function and normalized temperature were iterated on until the 2-norm of the Q residual was less than 10^{-5} .

(2) The relaxation factor used for the BSSOR iteration was 1.6 .

(3) In the IOM acceleration the maximum number of v's was 6 and each y_{j+1} was held orthogonal to the last 3 v's (i.e. $m = 6$ and $p = 3$).

(4) The outer iteration was carried out until the maximum relative change between two successive iterates of the boundary location or temperature inside the domain was less than 10^{-3} using an underrelaxation factor of $.5$.

Inspection of Table 4 reveals that Method 2 is not acceptable on a 10×10 spatial grid since the results for this grid vary in the second decimal place from all the

Table 4a - Example 2 Results

Method 1 - Transformed Rectangular Coordinates

$\Delta\tau = .0005$

	h=.1, k=.1,	h=.05, k=.05,	h=.025, k=.025
f(0,.01)	.897292	.901103	.903019
s(.01)	1.326704	1.330336	1.329210
f(0,.02)	.826844	.834052	.839480
s(.02)	1.558907	1.549772	1.546786
f(0,.04)	.724536	.740108	
s(.04)	1.904077	1.895329	
f(0,.06)	.650739	.672355	
s(.06)	2.182076	2.171485	
area(.06)	.67338	.66945	
CPU time	92 secs	385 secs	1427 secs

$\Delta\tau = .001$

	h=.1, k=.1,	h=.05, k=.05,	h=.025, k=.025
f(0,.01)	.898301	.901989	did not converge
s(.01)	1.331908	1.334606	
f(0,.02)	.828245	.835463	
s(.02)	1.562110	1.555068	
f(0,.04)	.725403	.741459	
s(.04)	1.911696	1.901168	
f(0,.06)	.650884	.672919	
s(.06)	2.193649	2.182008	
area(.06)	.68959	.67474	
CPU time	73 secs	335 secs	212 secs

$\Delta\tau = .002$

	h=.1, k=.1,	h=.05, k=.05,	h=.025, k=.025
f(0,.01)	.899933	did not converge	did not converge
s(.01)	1.339411		
f(0,.02)	.830157		
s(.02)	1.570111		
f(0,.04)	.728465		
s(.04)	1.921564		
f(0,.06)	.654456		
s(.06)	2.203022		
area(.06)	.68959		
CPU time	66 secs		

Table 4b - Example 2 Results

Method 2 - Transformed Polar Coordinates

$\Delta\tau$=.0005

	$h=\pi/20$, k=.1,	$h=\pi/40$, k=.05,	$h=\pi/80$, k=.025
f(0,.01)	.890876	.897909	.901247
s(.01)	1.355929	1.322911	1.321080
f(0,.02)	.818751	.829302	.836685
s(.02)	1.585667	1.542513	1.540517
f(0,.04)	.715077	.733563	-
s(.04)	1.961050	1.899340	-
f(0,.06)	.641915	.664942	-
s(.06)	2.278792	2.187707	-
area(.06)	.73001	.68161	-
CPU time	83 secs	717 secs	835 secs

$\Delta\tau$=.001

	$h=\pi/20$, k=.1,	$h=\pi/40$, k=.05,	$h=\pi/80$, k=.025
f(0,.01)	.892735	.899708	.902548
s(.01)	1.349598	1.318177	1.316708
f(0,.02)	.819121	.830861	.837608
s(.02)	1.581132	1.537463	1.535898
f(0,.04)	.713675	.733600	-
s(.04)	1.959307	1.895044	-
f(0,.06)	.640046	did not converge	-
s(.06)	2.278696	-	-
area(.06)	.72977	-	-
CPU time	55 secs	502 secs	601 secs

$\Delta\tau$=.002

	$h=\pi/20$, k=.1,	$h=\pi/40$, k=.05	$h=\pi/80$, k=.025
f(0,.01)	.895044	.901720	did not converge
s(.01)	1.340333	1.311445	
f(0,.02)	.822281	.833484	
s(.02)	1.571222	1.529443	
f(0,.04)	.717291	.736221	
s(.04)	1.947581	1.883447	
f(0,.06)	.643210	did not converge	
s(.06)	2.265249	-	
area(.06)	.7272	-	
CPU time	50 secs	348 secs	

others. There is approximately two and one half decimal figure agreement in the mound centre height and toe location for various grid sizes and time steps within and between the other results of Methods 1 and 2. Method 2 is somewhat faster than Method 1 in terms of CPU time and also is more robust in terms of time step selection for a given spatial grid. Again it appears that the lack of accuracy when using Method 2 is due to spatial errors since there is very good agreement when different time steps are used for a given spatial grid. It appears that for Method 1, using a 10×10 spatial grid with a time step of .001 gives results with acceptable numerical convergence while for Method 2 a 20×20 spatial grid is required.

The deteriorating accuracy apparent in Method 2 can again, as in Chapter 2, be explained by the lack spatial resolution at the toe of the moving boundary.

The subsidence mound is plotted at different times in steps of .01 from the results of Methods 1 and 2, for the given initial conditions in Figure 21 following. Unlike the results of the unheated problem dealt with in Chapter 2, the mound appears to become 'kinked' with a linear profile at the advancing toe.

Figure 21 – Comparison of Methods

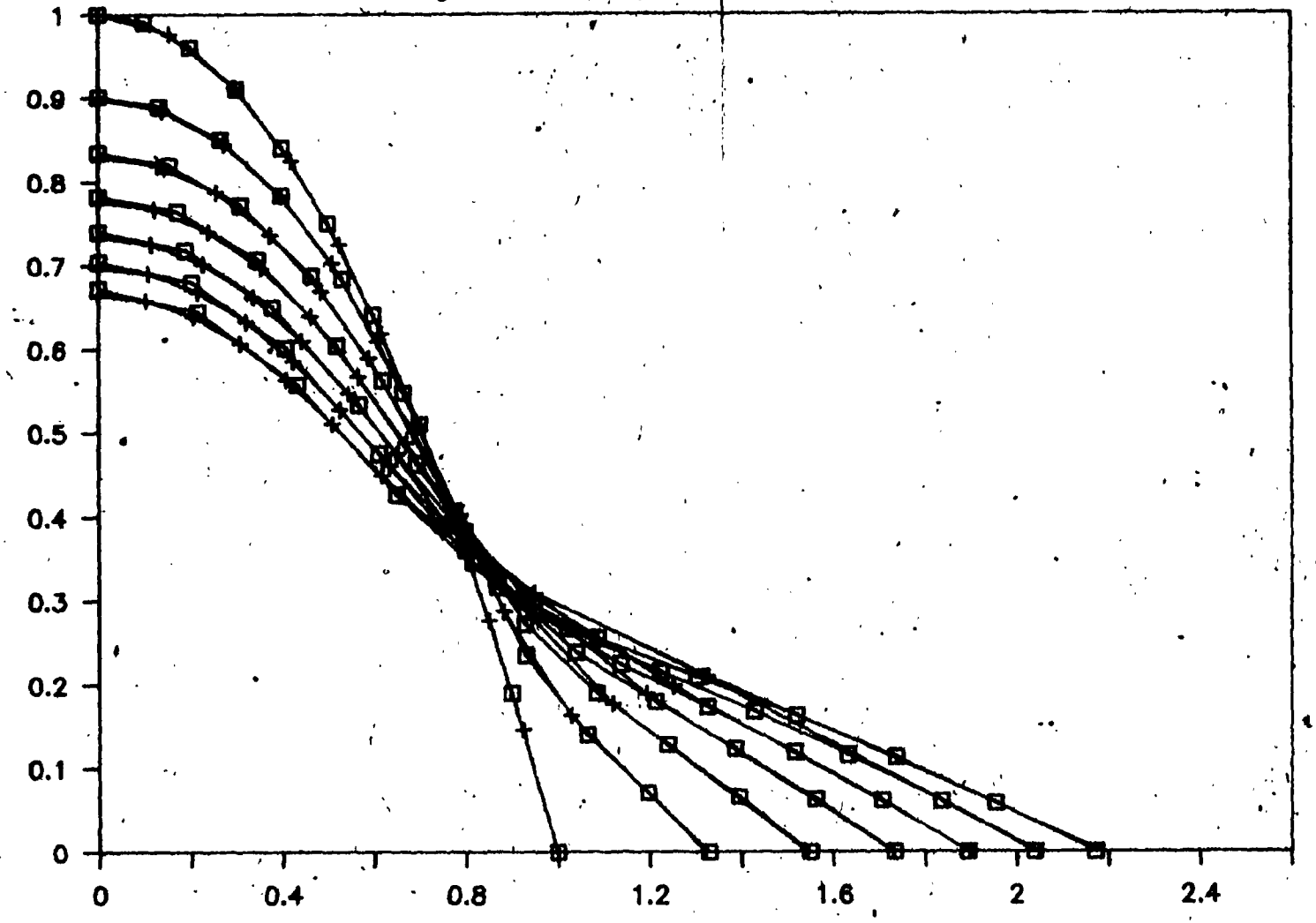

Note that the temperatures in the field predicted by Methods 1 and 2 are somewhat difficult to compare as the grid points are not in the same locations. It appears that the temperatures generally agree to about two or three decimal figures. There are, however, for both methods, some small oscillations (in the fourth decimal figure for Method 1 and somewhat larger for Method 2) in the temperatures of the fluid in the toe region . Additionally in the results reported later at higher Rayleigh numbers there are larger (in the first significant figure) oscillations in the temperature near the boundary in the center of the mound. The initial and later (at $\tau = .06$) temperature contours are plotted in Figures 22 and 23 respectively. Note that the region under the 'kinked' part of the toe is almost all very close to the boundary temperature of 1.

Parameter studies were done on the various parameters as follows:

(1) with $m = 3$, $Ra = 10$, $B\Delta T = .1$ and $\frac{\alpha_1}{\alpha_2 P} = 5$
K was varied from .5 to .9 (see Figure 24)

(2) with $K = .9$, $Ra = 10$, $B\Delta T = .1$ and $\frac{\alpha_1}{\alpha_2 P} = 5$
m was varied from 2 to 4 (see Figure 25)

Figure 22 – Isotherms at t = 0

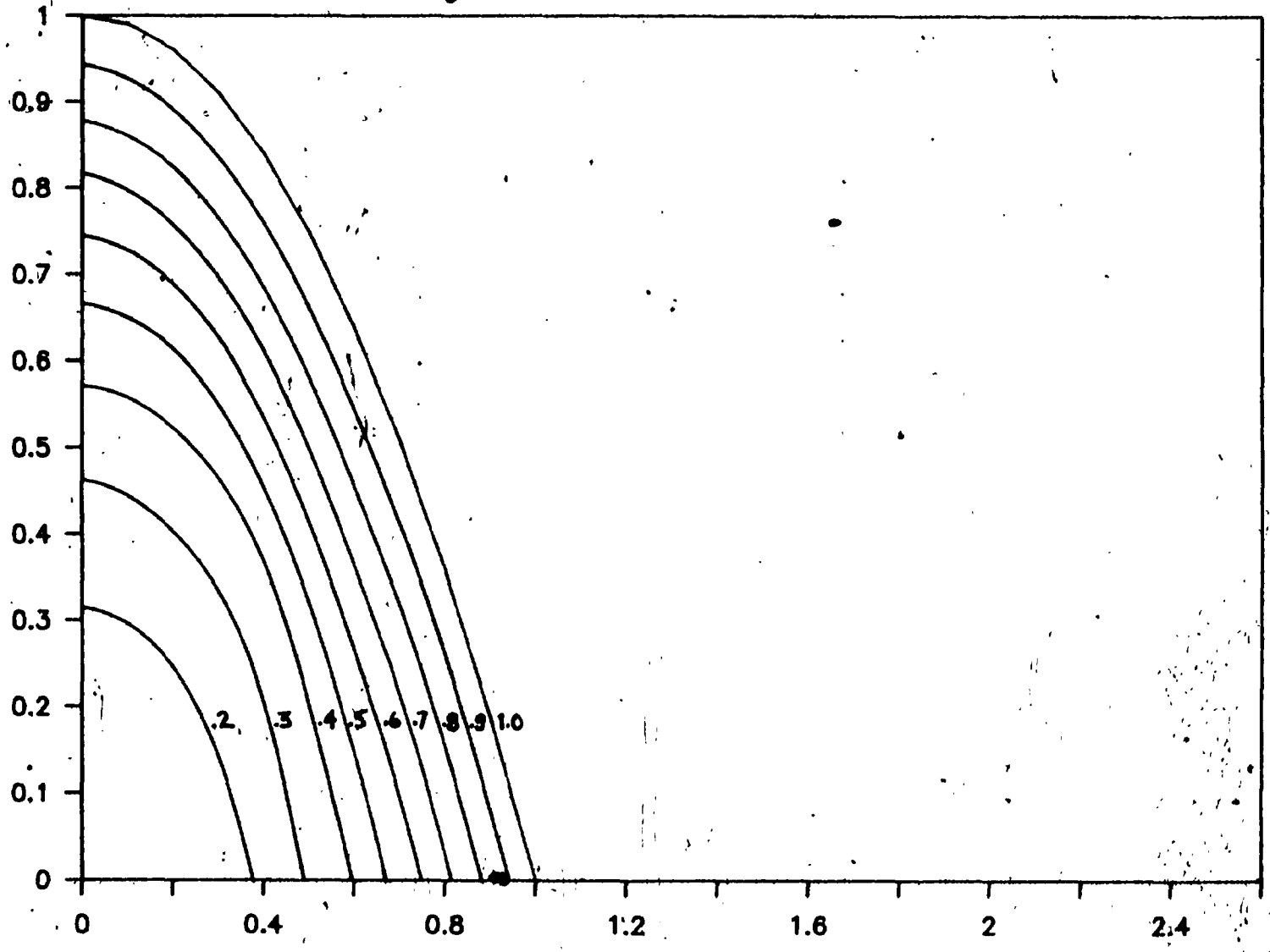

Figure 23 – Isotherms at t = .06

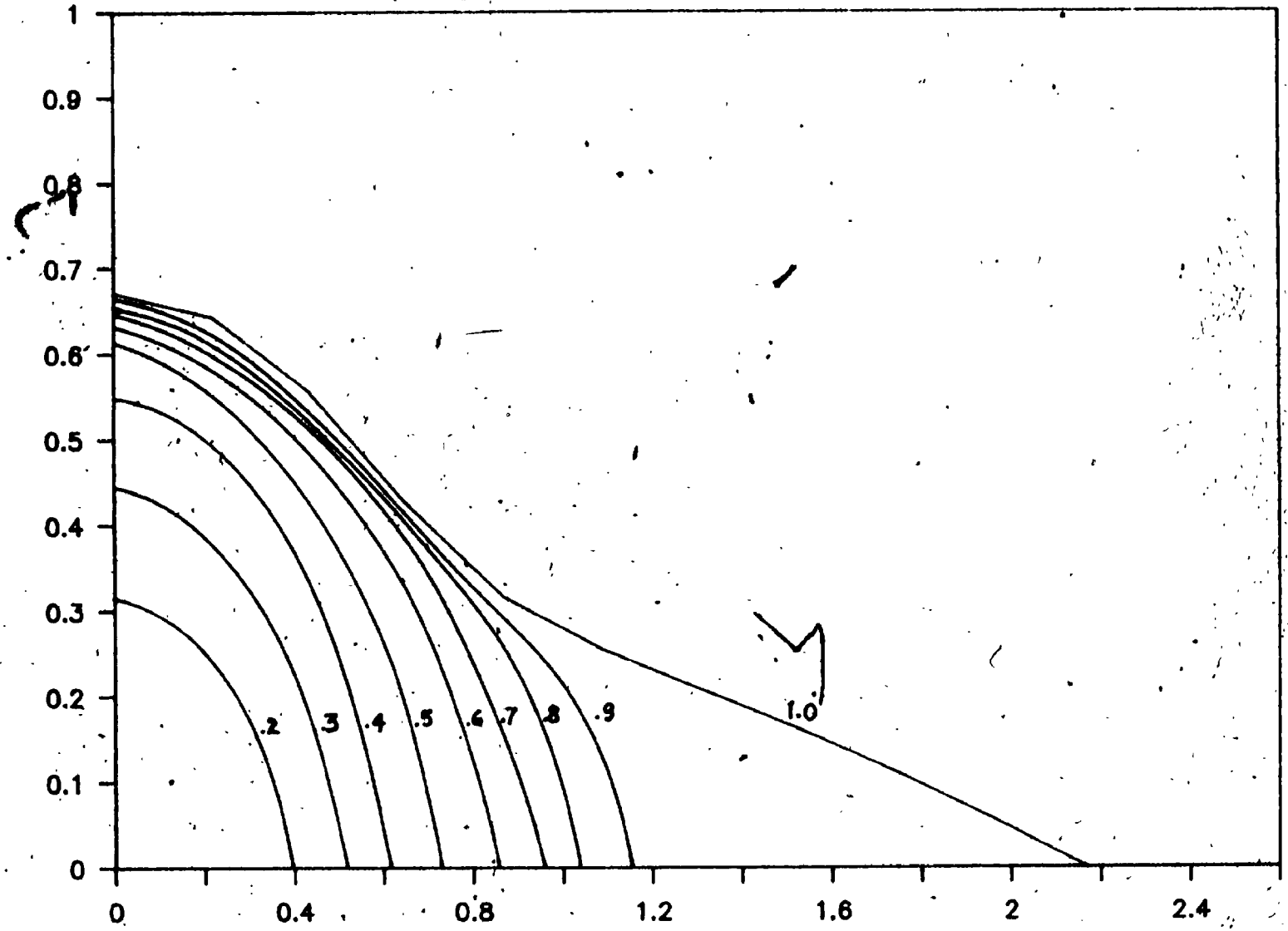

(3) with $K = .9$, $m = 3$, $\beta\Delta T = .1$ and $\frac{\alpha_1}{\alpha_2 P} = S$

Ra was varied from 1 to 800 (see Figure 26)

(4) with $K = .9$, $m = 3$, $Ra = 10$ and $\frac{\alpha_1}{\alpha_2 P} = S$

$\beta\Delta T$ was varied from .05 to .2 (see Figure 27)

(5) with $K = .9$, $m = 3$, $Ra = 10$ and $\beta\Delta T = .1$

$\frac{\alpha_1}{\alpha_2 P}$ was varied from 1 to 5 (see figure 28)

Except where noted these results were computed using Method 1 with a 20 x 20 spatial grid and a time step of .001 .

The effect of decreasing K (i.e. increasing the initial internal temperature of the mound) can be seen to be one of lessening the 'kinked' shape of the mound. Thus for lower values of K the centre of the mound drops faster while the toe spreads out only slightly faster than for higher values. This can be explained by the fact that at lower values of K the temperature, and thus viscosity differences of the fluid in different regions of the mound are much less than at higher values of K.

From the figures it can be seen that as m is increased the mound drops slower and spreads out slower emphasizing its 'kinked' appearance.

Figure 24a — Variation of Parameter K

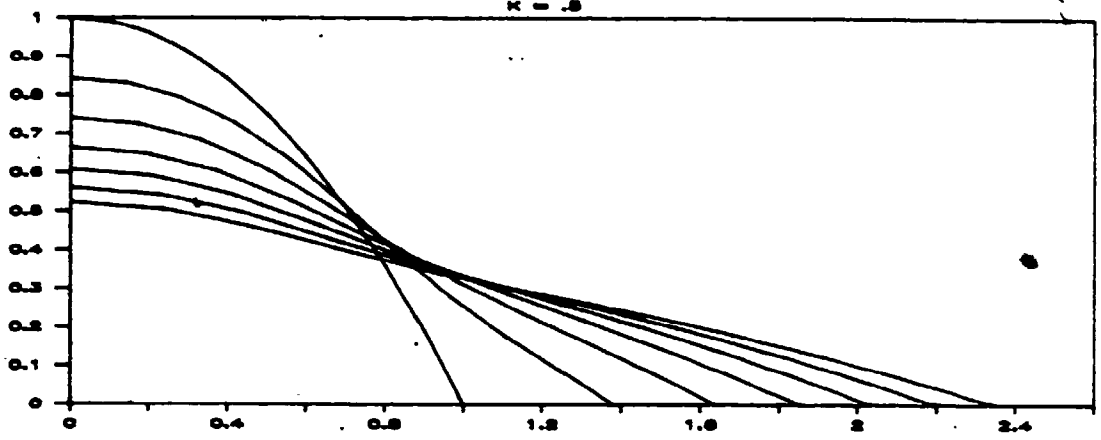

Figure 24b — Variation of Parameter K

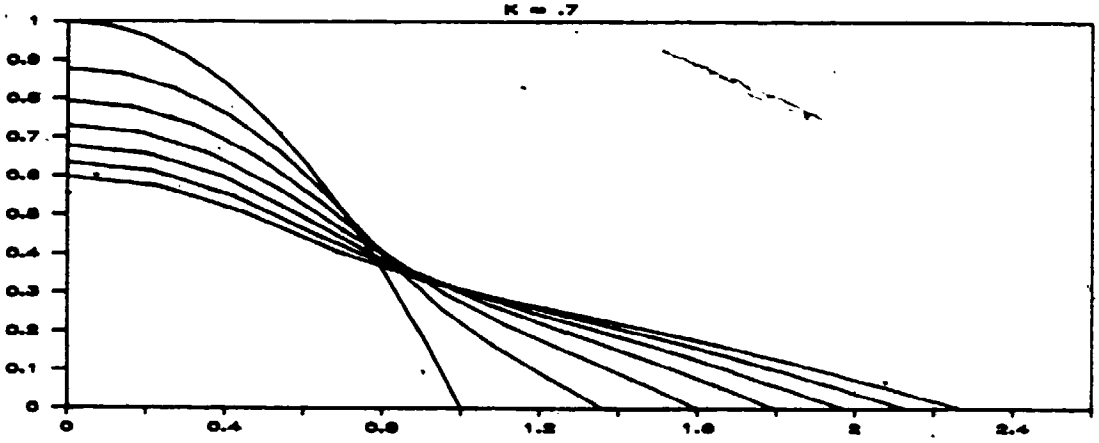

Figure 24c — Variation of Parameter K

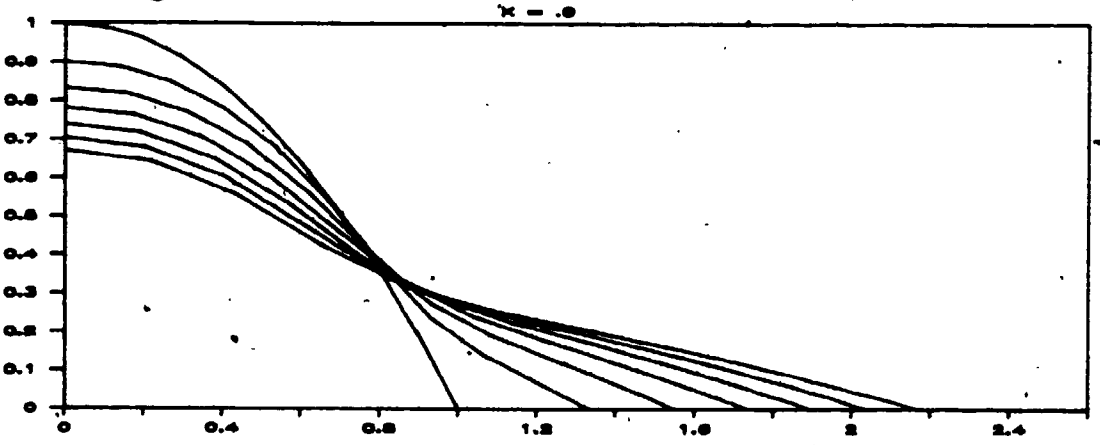

Figure 25a — Variation of Parameter m

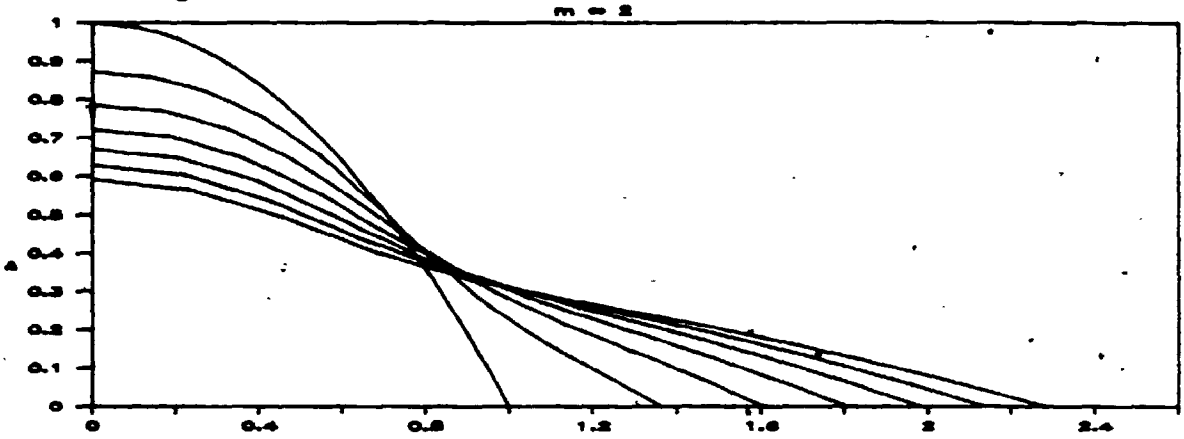

Figure 25b — Variation of Parameter m

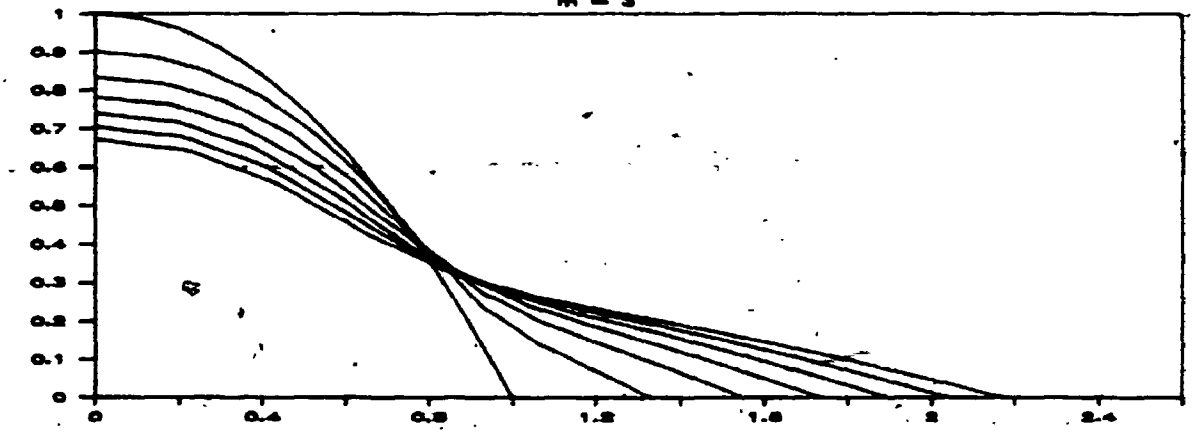

Figure 25c. — Variation of Parameter m

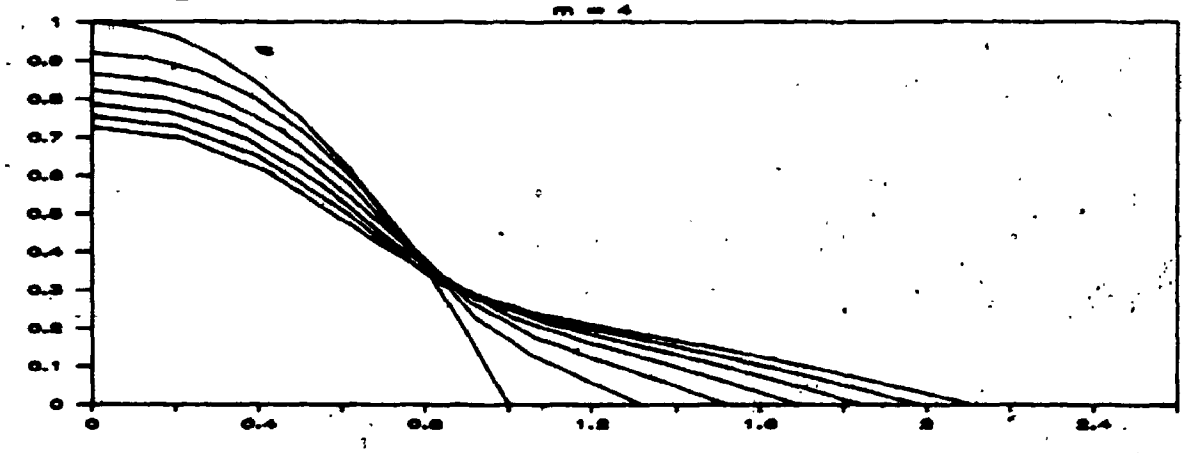

Figure 26a — Variation of Parameter Ra

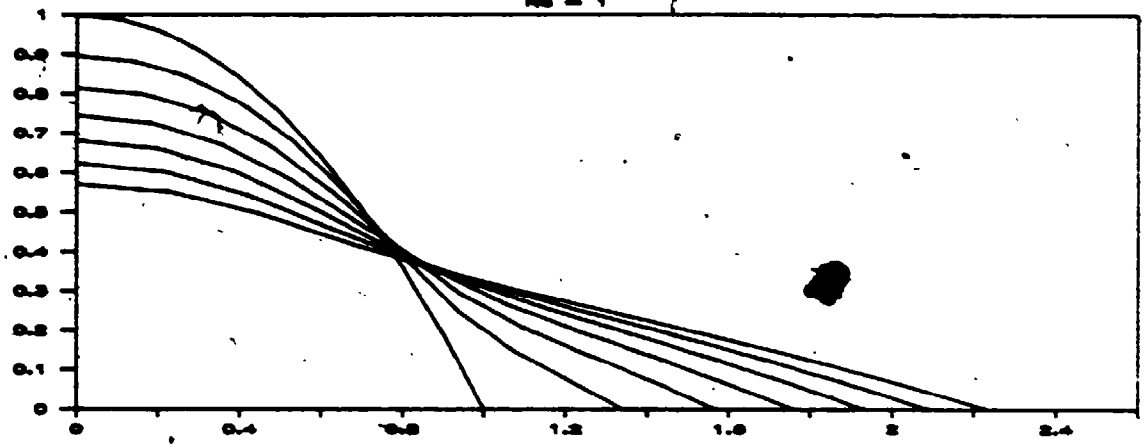

Figure 26b — Variation of Parameter Ra

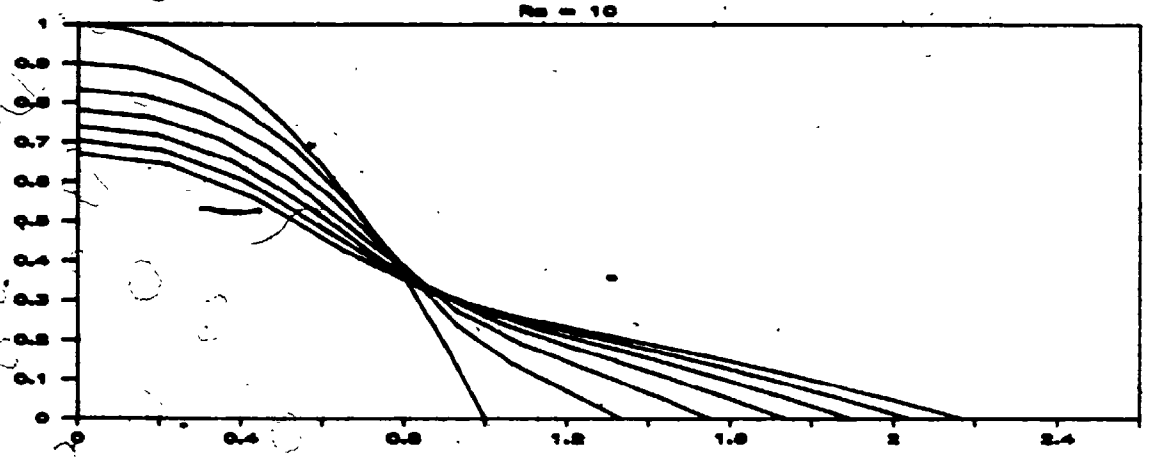

Figure 26c — Variation of Parameter Ra

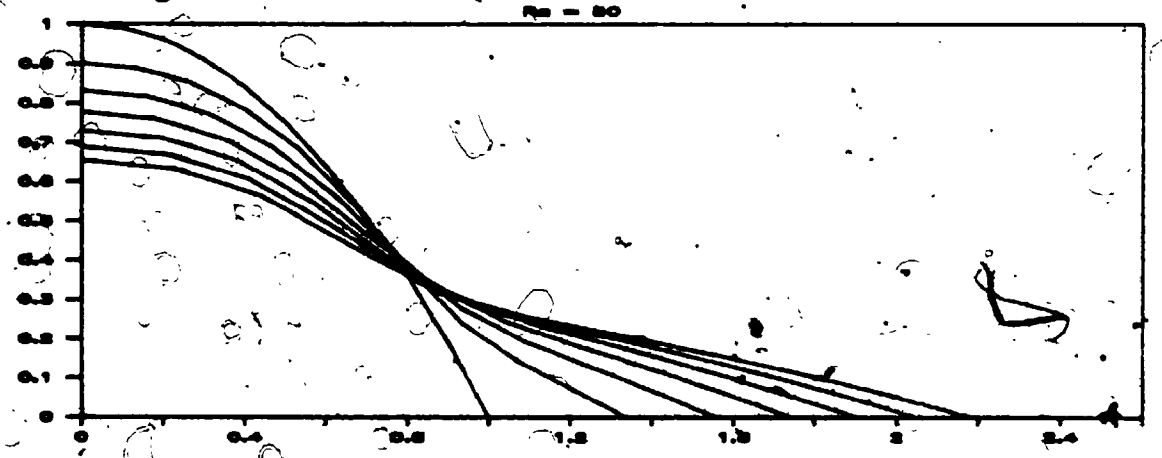

Figure 26d — Variation of Parameter Ra

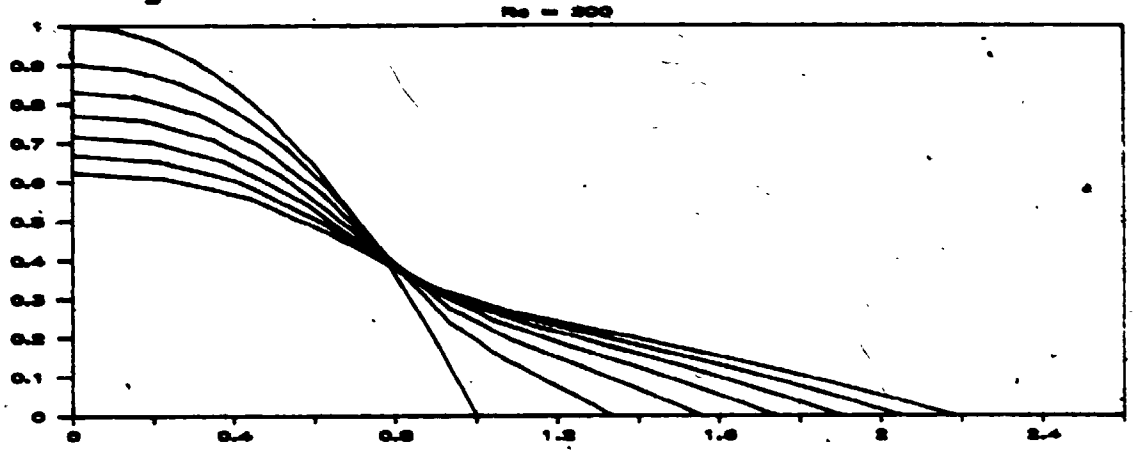

Figure 26e — Variation of Parameter Ra

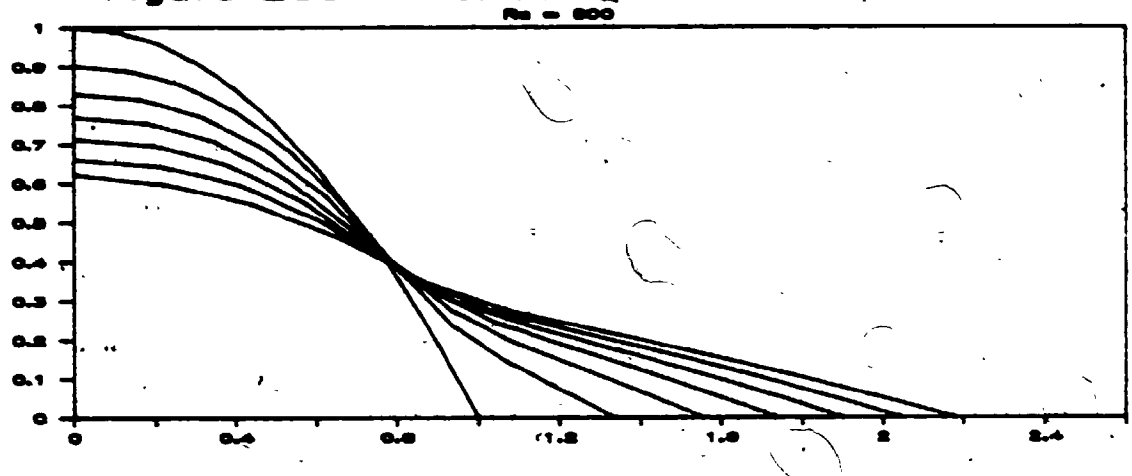

Figure 27a — Variation of Parameter $\beta\Delta T$

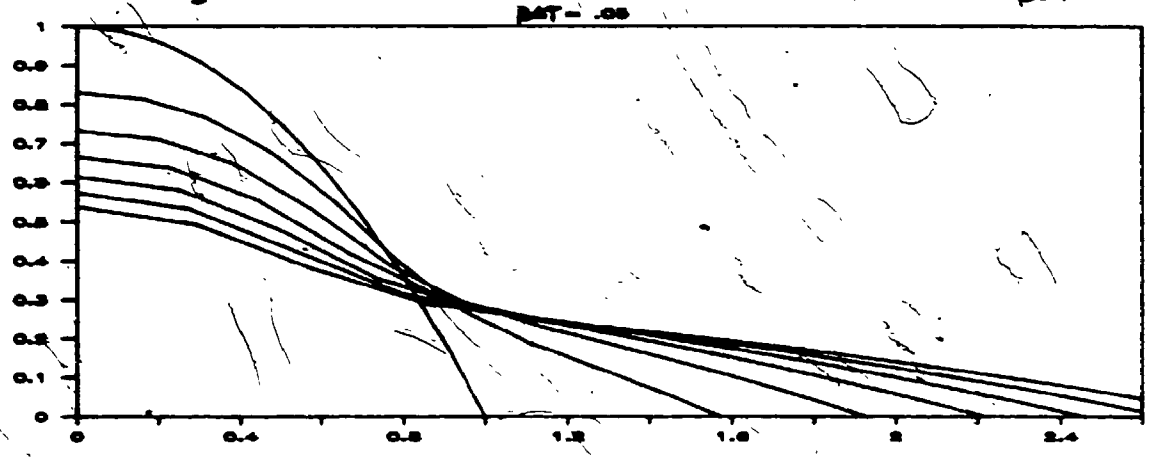

Figure 27b — Variation of Parameter $\beta\Delta T$

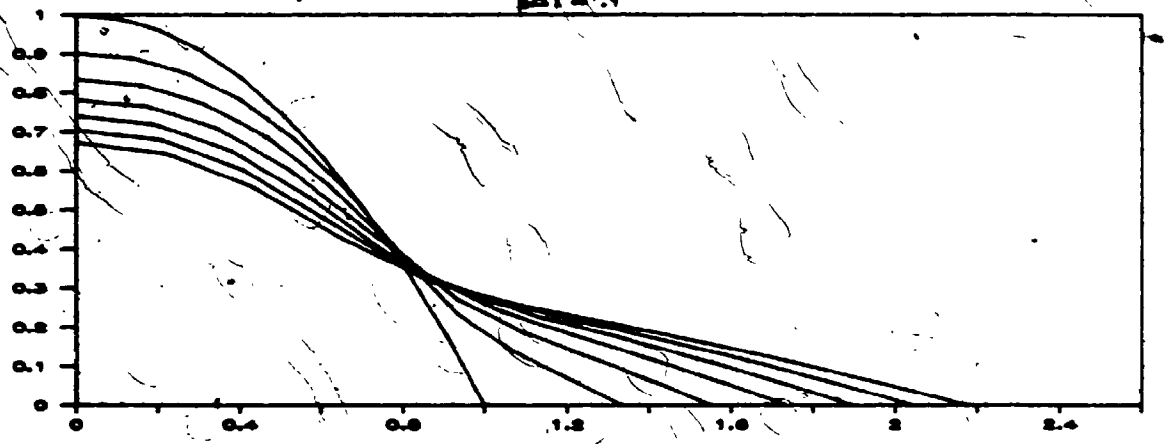

Figure 27c — Variation of Parameter $\beta\Delta T$

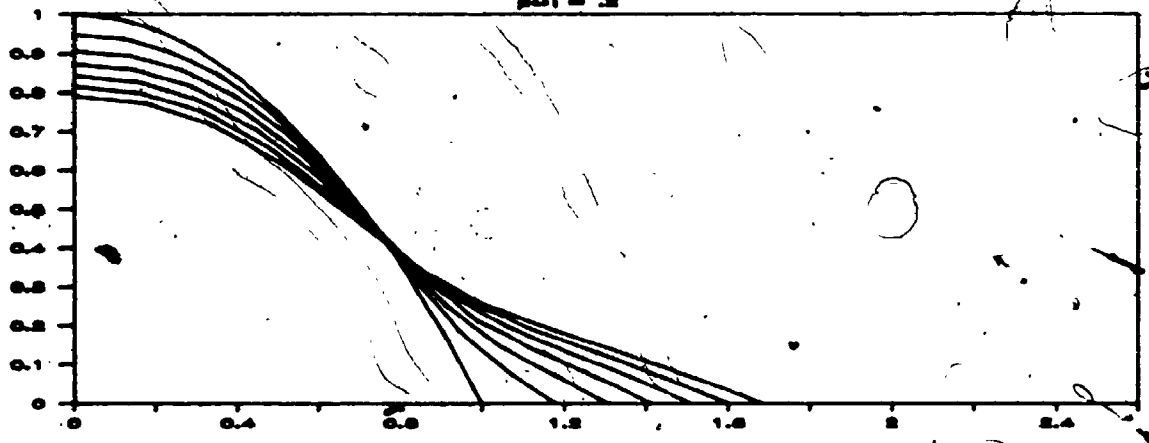

Figure 28a — Variation of Parameter $\frac{\alpha}{\alpha_1 p}$ $\frac{\alpha_2}{\alpha_1} = 1$

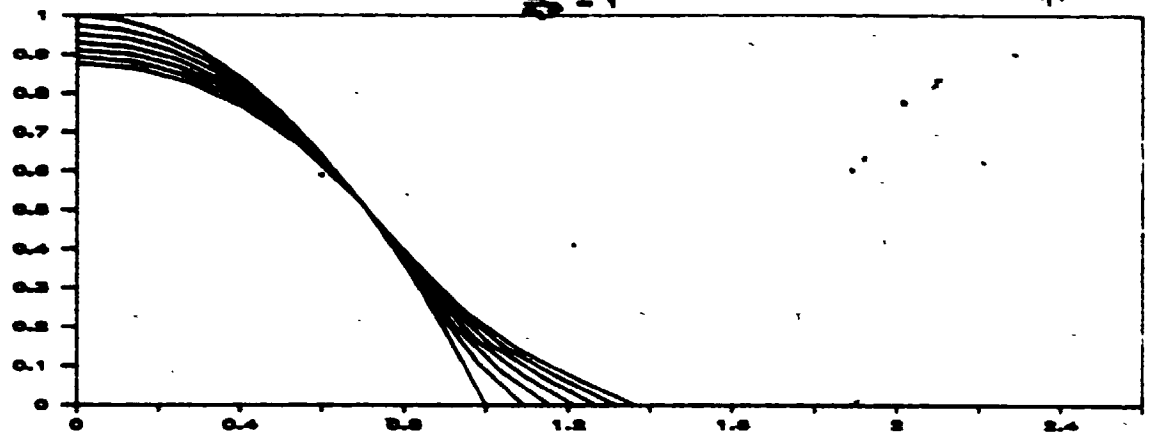

Figure 28b — Variation of Parameter $\frac{\alpha}{\alpha_1 p}$ $\frac{\alpha_2}{\alpha_1} = 3$

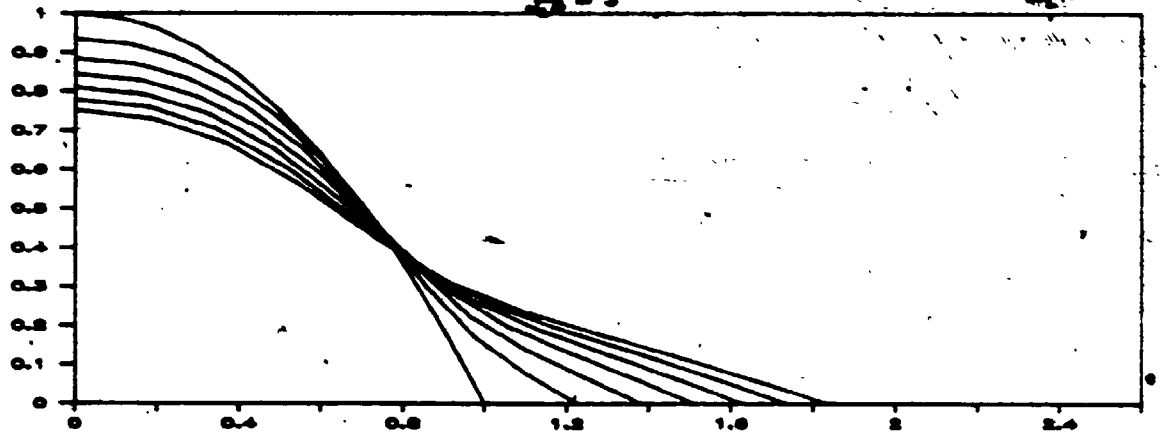

Figure 28c — Variation of Parameter $\frac{\alpha}{\alpha_1 p}$ $\frac{\alpha_2}{\alpha_1} = 5$

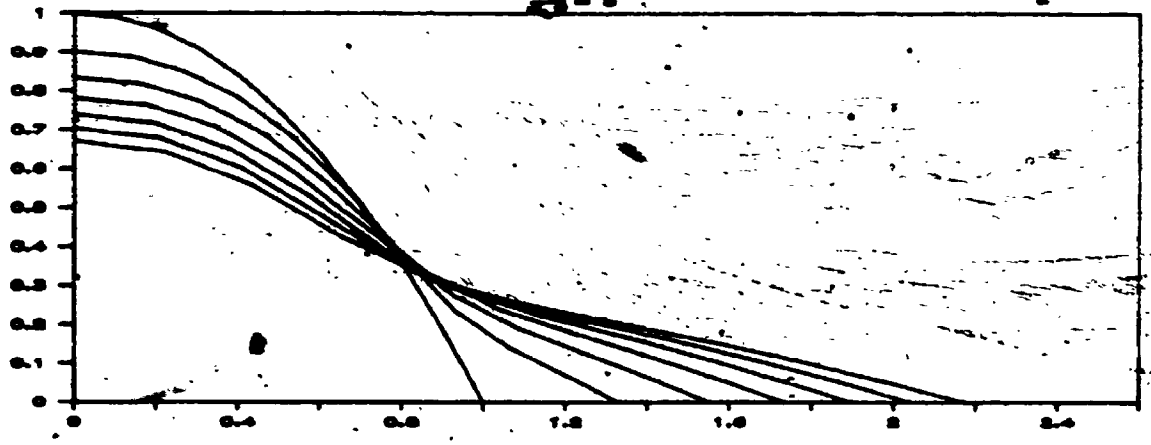

It can ~~also~~ be seen that the effect of increasing the Rayleigh number beyond 10 does not effect the motion of the toe but results in a slighty faster drop in the center of the mound the middle of which is somewhat wider. For a Rayleigh number of 1 the mound decays and spreads faster and appears much less 'kinked' than is the case for higher Rayleigh numbers.

The effect of increasing $\beta\Delta T$ appears to be one of slower motion. That is, the shape of the mound does not seem to be affected but its decay progresses more slowly.

Finally, the effect of decreasing $\frac{\alpha_1}{\alpha_2 P}$ is again one of slowing the speed of the mound's decay without affecting its 'kinked' appearance. This is very similar to the effect of increasing $\beta\Delta T$ as above.

3.7 Conclusions

As in Chapter 2, the transformed polar coordinate formulation of Method 2 is less accurate but more robust in terms of time step selection for a given number of spatial grid points than the transformed rectangular coordinate formulation of Method 1. This appears to be due to the lack of spatial resolution in the toe region of the subsidence mound.

The major effect of adding heating along the moving boundary to the subsidence mound problem of Chapter 2 is to change the mound's appearance. Typically, the mound attains a 'kinked' profile with the toe region spreading out faster than the cetral region of the mound. This is due to the large viscosity variations between the rapidly heated fluid in the toe region and the colder fluid elsewhere.

In this chapter a numerical scheme has been developed that allows for the calculation of interface motion between wet and dry regions in a porous media including the effects of heating along the interface. It should be possible to further refine this method so as to solve more realistic problems of interface motion as in for example, the in situ heating of heavy oils.

Appendix 1

In this appendix it is shown that the condition for non-negative coefficients of the difference equations from Chapter 2, for the potential of Method 2, cannot be established. Consider the coefficients of equation (2.7.11) and their definitions in (2.7.12)-(2.7.14). The condition that the coefficients $C^n_{0_{i,j}}$, $C^n_{1_{i,j}}$, $C^n_{2_{i,j}}$, $C^n_{3_{i,j}}$ and $C^n_{4_{i,j}}$ be non- negative implies that:

$$| B^n_{i,j} | \leq \min \left\{ A^n_{i,j} , \; C^n_{i,j} - | D^n_{i,j} | \right\} \qquad (A.1.1)$$

Now by definition

$$| B^n_{i,j} | = \left| \frac{\eta_i \left(f^n_{i+1} - f^n_{i-1} \right)}{2 k f^n_i} \right| \qquad (A.1.2)$$

Consider the difference equations adjacent to the leading edge of the toe where $I = M$. Suppose that in this region the moving boundary is linear in profile with slope $-S$. Note that the assumption of linearity of the profile of the moving boundary near its leading edge is quite reasonable as indicated by the computational results of Chapter 2. Thus

$$f_{M-1} = 2 S h \;\; , \;\; f_M = S h \;\; \text{and} \;\; f_{M+1} = 0 \qquad (A.1.3)$$

Substitution into (A.1.2) gives:

$$| B^{n}_{m,j} | = \frac{\eta_j}{k} = j - 1 \qquad (A.1.4)$$

which has a maximum of $(N-1)$ occuring when $j = N$.

Since the value of $A^{n}_{1,j}$ is defined to be 1 it is clear that (A.1.1) cannot be satisfied for any reasonable $N > 2$. Thus the non-negativeness of the coefficients of the difference equations for the potential of Method 2 cannot be established.

Appendix 2

In this appendix the local truncation error for the predictor-corrector scheme for propagating the moving boundary is established. This analysis is similar to that of Strikwerda and Geer (1980) for their shape of a slender jet calculation, however they do not analyse the accuracy of the predicted potentials as below. Assume that $\Delta\tau$, h and k are all of the same order (i.e. $O(\epsilon)$). The predictor-corrector scheme is:

$$\vec{u}_1^{\,*} = \vec{u}_1^{\,n} + \Delta\tau\, \vec{F}\left(\vec{u}_1^{\,n} , D_2\vec{u}_1^{\,n} , D_1\phi^n_{1,N-1} , \tau^n \right) \qquad \text{(A.2.1a)}$$

$$\vec{u}_1^{\,n+1} = \frac{1}{2}\left(\vec{u}_1^{\,n} + \vec{u}_1^{\,*} + \Delta\tau\, \vec{F}\left(\vec{u}_1^{\,*} , D_2\vec{u}_1^{\,*} , D_1\phi^*_{1,N-1} , \tau^{n+1} \right) \right) \qquad \text{(A.2.1b)}$$

Using a Taylor's expansion gives:

$$\vec{u}_1^{\,n+1} = \vec{u}_1^{\,n} + \Delta\tau \frac{\partial \vec{u}_1^{\,n}}{\partial\tau} + \frac{\Delta\tau^2}{2} \frac{\partial^2 \vec{u}_1^{\,n}}{\partial\tau^2} + O(\epsilon^3) \qquad \text{(A.2.2)}$$

The origional equation for the moving boundary gives:

$$\frac{\partial \vec{u}_1^{\,n}}{\partial\tau} = \vec{F}\left(\vec{u}_1^{\,n} , \frac{\partial \vec{u}_1^{\,n}}{\partial\xi} , \phi^n_{1,N-1} , \tau^n \right) \qquad \text{(A.2.3)}$$

Introduce the notation:

$$\vec{F}^n_{D_2} \equiv \vec{F}\left(\vec{u}^n_1 , D_2\vec{u}^n_1 , \phi_{n_1,N-1}^{n} , \tau^n \right)$$

$$\vec{F}^n_{D_3} \equiv \vec{F}\left(\vec{u}^n_1 , D_3\vec{u}^n_1 , \phi_{n_1,N-1}^{n} , \tau^n \right) \qquad \text{(A.2.4)}$$

then using Taylor's expansion:

$$\frac{\partial \vec{u}^n_1}{\partial \tau} = \frac{1}{2}\left(\vec{F}^n_{D_2} + \vec{F}^n_{D_3} \right) + O(\varepsilon^2) \qquad \text{(A.2.5)}$$

as long as

$$\frac{\partial \vec{u}^n_1}{\partial \xi} = \frac{1}{2}\left(D_2\vec{u}^n_1 + D_3\vec{u}^n_1 \right) + O(\varepsilon^2) \qquad \text{(A.2.6)}$$

which is the case for both the MacCormack based scheme for which D_2 and D_3 are first order backwards and forwards difference operators and for the Crank Nicolson based scheme for which D_2 and D_3 are both second order central difference operators.

Now

$$\Delta\tau \frac{\partial^2 \vec{u}^n_1}{\partial\tau\partial\xi} = \Delta\tau \frac{\partial}{\partial\tau}\left(\vec{F}\left(\vec{u}^n_1 , \frac{\partial \vec{u}^n_1}{\partial \xi} , \phi_{n_1,N-1}^{n} , \tau^n \right) \right) \qquad \text{(A.2.7)}$$

Using Taylor's expansion gives:

$$\Delta\tau \frac{\partial^2 \vec{u}_i^n}{\partial \tau^2} = \Delta\tau \frac{\partial}{\partial \tau} \left(\vec{F}_{D_3}^n + O(\varepsilon) \right)$$

$$= \Delta\tau \left(\frac{\partial \vec{F}_{D_3}^n}{\partial \vec{u}} \frac{\partial \vec{u}_i^n}{\partial \tau} + \frac{\partial \vec{F}_{D_3}^n}{\partial \vec{u}_\xi} \frac{\partial D_3 \vec{u}_i^n}{\partial \tau} + \frac{\partial \vec{F}_{D_3}^n}{\partial \phi_n} \frac{\partial \phi_{n_i, N+1}}{\partial \tau} + \frac{\partial \vec{F}_{D_3}^n}{\partial \tau} \right) + O(\varepsilon^2)$$

$$= \Delta\tau \left\{ \frac{\partial \vec{F}_{D_3}^n}{\partial \vec{u}} \frac{\left(\vec{u}_i^{n+1} - \vec{u}_i^n \right)}{\Delta\tau} + \frac{\partial \vec{F}_{D_3}^n}{\partial \vec{u}_\xi} D_3 \left\{ \frac{\left(\vec{u}_i^{n+1} - \vec{u}_i^n \right)}{\Delta\tau} \right\} + \frac{\partial \vec{F}_{D_3}^n}{\partial \phi_n} \left\{ \frac{\left(\phi_{n_i, N+1}^{n+1} - \phi_{n_i, N+1}^n \right)}{\Delta\tau} \right\} + \frac{\partial \vec{F}_{D_3}^n}{\partial \tau} \right\} + O(\varepsilon^2) \qquad \text{(A.2.8)}$$

Now since the starred values of the boundary position are the predicted values in (A.2.1a) they satisfy:

$$\vec{u}_i^* - \vec{u}_i^n = \Delta\tau \frac{\partial \vec{u}_i^n}{\partial \tau} + O(\varepsilon^2)$$

$$= \vec{u}_i^{n+1} - \vec{u}_i^n + O(\varepsilon^2) \qquad \text{(A.2.9)}$$

Finally a relationship between the starred and advanced time values of the derivative of the potential is required. Noting that these derivatives are evaluated on the moving boundary at the same time and on the same vertical line, the following Taylor's expansion is made:

$$\phi^{*}_{n_1,N+1} = \phi^{n+1}_{n_1,N+1} + (\,1,\ 0\,)\cdot\left(\vec{u}^{\,*}_1 - \vec{u}^{\,n+1}_1\right)\phi^{n+1}_{n n_1,N+1}$$

$$+ O(\varepsilon^2) \qquad \text{(A.2.10)}$$

Note that the dot product in the above expression represents the difference in the predicted boundary height and the boundary location at the advanced time. Using relation (A.2.9) and subtracting $\phi^{n}_{n_1,N+1}$ from both sides of (A.2.10) gives:

$$\phi^{*}_{n_1,N+1} - \phi^{n}_{n_1,N+1} = \phi^{n+1}_{n_1,N+1} - \phi^{n}_{n_1,N+1} + O(\varepsilon^2)$$

(A.2.11)

Substitution of (A.2.9) and (A.2.11) into (A.2.8) yields:

$$\Delta\tau\,\frac{\partial^2 \vec{u}^{\,n}_1}{\partial\tau^2} = \frac{\partial \vec{F}^{\,n}_{D_3}}{\partial \vec{u}}\left(\vec{u}^{\,*}_1 - \vec{u}^{\,n}_1\right) + \frac{\partial \vec{F}^{\,n}_{D_3}}{\partial \vec{u}_\xi} D_3\left\{\vec{u}^{\,*}_1 - \vec{u}^{\,n}_1\right\}$$

$$+ \frac{\partial \vec{F}^{\,n}_{D_3}}{\partial \phi_n}\left\{\phi^{*}_{n_1,N+1} - \phi^{n}_{n_1,N+1}\right\} + \Delta\tau\,\frac{\partial \vec{F}^{\,n}_{D_3}}{\partial\tau}\Big) + O(\varepsilon^2)$$

(A.2.12)

Finally substitution of (A.2.5) and (A.2.12) into (A.2.2) gives:

$$\vec{u}_1^{n+1} = \vec{u}_1^n + \frac{\Delta\tau}{2}\left\{ \left(\vec{F}_{D_2}^n + \vec{F}_{D_3}^n \right) + \frac{\partial \vec{F}_{D_3}^n}{\partial \vec{u}} \left(\vec{u}_1^* - \vec{u}_1^n \right) + \frac{\partial \vec{F}_{D_3}^n}{\partial \vec{u}_\xi} D_3 \left\{ \vec{u}_1^* - \vec{u}_1^n \right\} + \frac{\partial \vec{F}_{D_3}^n}{\partial \phi_n} \left\{ \phi_{n_{1,N+1}}^* - \phi_{n_{1,N+1}}^n \right\} + \Delta\tau \frac{\partial \vec{F}_{D_3}^n}{\partial \tau} \right\} + O(\epsilon^3) \qquad (A.2.13)$$

in which the terms involving $\vec{F}_{D_3}^n$ can be recognized as a Taylor's series for $\vec{F}_{D_3}^*$ about $\vec{F}_{D_3}^n$ accurate to $O(\epsilon^2)$. Thus

$$\vec{u}_1^{n+1} = \vec{u}_1^n + \frac{\Delta\tau}{2}\left(\vec{F}_{D_2}^n + \vec{F}_{D_3}^* \right) + O(\epsilon^3) \qquad (A.2.14)$$

Since $\vec{F}$ is linear in ϕ_n and D_1 is a second order backwards difference operator,

$$\vec{F}_{D_2}^n = \vec{F}\left(\vec{u}_1^n , D_2\vec{u}_1^n , D_1\phi_{1,N+1}^n , \tau^n \right) + O(\epsilon^2)$$

$$\vec{F}_{D_3}^* = \vec{F}\left(\vec{u}_1^* , D_3\vec{u}_1^* , D_1\phi_{1,N+1}^* , \tau^{n+1} \right) + O(\epsilon^2) \qquad (A.2.15)$$

Thus

$$\vec{u}_i^{n+1} = \vec{u}_i^n + \frac{\Delta\tau}{2}\left(\vec{F}(\vec{u}_i^n, D_2\vec{u}_i^n, D_1\phi^n_{i,N+1}, \tau^n) + \vec{F}(\vec{u}_i^{**}, D_2\vec{u}_i^{**}, D_1\phi^{**}_{i,N+1}, \tau^{n+1}) \right) + O(\epsilon^3) \tag{A.2.16}$$

which is the predictor-corrector (A.2.1) written as one step. This shows the second order local accuracy in time/space of the predictor-corrector scheme as required.

References

Beam, R. M. and Warming, R. F. (1980), Alternating direction implicit methods for parabolic equations with a mixed derivative, SIAM J. Sci. Stat. Comput., 1, 131-159.

Beam, R. M. and Warming, R. F. (1978), An implicit factored scheme for the compressible Navier-Stokes equations, AIAA J., 16, 393-402.

Bear, J. (1972), Dynamics of Fluids in Porous Media, McGraw-Hill Inc., New York, N. Y.

Bear, J. (1979), Hydraulics of Groundwater, American Elsevier Publishing Company Inc., New York, N. Y.

Butler, R. M., McNab, G. S. and Lo, H. Y. (1979), Theoretical studies on the gravity drainage of heavy oil during in-situ steam heating, paper presented at the 29'th Canadian Chemical Engineering Conference, Sarnia, Ontario, Canada.

Chan, T. F. (1984), Stability analysis of finite difference schemes for the advection-diffusion equation, SIAM J. Numer. Anal., 21, 272-284.

Cheng, P. (1978), *Heat transfer in geothermal systems*, in Advances in Heat Transfer, ed. T. F. Irvine and J. D. Hartnett, Academic Press, New York, N. Y.

Colgan, L. H. (1982), *Iterative methods for solving large sparse linear systems*, in Numerical Solutions of Partial Differential Equations, ed. J. Noye, North Holland Publishing Company.

Combarnous, M. A. and Bories, S. A. (1975), *Hydrothermal convection in saturated porous media*, Advances in Hydroscience, 10, 231-307.

Concus, P. and Golub, G. H. (1976), *A generalized conjugate gradient method for nonsymmetric systems of linear equations*, Stanford University research report CS-76-535.

Douglas Jr., J. (1983), *Finite difference methods for two-phase incompressible flow in porous media*, SIAM J. Numer. Anal., 20, 681-696.

Elder, J. W. (1967), *Steady free convection in a porous medium heated from below*, J. Fluid Mech., 27, 29-49.

Elman, H. C. (1984), *Iterative methods for non-self-adjoint elliptic solvers*, in Elliptic Problem Solvers II, ed. G. Birkhoff and A. Schoenstadt, Academic Press.

Forsyth Jr., P. A. and Rasmussen, H. (1979), *Solution of time dependent electrochemical machining problem by a co-ordinate transformation*, J. Inst. Maths Applics., 24, 411-424.

Forsyth Jr., P. A., and Rasmussen, H. (1980), *A Kantorovich method of a solution of time-dependent electrochemical machining problems*. Comp. Methods in Applied Mech. and Eng., 23.

Fruzeland, R. M. (1977), *A survey of the formulation and solution of free and moving boundary (Stefan) problems*, Brunel University TR/76.

Gary, J. and Kassoy D. R. (1981), *Computation of steady and oscillatory convection in a saturated porous media*, J. Comp. Phys., 40, 120-142.

Greydanus, J. (1983), *Numerical solution of three instability problems*, Ph. D. thesis, University of Western Ontario.

Gurtin, M. E., MacCamy, R. C. and Socolovsky, E. A. (1984), *A coordinate transformation for the porous media equation that renders the free-boundary stationary*, Quart. Appl. Math., 42.

Guvanasen, V. and Volker, R. E. (1980), *Numerical solution for unsteady flow in unconfined aquifers*, Int. J. Numer. Meth. Eng., 15, 1643-1657.

Hickox, C. E. and Gartling, D. K. (1981), *A numerical study of natural convection in a horizontal porous layer subjected to an end-to-end temperature difference*, J. Heat Transfer, 103, 797-802.

Horne, R. N. and O'Sullivan, M. J. (1978), *Convection in a porous medium heated from below: the effect of temperature dependent viscosity and thermal expansion coefficient*, J. Heat Trans., 100, 448-452.

Loh, C. Y. (1985), *Numerical techniques for free surface problems*, Ph. D. thesis, University of Western Ontario.

Loh, C. Y. and Rasmussen, H. (1984), *The free surface on a liquid filling a porous slab heated from its sides*, Int. J. Heat Mass Transfer, 27, 921-926.

MacCormack, R. W. (1978), *An efficient explicit-implicit-characteristic method for solving the compressible Navier-Stokes equations*, in Computational Fluid Dynamics, ed. H. B. Keller, SIAM-AMS Proceedings, 11, 130-155.

Meek, P. C. and Norbury, J. (1984), *Nonlinear moving boundary problems and a Keller box scheme*, SIAM J. Numer. Anal., 21, 883-893.

Mitchel, A. R. and Griffiths, D. F. (1980), The Finite Difference Method in Partial Differential Equations, John Wiley & Sons Ltd.

Prasad, V. and Kulacki, F. A. (1984a), *Convective heat transfer in a rectangular porous cavity - effect of aspect ratio on flow structure and heat transfer*, J. Heat Transfer, 106, 158-165.

Prasad, V. and Kulacki, F. A. (1984b), *Natural convection in a rectangular porous cavity with constant heat flux on one vertical wall*, J. Heat Transfer, 106, 152-157.

Rasmussen, H. and Silhani, D. S. (1981), *Unsteady porous flow with a free surface*, IMA J. Appl. Math., 27, 307-318.

Roache (1972), Computational Fluid Dynamics, Hermosa Publishers, Albuquerque, New Mexico.

Saad, Y. (1981), *Krylov subspace methods for solving large unsymmetric linear systems*, Math. Comput., 37, 105-126.

Saad, Y. (1984), *Practical use of some Krylov subspace methods for solving indefinite and nonsymmetric linear systems*, SIAM J. Sci. Stat. Comput., 5, 203-228.

Scheidegger, A. E. (1974), The Physics of Flow Through Porous Media, University of Toronto Press.

Strikwerda, J. and Geer, J. (1980), *A numerical method for computing the shape of a vertical slender jet*, SIAM J. Sci. Stat. Comput., 1, 449-466.

Todsen, M. (1971), *On the solution of transient free-surface flow problems in porous media by finite-difference methods*, J. Hydrology, 12, 177-210.

Warming, R. F. and Beam, R. M. (1978), *On the construction and application of implicit factored schemes for conservation laws*, SIAM-AMS Proceedings, 11, 85-129.

Whitaker, S. (1977), *Simultaneous heat, mass, and momentum transfer in porous media: a theory of drying*, in Advances in Heat Transfer, ed. T. F. Irvine and J. D. Hartnett, Academic Press, New York, N. Y.

Widlund, O. (1978), *A Lanczos method for a class of nonsymmetric systems of linear equations*, SIAM J. Numer. Anal., 15, 801-812.

Wooding, R. A. (1957), *Steady state free thermal convection of liquid in a saturated permeable medium*, J. Fluid Mech., 2, 273-285.

Young, D. M., Jea, K. C. and Kincaid, D. R. (1984), *Accelerating nonsymmetrizable iterative methods*, in Elliptic Problem Solvers II, ed. G. Birkhoff and A. Schoenstadt, Academic Press.